LATE PLEISTOCENE TO HOLOCENE EVOLUTION, SEDIMENTATION PROCESSES, AND ANTHROPOGENIC IMPACT OF A COASTAL SYSTEM: RARITAN AND SANDY HOOK BAYS, NEW JERSEY

by

ELANA A. KLEIN

A dissertation submitted in partial fulfillment of the requirements for the degree of
Doctor of Philosophy in Earth & Environmental Sciences,
The Graduate Center
City University of New York

2012

This manuscript has been read and accepted for the Graduate Faculty in Earth and Environmental Science in satisfaction of the dissertation requirement for the degree of Doctor of Philosophy.

Dr. Cecilia McHugh

Date — Chair of Examining Committee

Dr. Cindi Katz

Date — Executive Officer

Dr. John Chamberlain

Dr. Hari Pant

Supervisory Committee

THE CITY UNIVERSITY OF NEW YORK

ABSTRACT

LATE PLEISTOCENE TO HOLOCENE EVOLUTION, SEDIMENTATION PROCESSES, AND ANTHROPOGENIC IMPACT OF A COASTAL SYSTEM: RARITAN AND SANDY HOOK BAYS, NEW JERSEY

by

ELANA A. KLEIN

Dissertation Advisor: Dr. Cecilia McHugh

The objectives of this study were: 1) to decipher the late Pleistocene to modern- day evolution of a coastal system; 2) determine the impact of natural processes such as longshore currents and storms on its sedimentary patterns; and 3) assess the impact of anthropogenic activities due to the proximity of a large metropolitan region. An ultimate goal was to assess the health of the ecosystems within the coastal environment.

The study area included the Raritan and Sandy Hook Bays, New Jersey, located just south of the terminus of the maximum extent of the Laurentide ice sheet. The area has long been affected by the growth of a spit, storms, and anthropogenic pollution.

Seismic reflection profiles provided a framework for the evolution of this simple-fill estuary since the Last Glacial Maximum. Studies of Vibracores from Sandy Hook Bay revealed that the latest Holocene sediment in the bay is dominated by low energy deposition in a back-barrier environment created by the development of the Sandy Hook Spit, interrupted by storm events (e.g., storm surge, fluvial flooding) which have either left unconformities due to erosion, or mass-wasting deposits.

Radiocarbon ages of two shallow marine (i.e., low tide- 10 m) mollusks (*Anomia simplex; Anadara transversa*) suggest sea level entered the Sandy Hook Bay at ~6.1 cal. ka BP,

similar to estimates by Fairbanks (1989), Siddall et al. (2003), and Wright et al. (2009) that sea level reached its present day height ~ 6.0 ka BP. This suggests the land was not affected as greatly by the forebulge than areas previously depressed under the glacial ice.

Five mass-wasting deposits were dated (from 970 AD, 1399 AD, 1525 AD, 1591 AD, and 1778 AD; mean ages) with radiocarbon ages of shells retrieved from the cores and correlated with storm deposits identified in previous studies of Long Island, NY, and the New Jersey coast. These findings show that large areas of a coastline need to be studied to characterize a long-term prehistoric record of storms.

Results from X- ray fluorescence, magnetic susceptibility, loss on ignition, and short-lived radioisotopes, revealed that metal concentrations were greater in the upper sediments of the bay, primarily in the backbarrier sections and proximal to the beaches. Coarser-grained sediments near the tip of the spit were associated with less contaminants in the upper sediments, most likely related to dredging, or the higher energy related to tidal currents and waves.

Initial results from wet chemistry (ICP Spectrometer) tests conducted by an independent laboratory showed Pb was present at levels determined by Long et al. (1995) to have adverse effects on organisms. Future research is necessary to identify and designate sections of the bay where fish and shellfish should not be harvested from, due to metal concentrations that may adversely affect the health of organisms that inhabit the substrate.

ACKNOWLEDGEMENTS

I would like to thank my committee members; Dr. John Chamberlain and Dr. Hari Pant, and most of all, many thanks to my advisor, Dr. Cecilia McHugh who has been a constant source of encouragement, motivation, and guidance throughout the Ph.D. process.

I would like to thank Dr. Robert Sheridan and Dr. Gail Ashley at Rutgers University for offering the use of their archived sediment cores, and interpreted seismic reflection profiles from Sandy Hook and Raritan Bays.

Many thanks to my lab-mates, Damayanti Gurung, Adina Hakimian, and Vadim Acosta for their help and support.

Thank you to the Captain and Crew of R/V Lionel Walford. Partial funding was provided by: PSC- CUNY Grants; program year 38- 39; and Doctoral Student Research Grant; CUNY Graduate Center; 07-08.

I would like to thank my friends and family for their endless encouragement, support, and advice along the way.

TABLE OF CONTENTS

LIST OF TABLES

LIST OF FIGURES

INTRODUCTION

Estuarine environments are vulnerable to impact from natural processes such as tides, storms and longshore currents (e.g., Donnelly et al., 2001a; 2001b; Zhang et al., 2002; Rosati, 2005), anthropogenic activities such as pollution from metals, PCB's, and dioxin (Olsen et al., 1978; Olsen et al., 1984; Renwick and Ashley, 1984; Feng et al., 1998; Cohen et al., 2000; Feng et al., 2002; Rosales- Hoz, 2003; Tovar- Sanchez et al., 2004), and the effects of climate change including eustatic rise of sea level (Gornitz et al., 2002; Pendleton et al., 2005; Miller et al., 2011).

Estuarine sediment can preserve the record of past eustatic changes, storm activity, and effects of urbanization providing a useful tool for deciphering the timeline of such changes (e.g., Zaitlin et al., 1994; Gaswirth, 1999). The evolution and historical impact of eustatic changes, natural processes (e.g., storms, barrier/ spit growth) and anthropogenic activities related to estuaries can provide a framework for mitigation of effects of storms, remediation of contaminants and understanding of other urban estuaries world-wide.

More specifically, "simple-fill" estuaries that by definition preserved in their sediments the record of one eustatic cycle (Zaitlin et al., 1994), also contain in their stratigraphy evidence from previous storms and contaminants deposited since the onset of urbanization. The sedimentary record in these estuaries can be used to better understand the impacts of natural processes and anthropogenic activities.

The area encompassing the Sandy Hook and Raritan Bays is a simple-fill estuary, which was located adjacent to the southeast terminus of the Laurentide Ice Sheet during the Last Glacial Maximum (LGM). This coastal area was also subaerially exposed and incised by fluvial systems during the LGM (Swift et al., 1980; Teller, 1987; Goss et al., 1995; Gaswirth, 1999;

Peltier, 1998; 1999; Gaswirth et al., 2002; Clark and Mix, 2002; Carey et al., 2005; Nordfjord et al. 2005; 2006). After the ice retreated, eustatic rise flooded the region, sediments filled the bay and estuarine conditions developed (Gaswirth, 1999; Nordfjord et al., 2005; Miller et al., 2011). Previous studies of the Hudson River Estuary and Long Island Sound documented that the first sea water incursions occurred at ~11.5 cal. ka BP and ~13.5 to 10.0 cal. ka BP, respectively (Weiss, 1974; Lewis and DiGiacomo- Cohen, 2000; Uchupi et al., 2001; Thomas and Varekamp, 2007). The discrepancy in the ages is related to glacial ice depressing the land. The Raritan Bay, south of the ice front is expected to have experienced sea water incursion consistent with estimates by Fairbanks (1989), Siddall et al. (2003), and Wright et al. (2009) that indicate global sea level reached its present position ~6.0 ka BP.

Urbanization has left the estuary vulnerable to anthropogenic impact. The Hudson-Raritan Estuary is presently one of the most urbanized estuaries on the East Coast of the United States, with inputs from sewage treatment plants, industrial discharge, untreated wastewater from combined storm overflow, as well as runoff from throughout the watershed (Tovar-Sanchez et al., 2004).

This study will add to the knowledge of how contaminant metals are accumulating in the sediments of the Sandy Hook Bay by examining the pre-industrial to modern depositional history based on a chronology derived from short-lived radioisotopes and radiocarbon ages. Deposition of contaminants will be analyzed in correlation with studies of the natural processes that occur in the bay region, including transport due to longshore currents, storm activity, and the presence of a sand spit. This will provide more information about how natural processes affect the fate of contaminant accumulation in urban bays, which are partially protected from ocean waves by barriers and spits.

The objectives of this study can be summarized as the follows:

Statement of the Research Problem

1. How did the Raritan and Sandy Hook Bays evolve since the Last Glacial Maximum in the context of a eustatic cycle?
2. What are the impacts of storms and longshore currents on the evolution of Raritan and Sandy Hook Bays? How does the growth of a spit affect processes that occur in the bay?
3. How is a modern bay located in an urban setting affected by anthropogenic processes? How do natural processes such as the growth of a spit, and storms, affect the deposition and transport of anthropogenic contaminants in a bay setting?

BACKGROUND

Geography of Raritan and Sandy Hook Bays

The Sandy Hook Bay is contained within Raritan Bay and both are adjacent to the Lower New York Harbor (Fig. 1). The region forms part of the Gateway National Recreation Area which includes more than 45 km of shoreline in Staten Island, Jamaica Bay, and Sandy Hook, and 40 km^2 of Jamaica Bay salt marsh and tidal creeks (Ray, 2004; Pendleton et al., 2005).

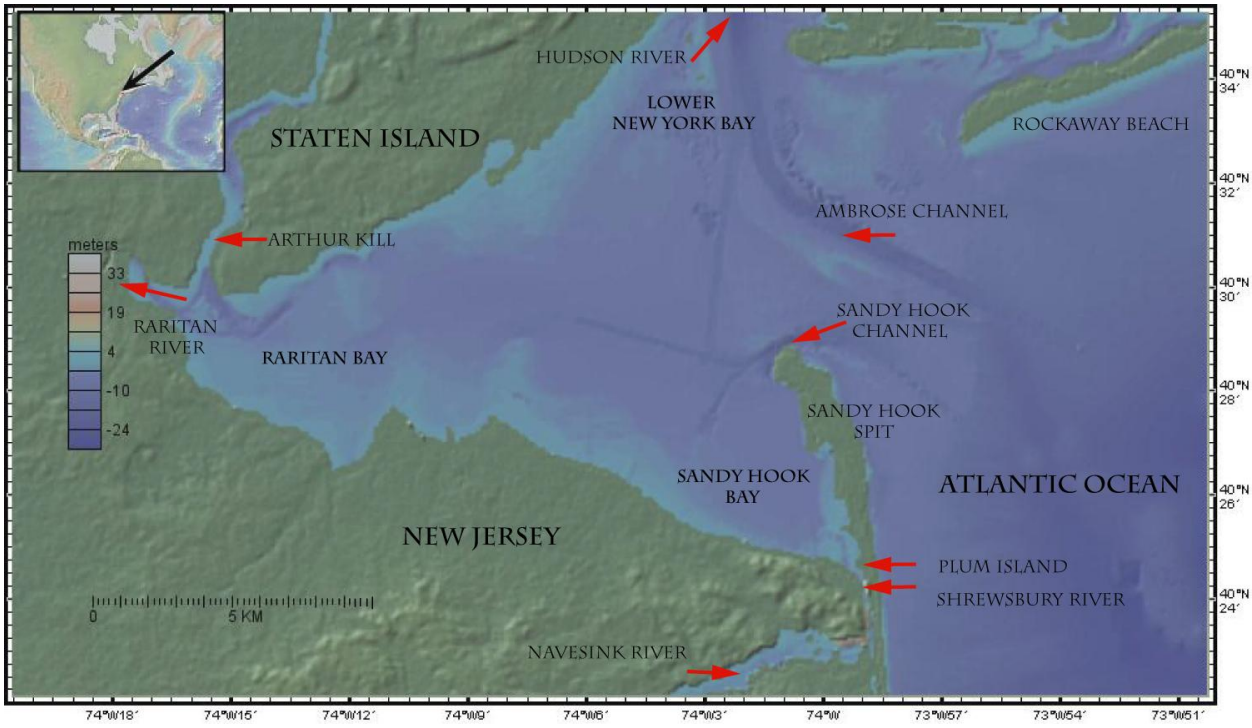

Figure 1: Map of coastal sections of New York and New Jersey, including the location of the study area. Locations of tributaries including the Shrewsbury River, Navesink River, Arthur Kill, Raritan River, and Hudson River are shown. (Adapted and modified from GeoMapApp ©).

The Hudson- Raritan Estuary is a two- layer estuary that is partially- mixed (Young and Hillard, 1984). The bathymetry of the Raritan Bay is flat and shallow (average 8 meters) and is deeper (3- 11 m) in dredged channels (U.S. Fish and Wildlife Service, 1997; Ray, 2004 and references therein).

The major water currents in the Raritan and Sandy Hook Bays flow in a counter-clockwise direction (Jeffries, 1962; NJDEP, 1998). The tidal range is microtidal, with an average of 1.5 m. It takes approximately 32- 42 tides to flush out the bays, over the course of 16 to 21 days. As the ebb tide enters the system, water moves in from the ocean through the opening between Sandy Hook and the Rockaway transect (e.g., Rockaway Beach), and then moves up the Hudson River. As the tide recedes, water travels out to the ocean from the Hudson and Raritan Rivers, and from the Raritan and Sandy Hook Bays (NJDEP, 1998; Ray, 2004; and references therein). The Raritan and Sandy Hook Bays range in salinity of 32‰, near the Sandy Hook, to 22 ‰ near the mouth of the Raritan River (Ray, 2004 and references therein).

The fluvial influx into the Raritan and Sandy Hook Bays is complex, as it includes several tributaries and potentially many sources of contaminants, which may accumulate in the bays (Paulson, 2005). The Raritan River is the major freshwater source to the system (Ray, 2004 and references therein). Other tributaries that flow into the Raritan and Sandy Hook Bays include the Shrewsbury River, Navesink River, Arthur Kill, and Hudson River (Fig. 1; U.S. Dept. of Interior, 1967; USGS Sandy Hook Quadrangle Topographic Map, 1998). There is also an influx of saline water landward (towards the Upper and Lower New York Bays) via shipping channels (e.g., Ambrose Channel; Paulson, 2005).

Late Pleistocene Glacial to Holocene Interglacial Evolution of the Coastal System

Last Glacial Maximum

The present- day Raritan Bay was located just south of the southeastern terminal moraine of the Laurentide Ice Sheet during the LGM (e.g., Teller, 1987; Goss et al., 1995; McHugh and

Olson, 2002). The sediments of this region recorded the late Pleistocene to Holocene glacial to interglacial history (Teller, 1987; Gaswirth, 1999; Peltier, 1998; 1999; Gaswirth et al., 2002; Clark and Mix, 2002; Carey et al., 2005; Wright et al., 2009; Miller et al., 2010; Figure 2).

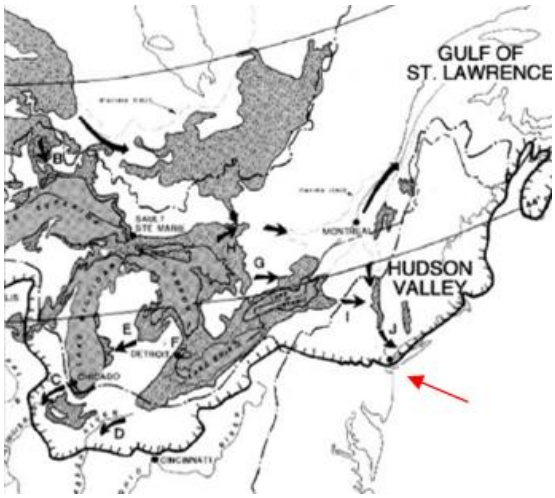

Figure 2: Map of the southeastern terminus of the Laurentide Ice Sheet during the LGM. The extent of the ice sheet is marked by a heavy black line. The location of study area is noted by a red arrow. (Modified after McHugh and Olson, 2002, and references therein).

At ~20,000 years BP, global sea level was ~120 m lower than today. This was estimated from sea level curves derived from various studies including those focused on corals (*Acropora palmata)* from cores retrieved offshore Barbados, $\delta^{18}O$ from benthic foraminifera. More recent studies dated unconformities and related them to seismic stratigraphy and sequence boundaries in the New Jersey continental margin, and offshore the eastern slope and shelf of New Zealand (Fairbanks, 1989; Peltier, 1998; Siddall et al., 2003; Peltier and Fairbanks, 2006; Miller et al., 2009; Wright et al., 2009; McHugh et al., 2010; Miller et al., 2011, and references therein; Engelhart et al., 2011a).

The New Jersey continental shelf was subaerially exposed during the Last Glacial Maximum (Swift et al., 1980; Gaswirth, 1999; Nordfjord et al. 2005; 2006; Wright et al., 2009).

Systems of braided streams meandered across the region beyond the margin of the ice and paleochannels related to these fluvial systems are evident in seismic reflection profiles (Gaswirth, 1999; Gaswirth et al., 2002; Gulick et al., 2005; Nordfjord et al. 2005; 2006).

Deglaciation

A transgression of sea level began as the ice sheet melted starting at 18,000 yrs BP (Peltier, 1999; Gaswirth et al., 2002; Duncan et al., 2002; Carey et al., 2005; Wright et al., 2009; Miller et al., 2009; Miller et al., 2011). According to Fairbanks (1989), sea level rose 24 m during melt-water pulse 1A at approximately 13,000 yrs BP. This was followed by a eustatic rise of 20 m from 17,100 to 12,500 yrs BP. The rate of sea level rise was lowest during the period of 11,000 – 10,500 yrs BP, associated with the start of the Younger Dryas cool period, with an increase in rates through to melt-water pulse (1B) at 9,500 yrs BP (Fairbanks, 1989). The meltwater associated with these 1A and 1B pulses entered the North Atlantic surface waters at rates of 14, 000 km^3/yr (1A), and 9,500 km^3/yr (1B) (Fairbanks, 1989). The melt-water pulse (1A) described by Fairbanks (1989) is consistent with minimum $\delta^{18}O$ values documented in Bard (1987) and Broecker et al. (1988; 1989). The $\delta^{18}O$ can be used as proxy for glacial ice volume because glacial ice has low $\delta^{18}O$ compared to seawater, which leaves the ocean water enriched in ^{18}O when ice sheets expand (Fairbanks, 1989; Peltier and Fairbanks, 2006).

As the Laurentide ice sheet retreated from 18,000 to 13,000 yrs BP, the melt water runoff became trapped by moraines and created glacial lakes along the ice margin in eastern North American and the Hudson Valley region. In the general area where New York, Connecticut and New Jersey states are today, several proglacial lakes were formed including Lake Connecticut, Lake Hudson, and Lake Passaic (Uchupi et al., 2001). It has been proposed that the lakes were

breached and catastrophically drained on the continental shelf, forming the Hudson Shelf Valley at ~10- 12 ka BP. The glacial Lake Hackensack drained through spillways in the moraine, into the present- day Raritan Bay and Lower New York Bay, as evidenced by paleochannels located where the drainage occurred. Glacial Lake Hackensack drained into the New Jersey continental shelf at approximately 15,000 yrs BP, via the present- day Raritan Bay (Uchupi et al, 2001; Donnelly et al., 2005; Rayburn et al., 2005; 2007; Thieler et al., 2007).

The exposed continental shelf was flooded at ~12,000 and 10,300 yrs BP when the terminal moraine (Harbor Hill Moraine) was breached at the Narrows between Staten Island and Long Island (Thieler et al., 2007). The breaching was possibly due to increased water levels in the Hudson basin from the glacial lakes Iroquois, Vermont and Albany, which drained through the Narrows, due to dam failure (Thieler et al., 2007). As a result, floodwaters from glacial Lake Hudson and other lakes drained through the Hudson Valley into New Jersey and Southern New England continental shelves and slopes (Uchupi et al, 2001, Donnelly et al., 2005, Thieler et al., 2007).

The course of the Raritan River was also affected by the deglaciation. According to Goss et al. (1995), and Gaswirth et al. (2002), the Raritan River used to flow northeastward before the Last Glacial Maximum. It was repositioned due to draining of glacial lakes to an eastward flow (Fig. 3).

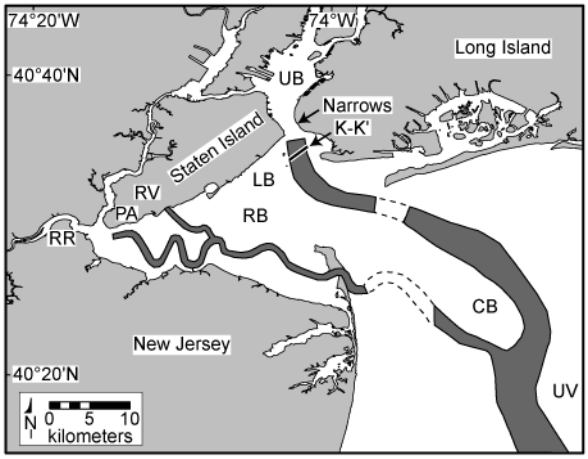

Figure 3: Locations of the paleo- Raritan and paleo- Hudson River, buried channels and spillways for glacial meltwater in present- day Raritan Bay and Hudson Shelf Valley. RB= Raritan Bay, LB= Lower New York Bay, CB= Christiansen Basin, RV= location of Richmond Valley Spillway, UV= Upper Hudson Shelf Valley, PA= Perth Amboy Spillway, RR= Raritan River, and UB= Upper New York Bay (Adapted with permission from Thieler et al., 2007).

Deglaciation of Long Island Sound

The present- day Long Island Sound was occupied by glacial Lake Connecticut that contained in its sediments varves and deltaic deposits (Lewis and Stone, 1991; Stone et al., 1998; Lewisand DiGiacomo-Cohen, 2000; Thomas et al., 2007). The lake formed as meltwater was dammed by moraines as the ice sheet retreated. Lake Connecticut ultimately drained through a spillway at the east end of the present- day Sound, (the Race) at approximately 15.5 ka BP (Lewis and Stone, 1991; Stone et al., 1998; Lewis and DiGiacomo- Cohen, 2000). As sea level rose through the Race beginning at ~13.5 ka BP, estuarine sediments were deposited on the lake floor (Stone et al., 1998; Lewis and DiGiacomo- Cohen, 2000). A ravinement surface was created by wave action as sea level rose into the region. The major sea level incursion that occurred at ~10 ka BP was marked by gray marine silts and sands containing abundant oysters (Varekamp et al., 2005; Varekamp and Thomas, 2005; Thomas et al., 2007).

Deglaciation in the Hudson River Valley

The local chronology for sea level change currently available for the Hudson River region is based on studies of cores from the Hudson River Estuary by Weiss (1974).Weiss (1974) used radiocarbon dates along with pollen, and foraminiferal assemblages, to determine that tidal and estuarine conditions reached the lower Hudson River Estuary before 12,000 yrs BP. Estuarine conditions did not developed upstream or the lower Hudson River until ~7,000 yrs BP. Weiss (1974) determined that the maximum incursion of brackish water into the Hudson River Estuary occurred ~6,500 yrs BP.

Deglaciation and Raritan Bay

In contrast to Long Island Sound and the Hudson River Valley, the Raritan Bay was located just south of the ice margin, and therefore may not have experienced a pronounced isostatic depression due to the weight of glacial ice. It has been proposed that the region located beyond the edge of the ice to the south of the ice sheet margin was instead up-warped as a proglacial forebulge (Dillon and Oldale, 1978; Peltier, 1998, Gornitz et al., 2002; Peltier and Fairbanks, 2006; Milne and Mitrovica, 2008; Engelhart et al., 2011a). Such areas including the regions south of the ice margin in present-day Raritan Bay would exhibit evidence of subsidence after deglaciation (i.e., more rapid rates of relative sea level rise than areas that were not previously up- warped; e.g., Peltier, 1998; Engelhart et al., 2011a). In contrast, the regions to the north of the glacial margin that were previously depressed by the glacial ice began to rebound (Dillon and Oldale, 1978; Peltier, 1999, Gornitz et al., 2002). This localized subsidence related to the up-warping of the forebulge was lessened by 5,000 BP (Miller et al., 2009).

Ages obtained from Long Island Sound, the Hudson River Valley and Raritan Bay suggest that relative sea level rise may have occurred later in Raritan Bay than in other regions to the north due to isostatic differences (Peltier et al., 1998; 1999; Miller et al., 2009; Wright et al 2009).

Isostasy and Holocene Sea- level Rise

It has been well documented globally that the eustatic rise reached the present shoreline at ~6,000 yrs BP and continues to rise locally in part due to isostasy associated with the last deglaciation and in part to the present melting of the ice sheets (Fairbanks 1989; Dillon and Oldale, 1978; Peltier, 1999; Gornitz et al., 2002; Peltier and Fairbanks, 2006; Milne and Mitrovica, 2008; Miller et al., 2009; Wright et al., 2009).

Recent studies have shown that the rate of pre- anthropogenic sea level rise for coastal New Jersey (1.8 mm/yr from ~5 ka to 0.5 ka cal. yrs BP) is consistent with that of the coastal regions spanning from southern New England to Delaware (~1.7 to 1.9 mm/yr, from 5,000 to 500 yrs BP) suggesting that the distance from the peripheral bulge has minimal impact after 5000 ka BP for this region (Miller et al., 2009). Furthermore, the rate of relative sea level rise at the New Jersey coast post- industrialization (~3.3 mm/yr) suggests much of the modern-day relative sea level rise (rates above the "background" rate of 1.8 mm/yr) is anthropogenically- driven (Stanley et al., 2004 and references therein; Miller et al., 2009).

More specifically, tidal gauge data for Sandy Hook Bay indicates a relative sea level rise rate of 3.8 mm/yr (Psuty, 1986; Gornitz et al., 2002; Pendleton et al., 2005; Miller et al., 2009). The greater relative sea level rise here (as compared to the aforementioned rates determined for the New Jersey coast; Miller et al., 2009) may be due to compaction of sediment (Psuty, 1986;

Gornitz et al., 2002; Stanley et al., 2004; Pendleton et al., 2005; Miller et al., 2009 and references therein).

Seismic Stratigraphy; Eustatic Cycles

Raritan Bay

The evolution of the Raritan and Sandy Hook Bays will be discussed in the context of seismic stratigraphy and previous seismic stratigraphic interpretations of the region related to the last eustatic cycle (Gaswirth, 1999; Gaswirth et al., 2002). According to Vail and co-workers (1977), a sea-level cycle is an interval of time during which a relative rise and fall of sea level takes place (Vail et al., 1977, part 3; Vail, 1987; Van Wagoner et al., 1987).

The system tracts described in the Raritan and Sandy Hook Bays are associated with a seismic stratigraphic sequence that is initiated with a Type 1 sequence boundary and includes lowstand, transgressive and highstand system tracts. A Type 1 sequence boundary is an erosional or non-depositional surface present between the lowstand and an earlier highstand system tracts (Vail, 1987; Van Wagoner et al., 1987; Gaswirth, 1999; Boggs, 2001).

The system tracts present in the Raritan Bay were interpreted in Gaswirth (1999) from primary reflection surfaces on the seismic profiles that were correlated to a well-documented lithostratigraphy of the region. The system tracts include: 1) a Type 1 sequence boundary which separates the Upper Cretaceous basement sediments from the late Pleistocene lowstand deposits; 2) late Pleistocene lowstand deposits; 3) Holocene transgressive sediments; and 4) Holocene highstand deposits.

A “lowstand system tract” is the lowermost unit in a depositional system, and overlies a Type 1 sequence boundary. Lowstand sediments are deposited at a lowered sea level relative to the paleoshoreline (Vail, 1987; Van Wagoner et al., 1987; Gaswirth, 1999; Boggs, 2001).

In the case of Raritan and Sandy Hook Bays, a Type 1 sequence boundary overlies tilted Cretaceous basement sediment layers, creating a significant unconformity between the Cretaceous and late Pleistocene. The lowstand deposits are associated with paleochannels, which are evident on the seismic reflection profiles of Raritan and Sandy Hook Bays. Fluvial deposits were recovered from the sediment cores where the seismic lines reveal paleochannel surfaces (Gaswirth, 1999).

Transgressive system tracts are associated with a eustatic sea level rise. The sea floods the shelf and marine sediments accumulate above fluvial deposits, which dominated the exposed shelf during a lowstand. However, if sediment supply is limited, incised valleys will not fill with sediments during the transgression of sea level (Vail, 1987; Boggs, 2001). The transgressive sequence is evident in the Raritan Bay where the paleochannels associated with gravels are infilled with finer- grained estuarine sediments (Gaswirth, 1999).

Highstand system tracts are generally composed of three sections, which include early highstand, highstand prograding complex, and late highstand complex. These can be associated with the late period of sea level rise, a sea level standstill, or the early part of sea level fall (Vail, 1987). The highstand deposits in the Raritan Bay are evident above a seismic reflector that marks the incursion of sea level, identified in sediments which penetrate the reflector by mollusk species which typically inhabit the low tide to ~ 9 m marine environment (e.g., *Anomia simplex*, *Anadara transversa*, Rehder, 1992), as well as a shift from silt and clay to medium sand (Gaswirth, 1999) further indicating a change in depositional energy. The late highstand complex

that according to Vail et al. (1987), occurs where sedimentation occurs above sea level is present in Sandy Hook and represented by the Sandy Hook spit (Vail, 1987; Boggs, 2001).

Seismic Facies; Raritan and Sandy Hook Bays

Seismic Reflection Profiles

Seismic reflection profiles were recovered from Raritan and Sandy Hook Bays by the Rutgers University and the New Jersey Geological Survey from the *R/ V James Howard* in 1994 (Fig. 4). The profiles are high- resolution Geopulse™ seismic profiles with approximately 100 m penetration (Gaswirth, 1999).

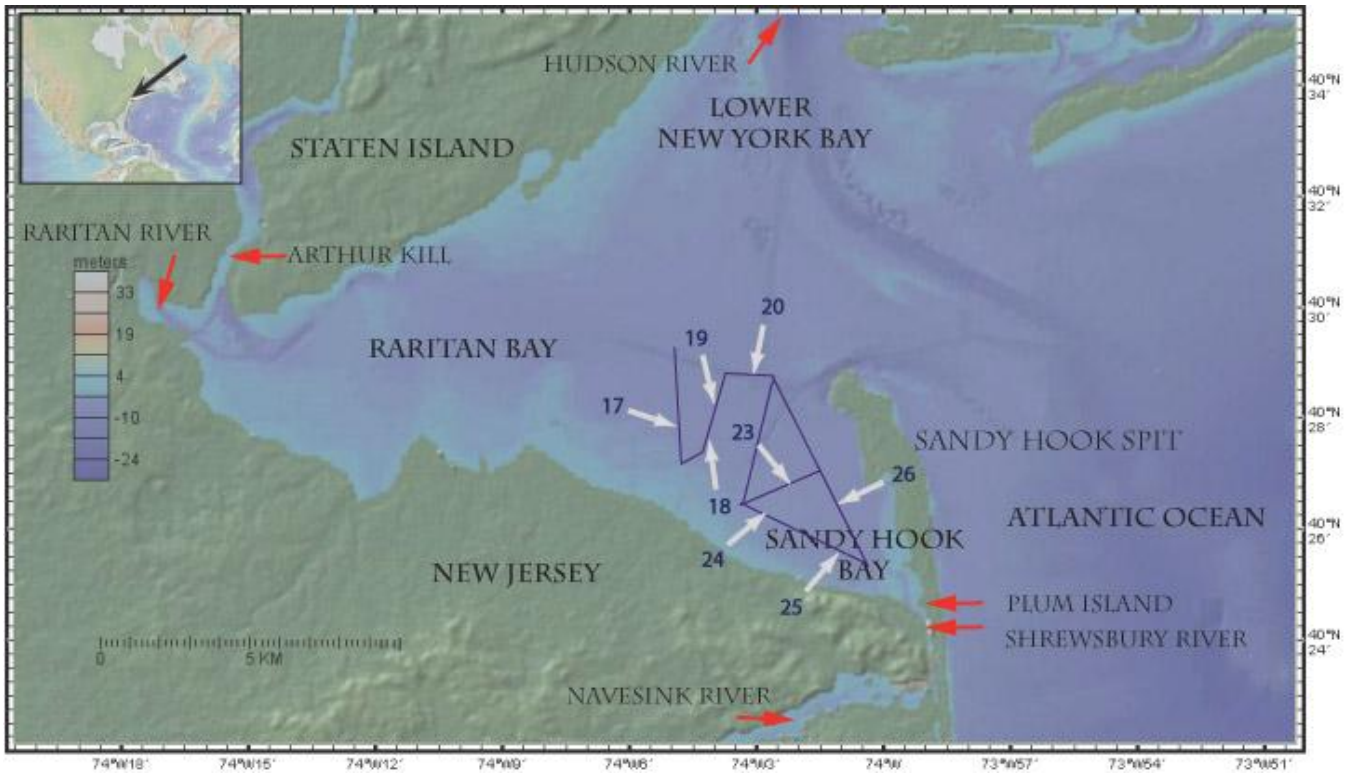

Figure 4: Map of Raritan and Sandy Hook Bays showing location seismic reflection profiles. Blue lines represent locations of seismic reflection profiles Lines 17, 18, 19, 20, 23, 24, 25, and 26, labeled with white arrows. The Sandy Hook Spit separates the bay from the Atlantic Ocean. (Adapted from GeoMapApp©; Gaswirth 1999; Gaswirth et al., 2002).

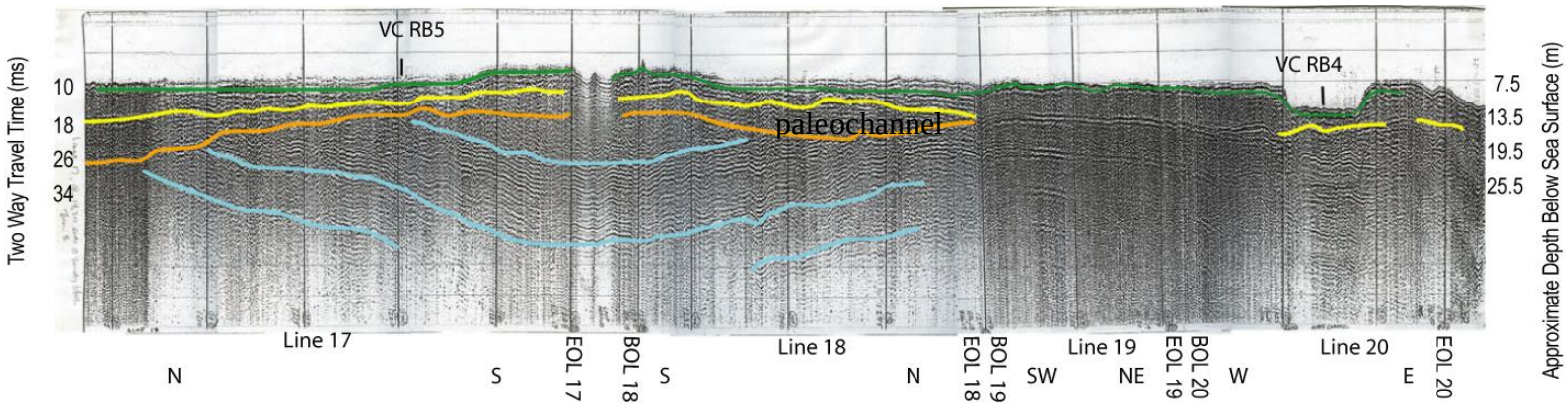

Figure 5: Interpretation of the seismic Lines 17, 18, 19, and 20 (Locations of lines are shown in Fig. 4). Line 17 trends N-S. Line 18 trends S- N. Line 19 trends SW- NE, Line 20 trends W-E. Also shown are the positions of Vibracores RB4 and RB5 along the seismic lines. EOL = end of line, BOL = beginning of line. Seismic reflectors interpreted as Cretaceous layers are traced in blue. Reflectors interpreted as late Pleistocene paleochannels are traced in orange. The reflector interpreted as the initial incursion of seawater is traced in yellow, and the reflector interpreted as the start of highstand deposition is traced in green. It is evident that Holocene deposition is minimal. (Adapted from Sheridan, unpublished, with permission; Gaswirth, 1999).

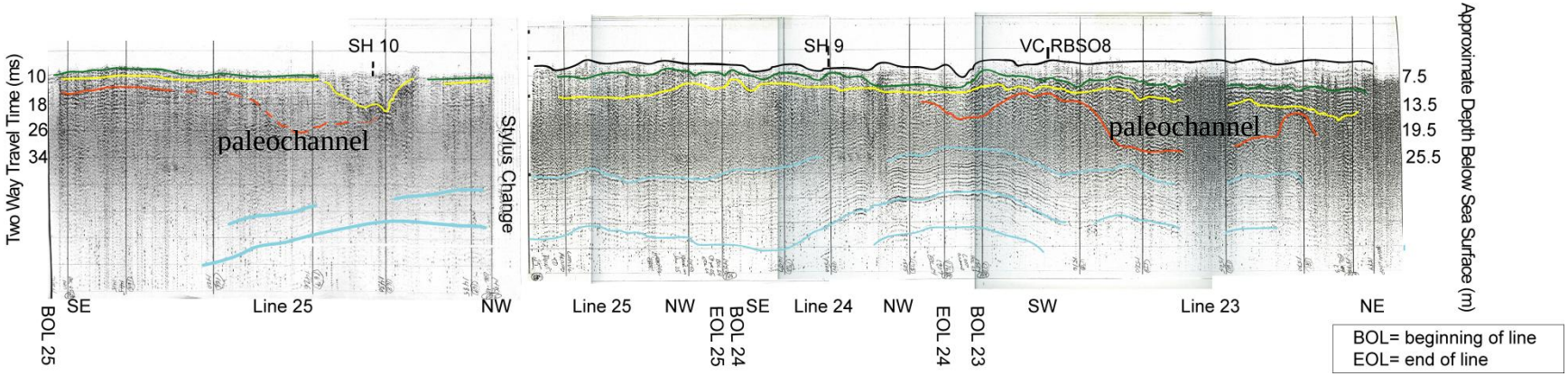

Figure 6: Interpretation of the seismic Lines 23, 24, and 25 (Locations of lines are shown in Fig. 4). Line 25 trends SE –NW. Line 24 trends SE-NW, and Line 23 trends SW- NE. Also shown are the positions of Vibracores SH 9, SH 10, and RB S08 along the seismic lines. Seismic reflectors interpreted as Cretaceous layers are traced in blue. Reflectors interpreted as late Pleistocene paleochannels are traced in orange. The reflector interpreted as the initial incursion of seawater is traced in yellow, and the reflector interpreted as the start of highstand deposition is traced in green (Adapted from Sheridan, unpublished, with permission; Gaswirth, 1999).

The late Pleistocene lowstand is noted by a deep (6-13 m) and wide (~200 m) channel, which incised Upper Cretaceous sediments (Gaswirth, 1999). The seismic reflector that marks the lowstand paleochannel deposits and erosional surfaces has been traced in orange. A second episode of channel incision is related to the initial flooding of the bay during the marine transgression in the early Holocene. This marks the incursion of seawater into the bay. The seismic reflector that denotes the second episode of channel incision has been traced in yellow. These are interpreted as tidal channels. The Late Holocene highstand sediments deposited from the initial transgression to the present are denoted by the seismic reflector traced in green (Gaswirth, 1999; Sheridan, unpublished).

Estuarine Evolution

Within the context of seismic stratigraphy, estuaries evolve when sea level begins to rise as deglaciation occurs and subaerially exposed river channels become tidal channels (Dalrymple, 1992; Gaswirth, 1999; Posamentier, 2001; Nordfjord et al. 2005; 2006). This estuarine evolution can be explained by a generalized seismic stratigraphic model. A fluvial valley is first carved by rivers during a lowstand of sea level. The floor of the river valley will later be marked by an unconformity as river sediments are deposited above the erosional surface. As sea level rises, the river valley is flooded with seawater and estuarine conditions are initiated. Estuarine sediments are deposited on top of the fluvial sediments and estuarine conditions move landward as sea level continues to rise. Holocene estuaries that are sediment starved such as the Hudson River estuary, filled with sediment during the lowstand of sea level and have not formed delta deposits offshore (Dalrymple et al., 1992; Posamentier, 2001; McHugh et al., 2004).

Regions where one period of lowstand to transgressive deposition is preserved are described as an estuary with a simple fill. Those described as a compound fill preserve more than one record of lowstand to transgression (Zaitlin et al., 1994). The Raritan Bay estuary can be described as a simple fill, only having preserved the latest cycle from the lowstand to present-day Holocene high stand of sea level (Goss et al., 1995; Gaswirth, 1999).

The general model for estuarine sedimentation based on physical processes is described in Dalrymple et al. (1992). Tidal and wave dominated estuaries have three separate zones based on the type of energy that dominates the system. The three sections include the marine zone which experiences wave and tide action, a central zone where marine and river energy are balanced resulting in a low energy environment, and a fluvial zone where mainly river processes dominate (Dalrymple et al., 1992). According to this model, the Raritan and Sandy Hook Bays are part of the marine zone.

Global comparisons

The Gulf of Cadiz in Southern Spain has preserved the sedimentary record of its evolution from the late Pleistocene to the Holocene and can be compared to the Raritan- Sandy Hook Bay region. Both estuaries are partially enclosed by spits. In the Gulf of Cadiz region, as in Raritan Bay, fluvial systems formed during the Last Glacial Maximum lowstand evolved into estuarine systems with Holocene eustatic rise (Dabrio et al., 2000). In contrast, the Chesapeake Bay described by Foyle and Oertel (1997), is a complex fill estuary with preservation of multiple Pleistocene sea level cycles in the sedimentary record.

Coastal Processes

Long Shore Currents

Sandy Hook spit has primarily formed as result of coastal processes: longshore currents, tidal currents, and storms. Longshore currents which travel along the New Jersey coast led to the development of the Sandy Hook Spit (Zhang et al., 2002; Gornitz et al., 2002; Hoffman, 2004; Rosati, 2005). Such currents are caused when waves hit the New Jersey coast obliquely, resulting in a current of water, which travels northward, parallel to the shoreline (Hoffman, 2004; Rosati, 2005; Pendleton et al., 2005). Sediments are transported by long shore currents along the coast in a process called littoral drift (Davis, 1983).

Aerial maps and photographs can be used to calculate the movement of sediments along the shoreline, and thus the rate at which sand spit is growing can be determined. Aerial photography and map outlines show past shorelines that are used to determine the changes that have occurred over time to the Sandy Hook Spit (Fig. 7). The northern tip of the spit has curved westward, which commonly occurs on spits due to long shore currents (Easterbrook, 1999). The western, bayside side of the spit has experienced erosion, as evident where past shorelines are situated further into the bay than the present shoreline. In contrast, the eastern side, seaward of the spit appears to be accreting and growing eastward. The sediment supply on the seaward side is due to the longshore current that travels along the Atlantic coast from central New Jersey northward to the Sandy Hook Spit (Ashley et al., 1986). The northern tip of the spit appears to have grown ~1125 meters between years 1836 and 2002, an average rate of 6.8 m per year (Fig. 7). According to Hoffman (2004), the rate of growth of the spit can be determined using the Sandy Hook lighthouse as a marker because the lighthouse was built in 1764, at a distance of

152.4 m (500 ft) from the hooked tip of the spit. In 1864, the lighthouse was ~1207 m (3960 ft), and is presently located ~2414 m (7920 ft) from the tip. The proximity of the lighthouse from the tip of the spit indicates a growth rate of ~9.4 m per year (~31 feet per year).

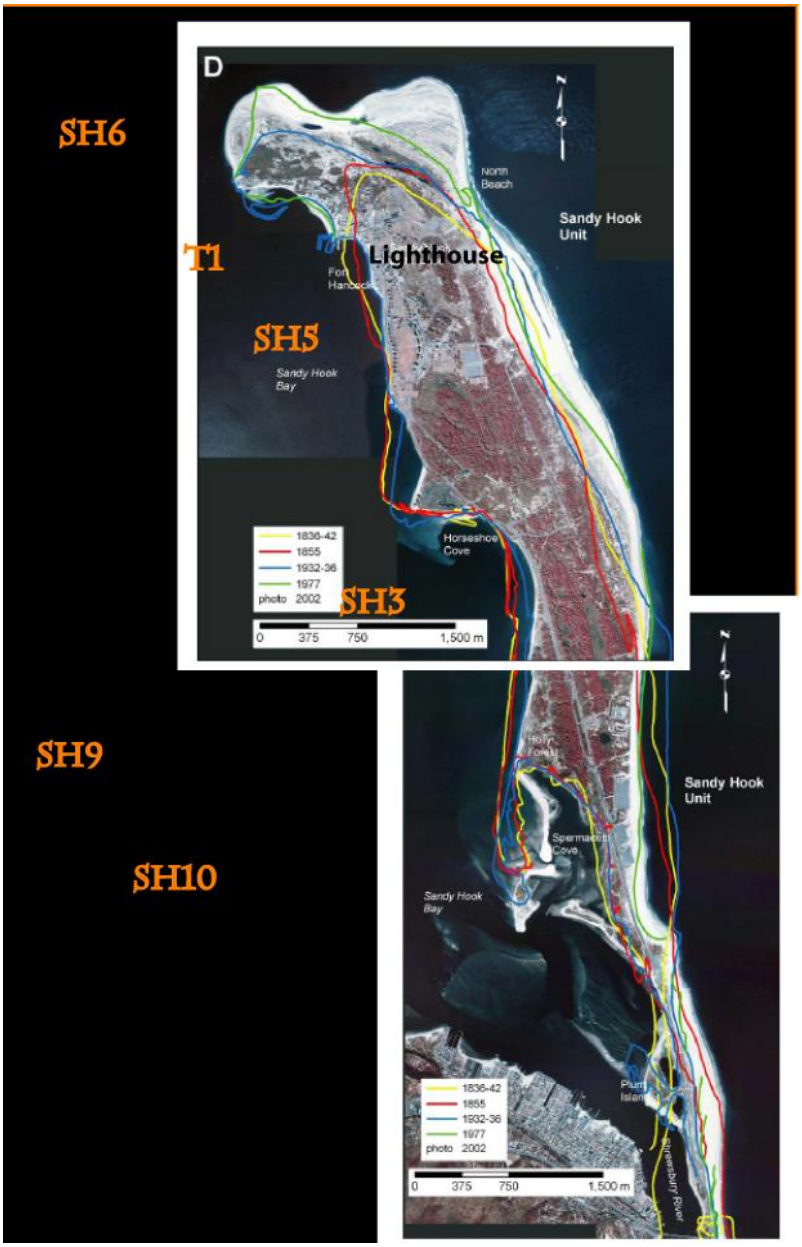

Figure 7: A compilation of aerial photos and historical data of Sandy Hook, New Jersey, modified from Pendleton et al. (2005, with permission). Colored lines represent dates of previous shoreline of the spit. Yellow= 1836- 1842, Red= 1855, Blue= 1932- 1936, Green= 1977, and the photograph represents the year 2002. Orange labels show approximate locations of Sandy Hook Bay cores used in this study (Cores SH 6, T 1, SH 5, SH 3, SH 9, and SH 10). The location of the lighthouse is shown.

Storms

Storms including Northeasters, tropical storms, and hurricanes have struck the east coast North America in the past and continue to affect these coastal regions (Dolan et al., 1988; Smith, 1999; Donnelly et al., 2001a; 2001b; Zhang et al., 2002; Landsea et al., 2003; Dougherty et al., 2004; Buynevich et al., 2004; Hill et al., 2004). Hurricanes hit the Northeast coast infrequently (e.g., 14 hurricanes hit NY- NJ from 1851 to 2006 AD; Blake et al., 2007) with an apparent frequency of impact of ~10 years during the period of 1851 to 1910 (Landsea et al., 2003).

Tropical storms impacted the Northeastern coast more frequently than hurricanes during the same period (Landsea et al., 2003). In contrast, Northeasters are common occurrences in the Northeast region and have been described as responsible for most of the annual storm- related erosion along the U.S. east coast (Zhang et al., 2000; Donnelly et al., 2001a; Dr. Nicholas Coch, person. commun. 2009).

It is important to determine historical effects of storms in the area because of its vulnerability to storm surge, waves, and even sea level rise (Landsea et al., 2003; Pendleton et al., 2005; Gornitz et al., 2002). In the study area, storm effects can be further augmented by the funnel shape of the New York Harbor, which allows water (i.e., storm surge) to build up into the harbor (Gornitz et al., 2002). Damage from storm surge has also increased due to man- made alterations to coastal areas (Coch, 1994).

Coastal Impact

Sediment transport along the shoreline is dominated by on- off shore movement and is accentuated during a storm, rather than the longshore currents which dominate fair- weather conditions. This can cause greater erosion of the shoreline, resulting in loss of property through

flooding, wind damage, and shoreline retreat (e.g., Donnelly et al., 2001; Gornitz et al., 2002; Dougherty et al., 2004).

Storm Effects on Sandy Hook and Raritan Bays

Studies by Donnelly et al. (2001; 2004) and Scillepi and Donnelly (2007) show storms have impacted the New Jersey coast in the past. These studies linked storm deposits from coastal NJ, and Long Island to prehistoric and historically- recorded storms. The documented New Jersey and Long Island washover deposits are characterized by sand layers interbedded with fine-grained mud, peat deposits, with sharp contacts at the lower boundaries of the deposits, and evidence of soft sediment deformation (Donnelly et al., 2001; 2004; Scillepi and Donnelly, 2007). For example, storm deposits from Whale Beach, NJ were dated as 1278- 1438 AD and described as evidence of a prehistoric hurricane (Donnelly et al., 2001b). Deposits from Brigantine, NJ, and Long Island were linked to a 1788 AD hurricane that hit the region (Donnelly et al., 2004; Scillepi and Donnelly, 2007), and deposits from Whale Beach and Brigantine, NJ, and Long Island were linked to an 1821 AD hurricane (Donnelly et al., 2001b; 2004; Scillepi and Donnelly, 2007).

A storm surge gauge at Sandy Hook recorded data from two Northeasters, which occurred January 25-30, 1933, and March 5-10, 1962. The storm in 1933 had a maximum surge of .92 m, and the 1962 storm had a storm surge of 1.3 m (Zhang et al., 2002). Another major storm in December 11- 12, 1992 also impacted the coastal region. The storm coincided with spring tides associated with the full moon, which allowed for great flooding. Tide gauges read 2.4 m above mean sea level (Gornitz et al., 2002 and references therein).

It is also noted that the right angle formed by Long Island and the coast of New Jersey could create a funnel effect, where storm surge would "pile" up in the direction of the New York Harbor. This has the potential to amplify storm surge, increasing the vulnerability of the area to flooding (Gornitz et al., 2002).

Hurricanes rarely hit the coasts of NJ and NY. Northeaster storms occur more frequently in the region and account for most of the annual storm activity responsible for erosion along the U.S. east coast (Zhang et al., 2000). Damage from storm surge has even increased due to man-made alterations to coastal areas (Coch, 1994). In examination of the storm deposits in the sediment cores, it is not known which deposits are related to a hurricane, and which are caused by northeaster storms.

Human Modifications of Coastlines

Human modification of coastlines, such as seawalls or beach nourishment projects, can also have an effect on the vulnerability to erosion (Pendleton, 2005). For example, when a sea wall was built in Sea Bright, along the New Jersey coast, it lessened the northward long shore current, which brings sand to Sandy Hook Spit. This allowed more erosion to occur on the coast of the Sandy Hook Spit, and less accretion to the spit (Gornitz et al, 2002).

Anthropogenic Impact

Sediment Contamination

Estuaries are vulnerable to the accumulation of pollution overtime (Olsen et al., 1978; Williams et al., 1978; Olsen et al., 1984; Renwick and Ashley, 1984; Wolfe et al., 1996; Kennish, 1997; Feng et al., 1998; Cohen et al., 2000; EPA, 2003; Bianchi, 2007). Pollutants

commonly become associated with highly- reactive fine particles (e.g., particles with an ionic charge) including organic material, and layered aluminosilicate clay minerals with high surface areas (Olsen et al., 1984; Lick and Huang, 1993; Stamoulis et al., 1996; Brady and Weil, 2002; Kersten and Smedes, 2002; Bianchi, 2007). Contaminants can also adsorb to coatings (e.g., composed of organic matter or Fe/Mn oxides) on a clay particle (Kersten and Smedes, 2002). Adsorption mainly occurs on the finer- grained fractions because coarse grains are generally composed of quartz or carbonate, which do not readily react with contaminants (Olsen et al., 1984).

Sediment Contamination in Raritan Bay

The mouth of the Raritan River has been described by Renwick and Ashley (1984) as a sediment sink, where contaminated sediments (organic and inorganic particulates) originating from landward sources (e.g., located between Perth Amboy and Bound Brook, NJ) can accumulate within the Raritan Estuary. Other sources of contaminants to the Raritan and Sandy Hook Bays include tributaries to the major waterways, runoff from urban areas, spills, atmospheric fallout, and landfills (Breteler, 1984 and references therein; Renwick and Ashley, 1984; Kennish, 1997 and references therein; Sañudo- Wilhelmy and Gill, 1999; Mecray et al., 1999; Gao et al., 2002; Tovar-Sanchez et al., 2004; Paulson, 2005).

More specifically, industries that may be point sources include organic chemical processing facilities, metal plating, pigment manufacturing, oil refineries, sanitary landfills, and a toxic waste landfill (Renwick and Ashley, 1984, and references therein). Sources might also be located seaward within the Hudson Raritan Estuary (Renwick and Ashley, 1984).

The toxicity of surface sediments (top 2 cm) within the Hudson- Raritan Estuary is variable across the estuary, as determined using different techniques including measurements of survival of organisms during exposure to the sediments collected from different sites in the study area, and analysis for metals (trace and heavy), along with polycyclic aromatic hydrocarbons, pesticides, polychlorinated biphenyls (NOAA, 1995; Wolfe et al., 1996; EPA, 1998, 2003).

Sections of the Hudson- Raritan Estuary were found to be toxic include an area near Throgs Neck, as well as sites in the East River, Kill Van Kull, Arthur Kill, Verrazano Narrows and Sandy Hook Bay based on survival rates of amphipods, bivalve larvae survival and development, and microbial bioluminescence. Sites are characterized as either non-toxic, or significantly toxic as compared to the control sediments in at least one test (NOAA, 1995; Wolfe et al., 1996; US EPA, 1998; 2003).

Water Quality and Health of Fish and Shellfish

The water quality of the Sandy Hook and Raritan Bays contains contaminants, which may affect the health of the ecosystem (e.g., Renwick and Ashley, 1984; Tiedemann, 1997; Cerrato, 2006). For example, the Raritan River water has been found to transport Cd, Co, Cu, Pb, Ni, and Zn in solution, and Al, Fe, and Mn as a solid, which can eventually become deposited in the sediments (Renwick and Ashley, 1984). Sections of the Sandy Hook and Raritan Bays have been described as "special restricted" and/or "prohibited" in regard to shellfish consumption based on bacterial coliform levels detected in the water, related to runoff, combined sewer overflows, and waste water treatment plants. Shellfish harvested from special restricted waterways require treatment prior to consumption, while prohibited waters are not allowed to be harvested for shellfish. Coliform, along with heavy metals and other chemicals, can accumulate

in the tissues of shellfish as they filter feed (NJDEP, 1998; Yuhas, 2002). More specifically, the Middlesex County Utilities Authority is one direct source of contamination to the bays, primarily affecting the western Raritan Bay, classified as a prohibited waterway for shellfish harvesting. This facility is permitted to discharge into the bay, therefore transporting viruses unharmed by chlorination processes used by the facility. In addition, heavy metals are released into the Raritan Bay at higher concentrations than Surface Water Quality Standards (NJDEP, 1998).

Water quality is also affected by influx of excess nutrients and organic matter into Sandy Hook Bay. The decomposition of organic matter and phytoplankton blooms (which spike due to excess nutrients) can lead to low dissolved oxygen, and subsequent fishkills. Major sources of the nutrients to the Sandy Hook Bay include the Raritan River, Hudson River, Arthur Kill and the Middlesex County sewage outfall (Reid et al., 2002, and references therein).

Negative Effects of Pollution on Wildlife

Survival, development, and reproduction of organisms can be adversely affected by contaminated water and sediments (Gochfeld and Burger, 1982; Jones and Lee, 1988; Gottholm et al., 1993 and references therein; NOAA, 1995; Wolfe et al., 1996; Tiedemann, 1997; Botton et al., 1998; NJDEP, 1998; Chang et al., 1998; Itow et al., 1998).Studies of tissue from mollusks which inhabit the study area (e.g., soft clams; *Mya arenaria*, and blue mussels; *Mytilus edulis*) have determined the presence of toxic heavy metals including Pb, Cr, Cu, Hg, Ni, and chemicals including DDT and PCB's (NJDEP, 1998, and references therein). Metals were also present in tissue from birds found within the proximity of the study area, as well as in livers of winter flounder (Gottholm et al., 1993 and references therein; Chang et al., 1998; Cohen et al., 2000).

METHODS

Seismic Facies; Raritan and Sandy Hook Bays

Seismic Reflection Profiles

Seismic reflection profiles described in the Background Section provide a framework for sediment facies analysis and the chronology of the sea level changes associated with the evolution of the Raritan and Sandy Hook Bays since the last glacial to interglacial cycle.

Sediment Cores

Two sets of cores were used for this study. Three long vibracores (3-5 m long; RB-04; RB-05 and RB-S08; Table 1) recovered from the *R/V Atlantic Twin* from Raritan and Sandy Hook Bays in September, 1994. The cores were first described by Gaswirth (1999) and sampled for radiocarbon dating from the archives at the Livingston campus, Rutgers University, NJ. The second set consisted of short vibracores recovered from Sandy Hook Bay onboard the *R/V Lionel Walford* in 1998 and are being curated at Lamont-Doherty Earth Observatory Core Repository (Table 1).

Core ID	Latitude	Longitude	Core Length (cm)	Water Depth (m)
RB 04	40º 28' 17.67" N	74º 02' 11.15" W	370	14
RB 05	40º 27' 28.43" N	74º 04' 15.40" W	520	6.1
RB S08	40º 26' 26.58" N	74º 02' 31.38" W	500	4.6
SH 3	40º 26' 18.6" N	74º 00' 30" W	187.5	6
SH 5	40º 27' 30" N	74º 01' 00" W	165.5	6
SH 6	40º 28' 30" N	74º 1' 48" W	95	9
SH 9	40º 26' .6" N	74º 02' 30" W	215.5	6
SH 10	40º 25' 30" N	74º 01' 30" W	145.5	7
T1	40º 27' 58" N	74º 01' 20" W	138	7

Table 1: Core ID, location, core length, and water depth from which the cores were recovered are shown. Core T1 was retrieved in 1997.

The six short vibracores retrieved from Sandy Hook Bay were sampled every 5 cm to characterize Holocene sedimentation. The sample volume was approximated by taking 2 cm of sediment at each interval, for half the diameter of the core. These cores were retrieved parallel to the Sandy Hook Spit and can be used to interpret the growth of the spit and its effect on sedimentary environments within the bay. Visual description of the archived half of each core included sedimentary structures, grain size changes, whole shells, and shell fragments. Effects of the core retrieval process were noted where sand had washed out (bottom of SH 6), similar to coring effects discussed in Psuty (1986).

Sediment Analyses

Grain Size

Grain size data was determined using wet and dry sieving techniques and the SediGraph 5100. Similar to methods used in McHugh et al. (2010), wet sediment samples were retrieved from the cores at an interval of 5 cm, weighed, and dried overnight in the fume hood. Once dried, samples were reweighed to calculate water content. Each sample was divided into two sections; one to be used for grain size analysis and one to be used in X- Ray fluorescence (XRF) and Loss on Ignition (LOI) analyses.

Dry samples were soaked in distilled water and in a solution of sodium metaphosphate to break up flocs of clay. Sediment samples were wet sieved through 63 micron sieves in order to separate samples into two fractions: coarse (>63 μm) and fine (< 63 μm). The dried fine- grained sediments were weighed, and saved for use in SediGraph analysis. The coarse- grained fraction

(>63 μm) was further analyzed using dry sieving techniques, separated by grain sizes shown in Table 2: (Boggs, 2001)

Sieve Size (diameter in μm)	U.S. Standard Sieve Mesh #	Grain size (phi)	Wentworth size class
63-125	230	4	very fine sand
125-250	120	3	fine sand
250-420	60	2	medium sand
420-1000	40	1.25	coarse sand
>1000	18	0	≥ very coarse sand

Table 2: Sieve sizes used in grain size analysis (dry sieving). Diameter is shown in μm, U.S. Standard Sieve Mesh Number, Grain Size (phi) and the Wentworth size class (Boggs, 2001).

In general, shell fragments were not removed before sieving, and are included as part of the coarse fraction. However, large shells were not sampled from the cores, and hence not included in the sieving process. The abundance of each grain size was derived for each sample as weight percent by dividing the weight of sediment left in each sieve by the total weight of the sample.

The fine- grained sections (<63 μm) were analyzed using a SediGraph 5100 with Mastertech autosampler at Queens College to ultimately determine the weight percentages of both clay, and silt grain sizes in each sample. The main purposes of this procedure were: to 1) correlate and confirm, lithological changes noted in the core descriptions (Camerlenghi et al., 1995; Meyer and Fisher, 1997), 2) link processes (e.g., shifts in transport energy) with temporal variability of silt and clay (Poppe et al., 2000; Cavin et al., 2000) and spatial distribution in the bay, and 3) correlate fine-grained data with metal contaminant variability (Kersten and Smedes, 2002).

Initially, ~2 g of the <63 µm fraction of each sample was used. Samples were soaked overnight in 50-60 ml of sodium metaphosphate solution of 0.5 g/l (Nichole Anest, person. commun., 2008). Sediments were mixed manually prior to loading in Mastertech autosampler in order to break up flocs of clay and analyzed at high resolution, using the sodium metaphosphate solution as the analysis liquid. A baseline of the analysis liquid was run with every new batch of solution and garnet was used periodically as a standard (Nichole Anest, person. commun., 2008; Micromeritics SediGraph 5100 operator's manual). The SediGraph was set to determine cumulative mass finer percent of each grain size (mm) for each sample interval for the following grain size fractions (Table 3):

Wentworth size class	diameter (mm)	diameter (µm)
very fine to fine-grained clay	< 0.001	< 1
medium clay	.001- 0.002	1 - 2
coarse clay	0.002 -0.004	2–4
very fine silt	0.004 - 0.008	4–8
fine silt	0.008 - 0.016	8 - 16
medium silt	0.016 - 0.031	16–31
coarse silt	0.031 - 0.062	31 - 62

Table 3: Grain size intervals measured by the SediGraph, shown in mm and µm (Boggs, 2001; Nichole Anest, person. commun., 2008).

The weight percent data was derived from cumulative mass finer percent values using a spreadsheet modified after a template provided by Rusty Lotti- Bond and Nichole Anest at Lamont- Doherty Earth Observatory, Palisades, NY (person. commun. 2008). The weight percent of the silt and clay fractions was ultimately calculated out of the mass of the total sediment sample (i.e., fine and coarse grains).

Sediment Composition

The description of the sediment components was based on the >63 µm size fraction of the sieved samples using a binocular microscope. The components for which percentages were determined include: quartz, pyrite, iron oxide (present as both small pieces of cement and as coating on smaller grains), shell fragments, and benthic foraminifera. These percentages were graphed by depth to show vertical changes in sediment components of the cores. Additional components noted in the sediments include gypsum, mica, glauconite, and organic material (e.g., periostracum fragments, Rehder, 1992).

Sedimentary Structures

Structures were noted upon visual description of the sediment cores, including soft sediment deformation features such as contorted beds and mud clasts, current-generated structures including micro ripples, and gas voids.

Mollusks and Other Shell Material

The quality of preservation of the shells was used to determine the energy of the environments in which deposition occurred. For example, sediment reworking and storm activity leads to deposition of broken shells, while the presence of well- preserved whole bivalves suggests the shells were buried in situ without reworking (Miall, 1984; 1990; Kovanen and Easterbrook, 2002).

The species of mollusks (Table 4) were used to determine the paleoenvironment, such as water depth and salinity, based on habitat as well as local distribution within the Hudson- Raritan Estuary (Tiedemann, 1997). The shells found in the cores include species of clams (*Mercenaria*

mercenaria), slipper shells (*Crepidula fornicata*), jingle shells (*Anomia simplex*), mussels (*Mytilus edulis*), and razor clams (*Ensis directus*).The presence of these shells was interpreted to mean there were shallow marine environments (Rehder, 1992; Abbott and Morris, 1995).Shells used to date the marine incursion into Raritan Bay included species which live at known salinity and depth ranges and are ideal for tracking sea level changes by marking paleosalinity and depth (e.g., *Anomia simplex, Mulinia lateralis, Anadara transversa*, *Ensis directus*; Figure 8, Table 4).

Mollusk Species	Common Name	Water Depth (m)	Salinity Range
Mercenaria mercenaria	Northern Quahog	intertidal flats to 15 m	Higher salinities, lower HR Estuary
Anomia simplex	Common Jingle Shell	low- tide line to 9 m	
Crepidula fornicata	Atlantic Slipper Shell	intertidal to 15 m	lower reaches of HR Estuary
Mulinia lateralis	Dwarf Surf Clam	0.6 - 55 m deep	bays, lagoons, by creeks
Geukensia demissa	Atlantic Ribbed Mussel	intertidal	salt marshes, in mud flats, lower reaches of HR Estuary
Mytilus edulis	Blue Mussel	near low- tide line	Slightly brackish, lower reaches of HR Estuary, rocky places
Anadara transversa	Transverse Ark	tidal to 9 m	ocean; algae beds in bays
Ensis directus	Atlantic Jackknife Clam	in sand, intertidal	estuaries

Table 4: Mollusk species discussed in this study. HR= Hudson- Raritan (Maurer et al., 1974; Rehder, 1992; Abbott and Morris, 1995; Tiedemann, 1997).

Figure 8: Photographs of select shells and shell fragments retrieved from the sediment cores.

Physical Properties

Physical properties including bulk density, and magnetic susceptibility were measured at an interval of 1 cm after the retrieval of the sediment cores from the bay using a GEOTEK Multi Sensor Core Logger at the Lamont- Doherty Core Laboratory (Losefski, person. commun. 2008). Physical property data is available for cores SH 3, SH 6, SH 9, SH 10, all representatives of the different depositional environments found within the bay. Physical properties were graphed by depth to show variations over time, and data were incorporated into multiple regressions as predictor variables for metal concentrations in the sediments.

Loss on Ignition

Loss on ignition was conducted at Lehman College. The dried sediment samples were grounded with mortar and pestle, and separated into three sections with approximate mass of 1 g each. An interval of 5 cm was used. Each sample was weighed and put in a drying oven for one hour at 100° C to ensure the analysis is conducted with completely dried sediments. Samples were then placed in a muffle furnace to burn for 5 hours at 550° C. After the organic matter burned off, the samples were reweighed. The percent of organic matter present in each sample was calculated using the following formula, using a spreadsheet provided by Dr. Hari Pant (person. commun. 2008): % Organic Matter = (loss in sample weight after 5 hours/ mass of initial sediment sample) x 100.

Subsequently, the percent of total organic carbon was derived from the percent organic matter results using the following formula: % Organic Carbon= 0.58 x (OM x 0.8 – 0.23) (Cohen et al., 2000 and references therein). This formula was chosen because it was used in a previous study performed proximal to this study area (Cohen et al., 2000). The correction factor applied to

the formula (i.e., OM x 0.8 - 0.23) was derived from regression analysis using Loss on Ignition data from soils in Pennsylvania (A. Wolf, person. commun., 2012). Results from each of the three trials run for each sample were averaged and graphed to show trends over time in the sediment cores (Veres, 2002; Hari Pant, person. commun., 2008).

Storm Deposits

Deposits were identified at depths in the Sandy Hook Bay sediment cores that exhibited abrupt changes from low energy muds, or sands, to higher energy deposits composed of larger clasts, with inclusions of mud clasts, pebbles, and broken shells. Sharp angular contacts were also present. As discussed in Miall (1984; 1990), the depositional energy of clastic sediments can be interpreted using grain size because larger grains (i.e. sand, pebbles) need higher energy mode of transport than finer grains (i.e. clay). Furthermore, the presence of bioclastic debris (i.e. broken shells) and concentrations of pebbles can indicate the possibility of storm activity (Miall, 1990).

Approximate dates associated with these deposits were determined from radiocarbon ages derived from mollusk shells below each deposit. Results were compared with previous studies of historical storms known to have affected the Northeastern coast, as well as prehistoric storms documented in sediment deposits in nearby study areas.

Chronology

The chronology was based on radiocarbon dates from mollusks and woody material retrieved from the cores as well as short-lived radioisotopes measured in the sediments (Figs. 8, 9). Radiocarbon dates were used to determine the timing of the sea level rise into the Raritan and

Sandy Hook Bay region as well as to date storm deposits in order to link results with historical and pre- historical storm events. Short- lived radioisotopes were used along with metal contaminant data in order to study of the contaminant history of the bays.

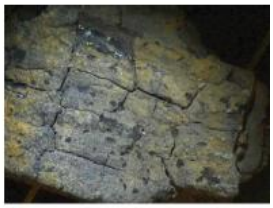

Wood Fragment

Figure 9: Photograph of a select wood fragment retrieved from the sediments.

Radiocarbon Chronology

Radiocarbon dating was conducted by The National Oceanic Sciences Accelerator Mass Spectrometry Facility (NOSAMS) at Woods Hole Oceanographic Institution, in Woods Hole, MA. Radiocarbon ages were calibrated using Calib 6.0 (Stuiver et al., 2005; Hughen et al. 2009, Reimer et al. 2009), CALIBomb (ages younger than 550 ^{14}C yr BP; Stuvier et al., 2005), and CalPal-2007online (ages younger than 550 ^{14}C yr BP; Danzeglocke et al., accessed 2010). The Marine09.14c calibration dataset for marine shells (which uses the 400 yr reservoir correction) and the calibration Intcal09.14c dataset for woody material (Stuiver et al., 2005; Miller et al., 2009 and references therein) were used in the calibration process. The local marine reservoir correction for Shark River, New Jersey of ΔR 130 (ΔR 60 error) was applied to resolve the deviation from the standard 400 yr correction due to local factors (Stuiver et al., 2005; McNeely et al., 2006). Shark River is the closest location to the Sandy Hook Bay for which a ΔR value is available (Stuiver et al., 2005; Calib Marine Reservoir Correction Database).

Shells and woody pieces retrieved from the cores for radiocarbon dating were chosen based on the quality of preservation, at depths based on facies classification (of shorter vibracores; SH 6, T 1, SH 5, SH 3, SH 9, SH 10; Table 1), and approximated depths of the seismic reflectors previously interpreted in Gaswirth (1999) and Sheridan (unpublished) to be the incursion of sea level since the retreat of the LGM (longer vibracores; RB 4, RB 5, RB SO8; Table 1).Shells that were whole and showed little evidence of weathering and transport were preferred in the dating process to minimize possibility of using fossil shells of much older age than the surrounding sediments (Miall, 1990; Rick et al., 2005). Furthermore, multiple shells were dated from the same depths wherever possible to confirm ages and attain accurate results (Rick et al., 2005).Shells were cut along multiple growth lines to incorporate an average age for the shell, a procedure discussed in previous studies (e.g., Rick et al., 2005).

Short-lived Radioisotope Chronology

Sediments were initially sampled from the cores at 10 cm intervals from 0 to 30 cm and analyzed for short- lived radioisotopes (i.e., ^{137}Cs; half-life of 30 yrs; Valette-Silver, 1993). If short-lived radioisotopes were detected, the cores were then sampled every 5 cm for better precision. Wet sediments were weighed and dried for one week. Dried samples were weighed, shells were removed, and sediments were ground with mortar and pestle and canned. Samples were analyzed by gamma counting at the Lamont- Doherty Earth Observatory.

After graphing the results with depth, the following dates were assigned to the sediment cores: The first appearance of ^{137}Cs, from the deepest part of the cores upwards, was assigned the calendar year 1954, related to the beginning of global nuclear testing. The first peak in concentration was assigned the calendar year 1963, related to a peak in global fallout (Olsen et

al., 1978; Williams et al., 1978; Olsen et al., 1981; Bopp et al., 1982; Olsen et al., 1984- 1985; Bopp and Simpson, 1989; Bopp et al., 1991).

Analysis of Metals

X-Ray Fluorescence (XRF)

The spatial distribution of contaminants among the different depositional environments related to the Sandy Hook Spit in the bay was examined along with temporal changes in the sediments in order to characterize the effects various physical processes (e.g., mass-wasting events, growth of the sand spit) might have on the accumulation of metal contaminants. Approximations of possible locations of contaminant sources, as well as changes in input over time were also inferred from the spatial and temporal variability of the metals.

The metal concentrations in the sediments were determined using a handheld X-Ray fluorescence spectrometer (Innov-X Systems Alpha Series™ X-Ray Fluorescence Spectrometer; Queens College, NY) at an interval of every 5 cm, and subsequently every 2 cm for enhanced resolution. Standardization was achieved by pointing the XRF at a metal alloy disk. The resulting spectrum of this procedure was automatically compared with the known results by the XRF software. XRF output data was verified using Standard Reference Materials manufactured by the National Institute of Standards and Technology (NIST), for which concentrations of different elements have already been determined from several analysis methods, including ICP-MS, ICP, ID TIMS, and AAS (NIST Certificate of Analyses for SRM 2702, 2709, 2710, 2711, and 2781; Kenna et al., 2011). For example, the known values of lead concentrations for SRM 2709, 2710,

and 2711 vs. the concentrations measured with the XRF resulted in a linear relationship with R^2=0.999 (Fig. 10).

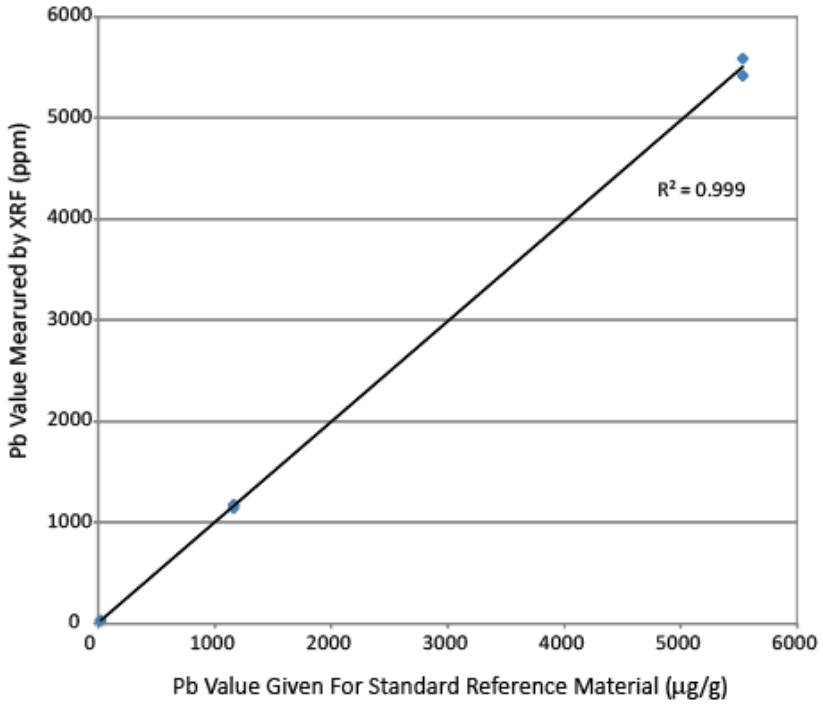

Figure 10: The linear correlation (R^2=0.999) of lead concentrations for known values for Standard Reference Materials 2709, 2710, 2711 vs. results measured by the XRF. Plotted with SPSS, 16.0 (Microsoft, 2007)

Resolution

The 5 cm analysis was conducted using the XRF mounted in the stand in the laboratory at Queens College on all of the sediment samples that were previously dried and archived in clear plastic bags. The purpose was to determine variability of metal concentration in all of the Sandy Hook Bay sediment cores, as well as to constrain background levels characterized by minimal metal concentrations present in deeper sediments. Four different NIST (National Institute of Standards and Technology) standard reference materials including a blank (SiO_2), SRM 2709 (San Joaquin soil), SRM 2711 (Montana II soil), and SRM 2710 (Montana I soil) were used to test the performance of the XRF (Stallard et al., 1995; Gill, 1997; Soil Appendix, Innov-X User

Manual Version 2.2, 2006; Kenna et al., 2011). Each sample was analyzed for 60 seconds, with the XRF set to "soil mode." Output data included concentrations of elements in parts per million (ppm).

The higher resolution analysis (2 cm) was performed with the handheld XRF at the Core Repository Laboratory at the Lamont- Doherty Earth Observatory. The upper sections of the wet sediment cores were used, for depths where metal concentrations were previously detected above background levels (determined from 5 cm resolution results). In order to maintain contact between the XRF equipment and the cores, clear plastic wrap was used to prevent damage and contamination of the analyzer. NIST standard reference materials used include a blank (SiO_2), NIST 2702 (inorganics in marine sediment), and NIST 2781 (domestic sludge).

RESULTS

The main goals of this study were to: 1) determine the timing of when relative sea level reached the present- day Raritan and Sandy Hook Bays and how it relates to relative sea level rise in nearby regions and globally, 2) classify the sediment facies, 3) relate storm deposits to historical storms and previous studies along the northeastern coast of the United States, 4) decipher the anthropogenic history of metal contamination in the Sandy Hook Bay, and 5) determine how sediment composition (i.e., grain size variability, total organic carbon) may have affected the accumulation of metal contaminants in different depositional environments within an urban bay The following is a compilation of the results used to answer these questions.

Sediment Analysis

The six sediment cores retrieved from Sandy Hook Bay represent varying depositional environments. These include: 1) protected areas behind the spit dominated by low-energy deposition of mud, 2) areas with punctuated high-energy deposition manifested by larger grains (e.g. sand and gravel) and shell fragments such as those near the end of the spit and proximal to the Sandy Hook Channel, and 3) offshore from the Sandy Hook Bay beaches (Table 5; Figs. 11-13). Core SH 6 was retrieved from the bay 1 km west of the northwestern end of the spit and proximal to Sandy Hook channel. Core T 1 was retrieved 0.4 km west of the spit; Core SH 5 was retrieved 1 km west of the spit on the bayward side. Core SH 3 was retrieved 1.2 km west of the spit and 3.5 km northwest of the mouth of the Shrewsbury River; Core SH 9 was retrieved 1.5 km north of the beaches. Core SH 10 was retrieved 1 km north of beaches and 3 km northwest of the river mouth

The sediment variability was analyzed to define the facies, which are described in the Discussion section, based on the following: 1) grain size; 2) sedimentary structures; 3) components (minerals such as iron oxide and pyrite and accessories such as woody material and shells); 4) total organic carbon (TOC); and 5) physical properties (magnetic susceptibility, bulk density). The sedimentary facies were defined based on an age model constructed from radiocarbon derived from mollusk shells, and from short-lived radioisotopes (i.e., ^{137}Cs).

	Tip of the Spit		Backbarrier		Offshore from Beaches	
Core ID	**SH 6**	**T1**	**SH 5**	**SH 3**	**SH 9**	**SH 10**
Latitude	40° 28' 30" N	40° 27' 58" N	40° 27' 30" N	40° 26' 18.6" N	40° 26' .6" N	40° 25' 30" N
Longitude	74° 1' 48" W	74° 01' 20" W	74° 01' 00" W	74° 00' 30" W	74° 02' 30" W	74° 01' 30" W
Core Length	95 cm	138 cm	165.5 cm	187.5 cm	215.5 cm	145.5 cm
Water Depth	9 m	7 m	6 m	6 m	6 m	7 m

Table 5: The Sandy Hook Bay sediment cores are listed with their interpreted depositional environments, latitude, longitude, core length, and water depths. See Figures 11- 13 for locations of the cores, lithology, and photographs, according to depositional environment.

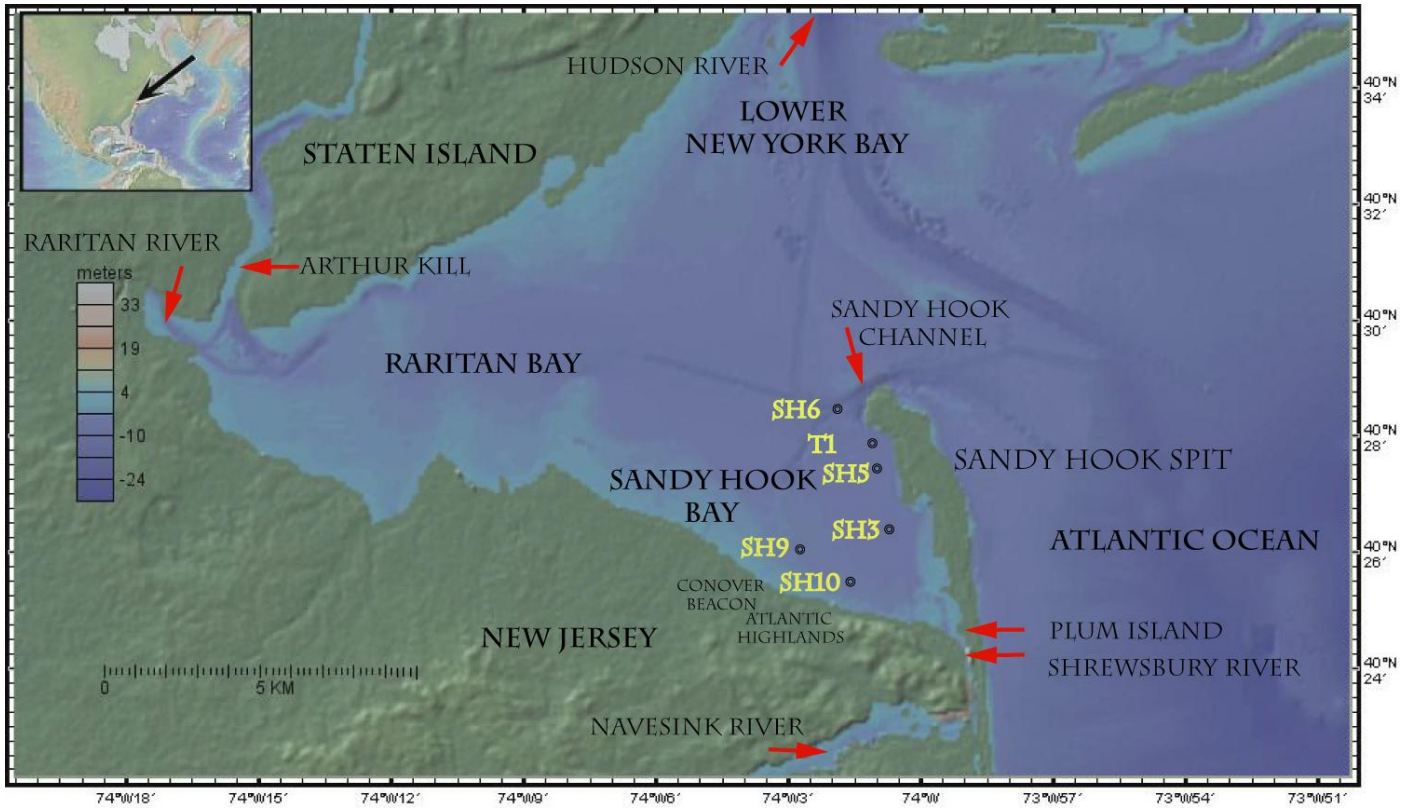

Figure 11: Map of Raritan and Sandy Hook Bays showing location of cores: SH 6, T 1, SH 5, SH 3, SH 9, and SH 10. The Sandy Hook Spit separates Sandy Hook Bay from the Atlantic Ocean. The locations of the Navesink River, Shrewsbury River, Arthur Kill, Hudson River, Sandy Hook Channel, Raritan River, the borough of Atlantic Highlands, and Conover Beacon are indicated on the map. Plum Island was deposited during a storm washover event (USGS, 2003) (Adapted from GeoMapApp©).

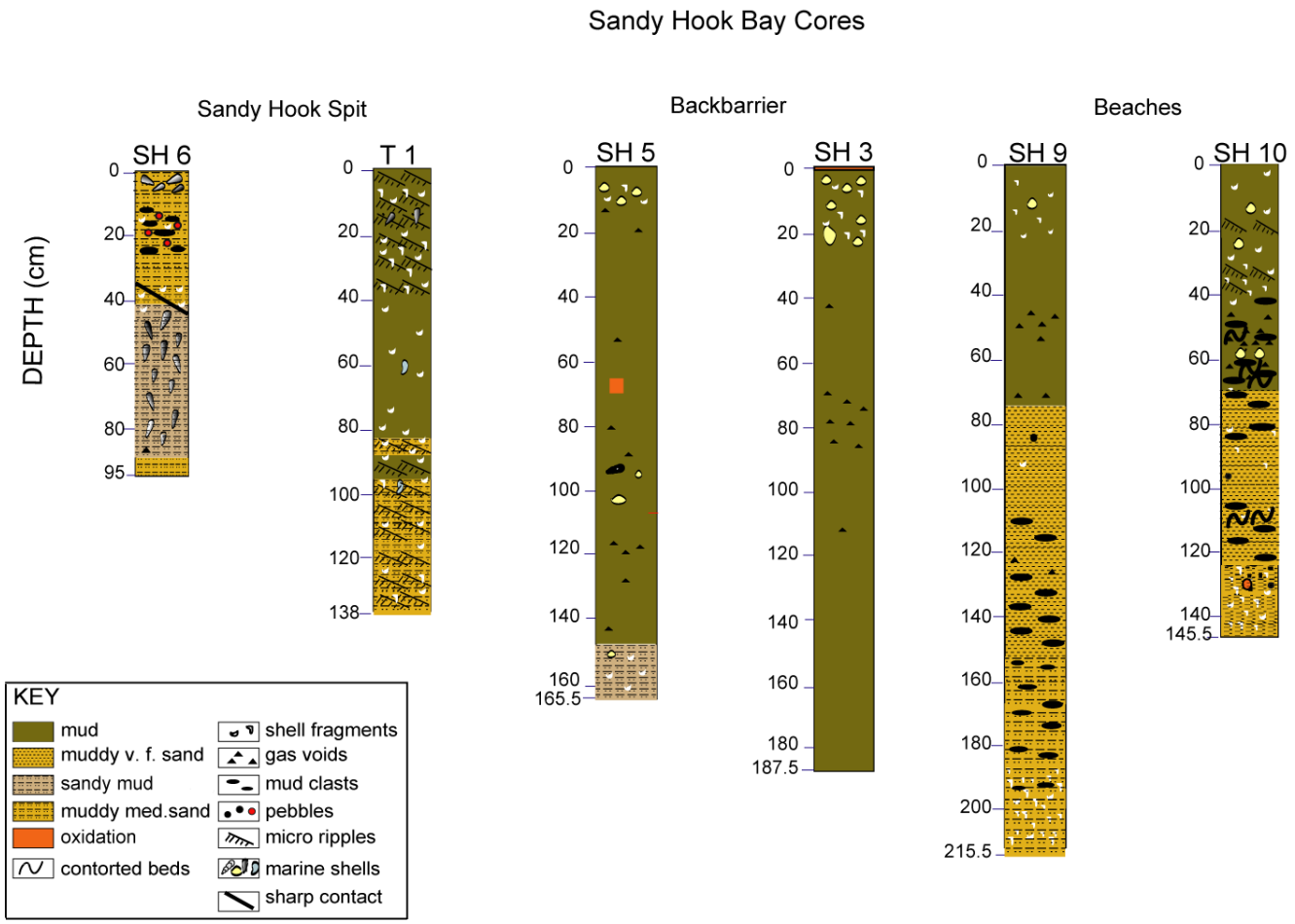

Figure 12: Lithological interpretation of cores used to define depositional environments (Table 5). Sediments range in grain size from mud to muddy very fine sand, muddy medium sand, and sandy mud. Oxidized sediment layers are marked in orange. Contorted beds are marked by a curved black line. Gas voids (black triangle), mud clasts (black oval), pebbles (circle), micro ripples, shell fragments, and marine shells are noted on the diagram. Grain size fines upwards across the bay. Mud clasts and shells are found within a muddy sandy matrix.

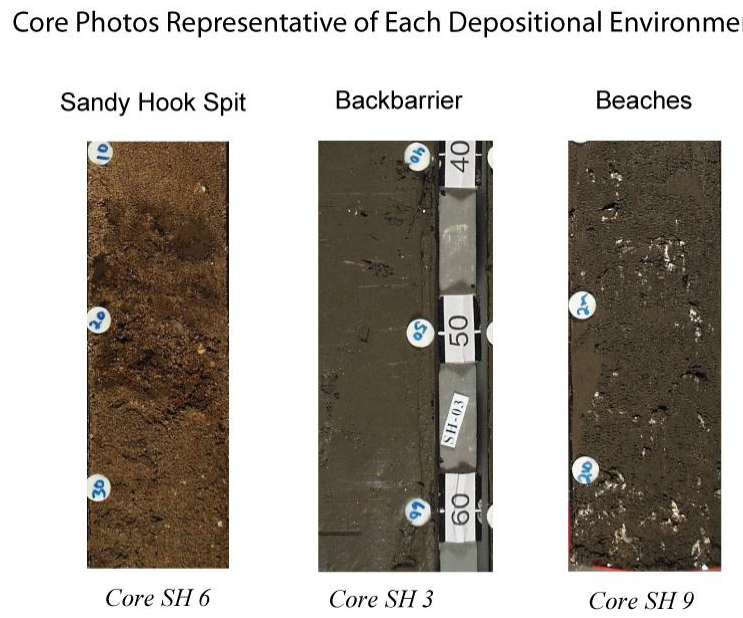

Figure 13: Core photos representative of each depositional environment; the spit (i.e., Core SH 6), behind the barrier (i.e., Core SH 3), and 1.5 km offshore from the beaches (i.e., Core SH 9). The end of the spit is a higher energy regime associated with the Atlantic Ocean, tides, waves, storms, and longshore current. This leads to deposition of coarser- grained sediments (i.e., gravel beds, sands). Behind the barrier, low energy leads to accumulation of finer-grained silts and clays. The sediment near the beaches fines upwards from muddy very fine to medium sand, to silt and includes whole shells and shell fragments, due to higher energy conditions as well as fluctuations in energy levels from waves, storms, and river discharge.

Deposits of Mass-Wasting and Sediment Reworking

Six deposits interpreted as mass-wasting and sediment reworking were characterized in the cores from their sedimentary structures such as contorted beds and mud clasts, coarser grain size of pebbles or sand, sharp upper and lower contacts, and broken shell fragments. Below is a description of each of the following deposits; Deposits SH10-3 (122- 145.5 cm), SH9-2 (195-215.5 cm), SH9-1 (110-195 cm), SH10-2 (102-122 cm), SH6-1 (10- 42 cm), and SH10-1 (40-84 cm) (Fig. 14).

Deposit SH10-3 is ~23 cm thick and characterized by muddy medium sand, shell fragments, pebbles and a rock fragment (7 cm) of redbed sandstone (Figure 15). Its upper boundary is marked by an abrupt change to muddy very fine sand with mud clasts.

Deposit SH9-2 is ~20 cm thick and characterized by muddy medium sand with sub-rounded quartz pebbles, abundant shell fragments and whole shells including an intertidal estuarine mollusk (*Anomia simplex*).The upper boundary of the deposit is marked by a change in lithology from muddy medium sand with abundant shell fragments to sand without shell fragments.

Deposit SH9-1, ~85 cm thick, is composed of muddy medium sand containing floating mud clasts, a fish tooth, pebbles and shallow water marine shells such as razor clams (*Ensis directus)*. The upper boundary grades upward from muddy medium sand to muddy very fine sand.

Deposit SH10-2, ~20 cm thick, is composed of muddy very fine sand, with contorted beds and floating mud clasts, shell fragments, and pebbles. The lower boundary is marked by an erosional surface, which separates two mass-wasting events. The upper boundary is gradational and noted by an absence of mud clasts.

Deposit SH6-1 is ~32 cm thick and composed of muddy medium sand with mud clasts, shell fragments, quartz pebbles and iron oxide cement fragments. A sharp, angular dipping contact marks the lower boundary of this deposit. The upper boundary is marked by a repopulation of the seafloor by a mussel community.

Deposit SH10-1, ~44 cm thick is characterized by mud with abundant gas voids and contorted floating mud clasts, overlying (with a gradational contact) muddy very fine sand. Its upper boundary grades to mud.

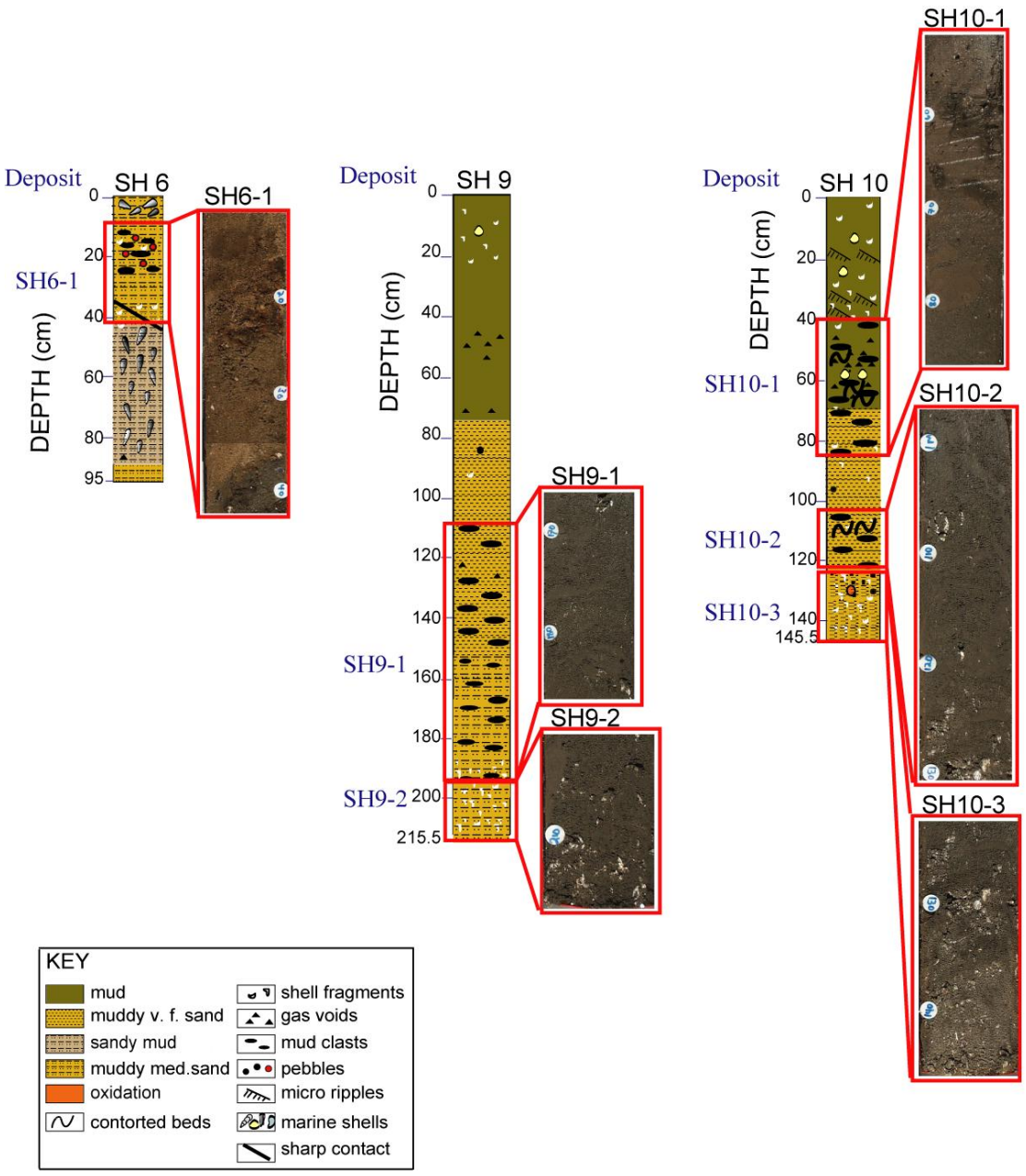

Figure 14: Lithology and photographs of sediment cores with mass-wasting deposits, including Deposits SH10-1, SH10-2, SH10-3, SH9-1, SH9-2, and SH6-1, each outlined in red.

Figure 15: Red sandstone fragment, 7 cm diameter, found in Core SH 10 (at 125-130 cm).

Grain Size

Grain size analyses show temporal and spatial variability: 1) there is spatial variability from a dominance of sand at the tip of the spit, to silt in the backbarrier, to a significant shift from sand to silt upwards in sediments offshore from the beaches (Fig. 16), and 2) temporal variability shows fining upwards with the deepest sediments composed of coarser grain sizes than the overlying sediments (e.g., Cores SH 5, SH 10; Figs. 18, 20) indicating changes in depositional energy over time for the bay as a whole.

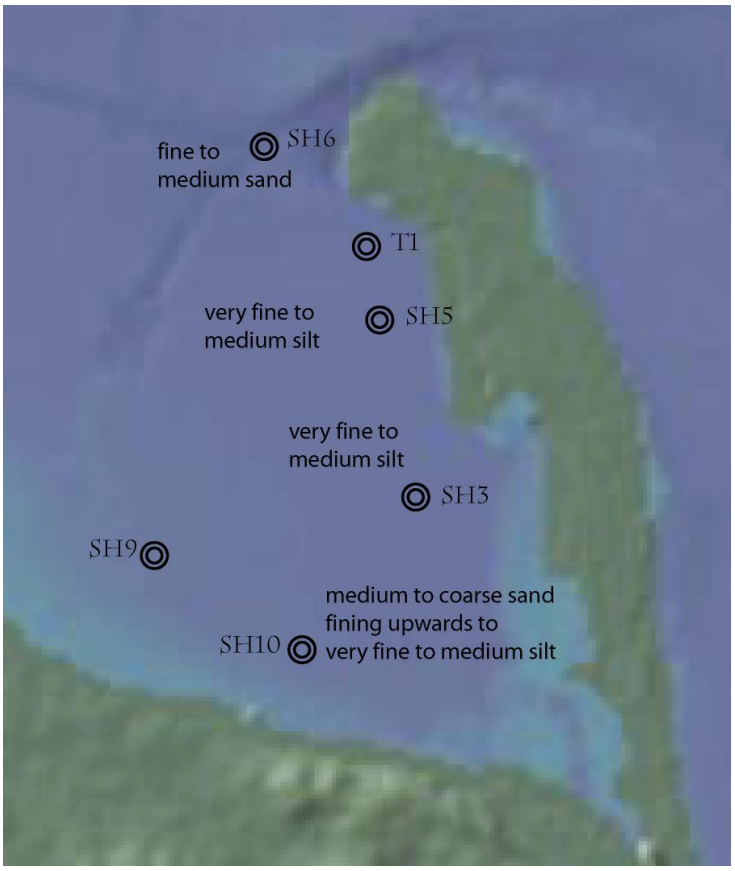

Figure 16: Dominant grain size for each depositional environment (based on weight percent, Figs. 17-20). From north to south along the bayside of the spit, sediments shift from sand at the tip of the spit (i.e., Core SH 6), to silt in the backbarrier (i.e., Cores SH 5, 3). The sediments offshore from the beaches (i.e., Core SH 10) are predominantly sand in the older sediments, with a shift to greater silt composition upwards.

Results indicate that the spatial variability of the fine and coarse- grained sediments is dependent upon the depositional environment (Figs. 16- 20; Table 5 for depositional environments).

Sandy Hook Spit: These sediments are characterized from the base upwards by muddy fine to medium sand (i.e., Core SH 6; Figure 12). Gravel beds are also present (Core SH 6; at 15 - 25 cm; Figs. 12, 14). The fine- grained fraction of silt and clay (< 1%) is limited to undisturbed

sediment, indicated by layers of whole, well-preserved mollusk shells, the lack of ripple marks or broken shell fragments (i.e., Core SH 6; 50- 80 cm; Figs. 12, 17).

Backbarrier: Sediments are relatively homogeneous throughout the core, indicating little variation in depositional energy over time. Clayey silt coincides with a low energy regime protected from the ocean waves (Figs. 18, 19). Sediments also contain shell fragment and shells, and a slight increase in sand, near the core tops (i.e. Cores SH 3, SH 5; 0- 20 cm depth; Figure 12).

Beaches: The sediments fine upwards from medium to coarse sand, to sandy silt (Cores SH 9, SH 10; Fig. 12). Shell fragments are also present (Core SH 9, 195-215.5 cm; Core SH 10, 0-40 cm, 125-145.5 cm; Figure 12). The overall depositional pattern of fining upwards is evident in both cores recovered from this setting (Fig. 20).

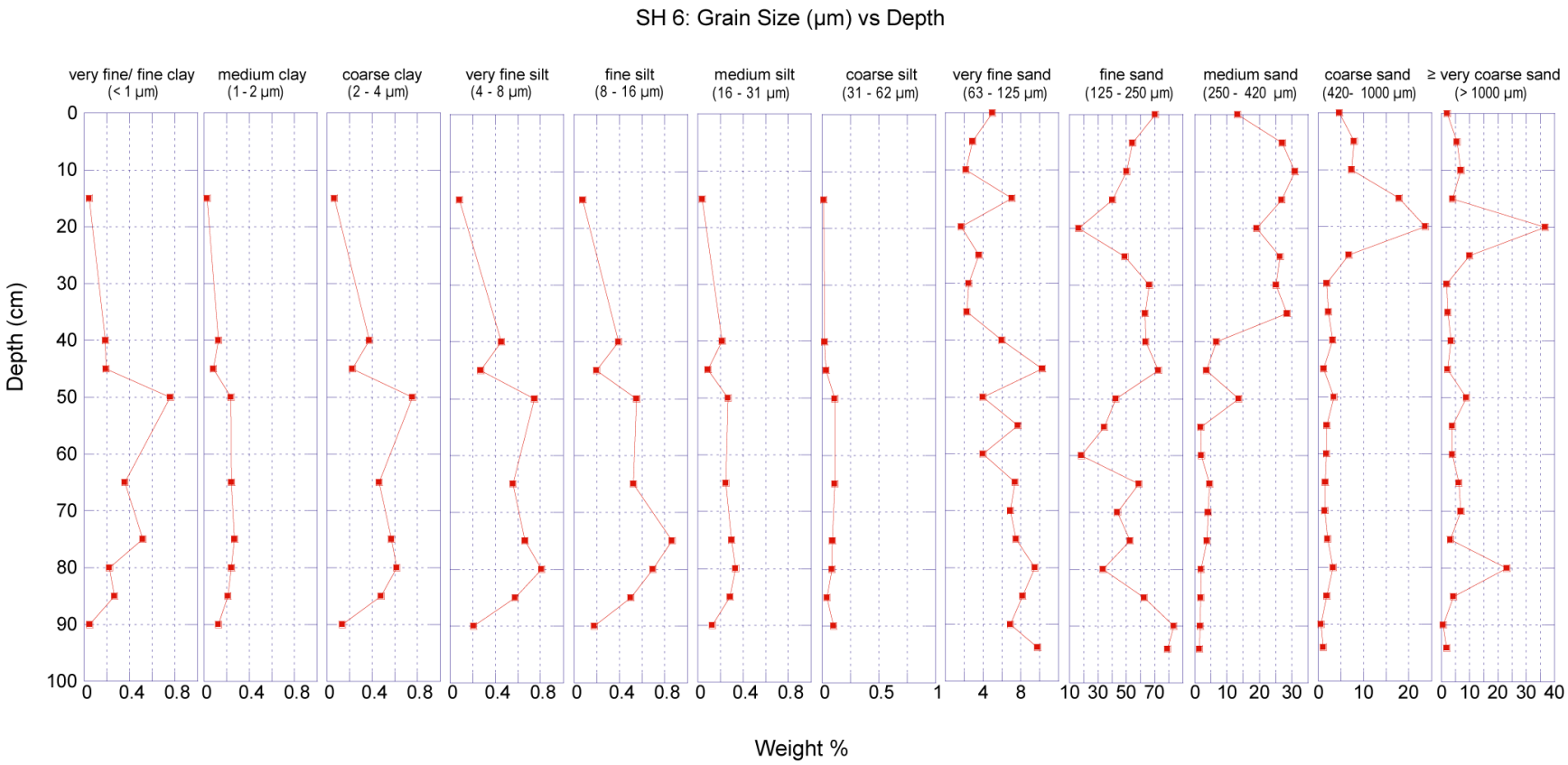

Figure 17: Grain size (weight %) versus depth (cm) results for core SH 6. Fine- grained sediments (< 63 µm) were scarce at the top of the core. The core is dominantly composed of fine sand (125- 250 µm), and coarsens from 5- 35 cm to medium sand (250- 420 µm). There is a punctuated increase in coarse and very coarse sand at 20 cm related to a thin layer of pebbles.

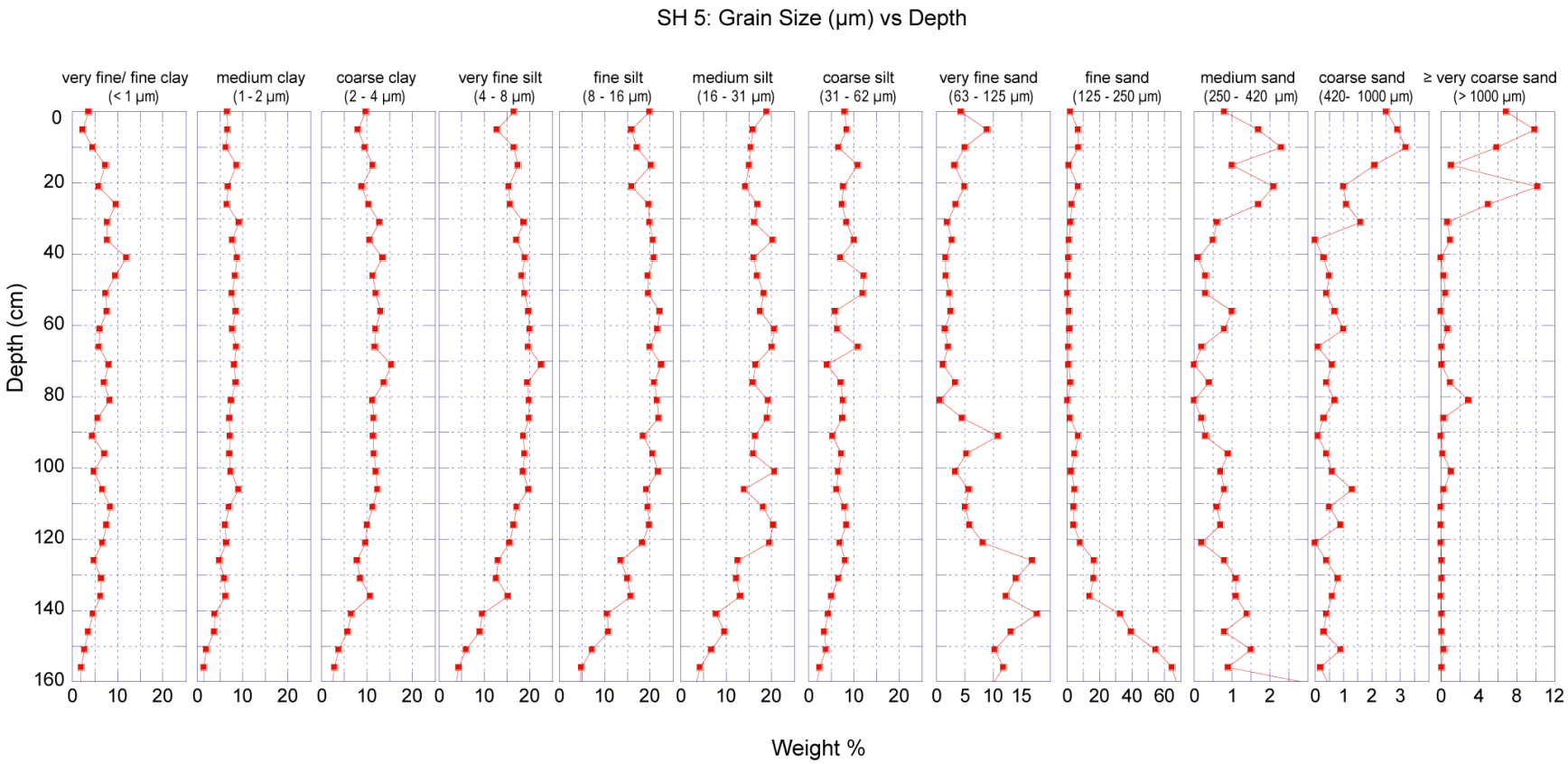

Figure 18: Grain size (weight %) versus depth (cm) results for core SH 5. Results show that this location is dominated by very fine, fine, and medium silt (i.e., range of 4- 31 µm). The deeper sediments (i.e., 120 – 165.5 cm) have a greater coarse- grained content (i.e., very fine and fine sand; 63- 250 µm) than overlying sediments. Coarsening upwards from 30 cm to the top of the core is coincident with an increase in shell fragments (Fig. 12).

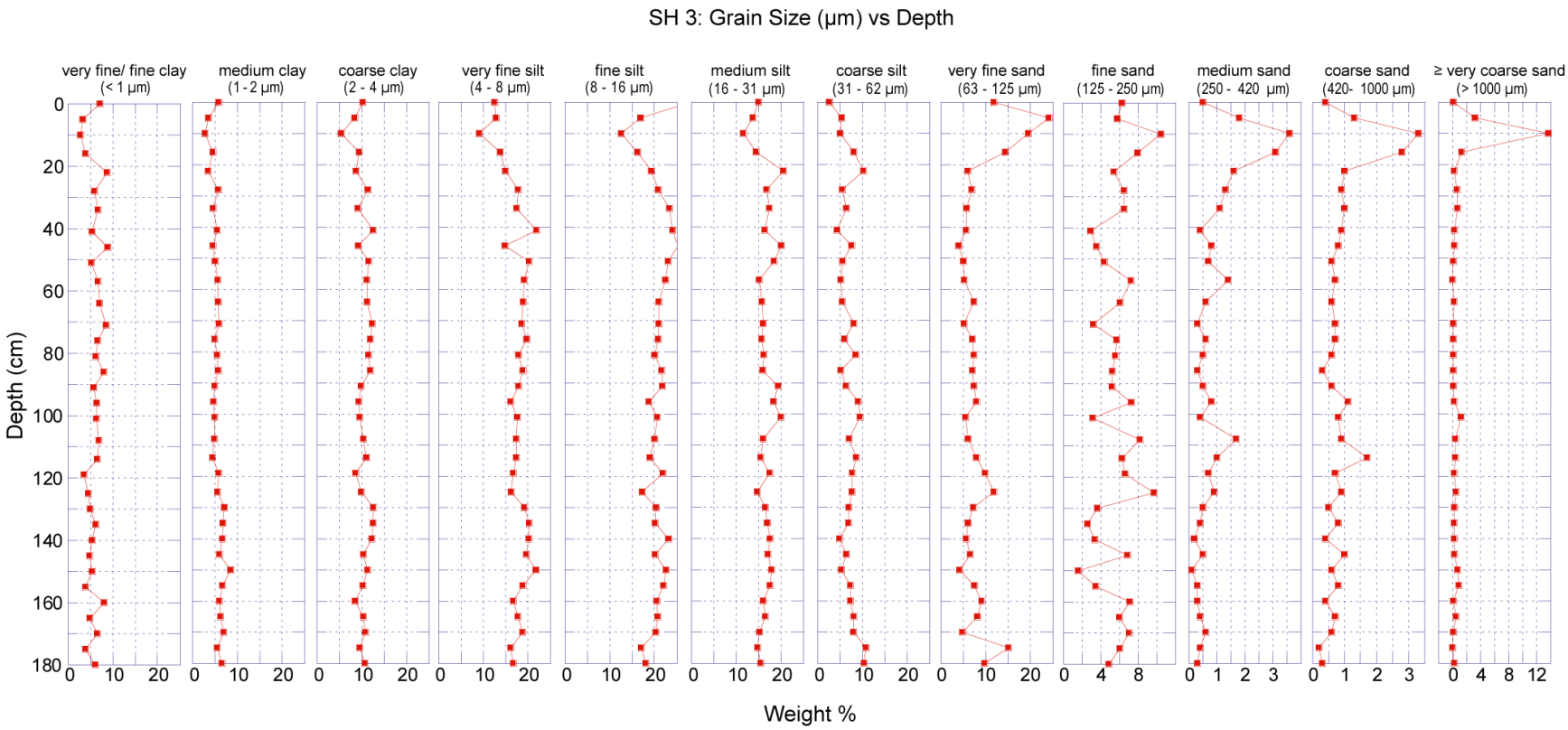

Figure 19: Grain size (weight %) versus depth (cm) results for core SH 3. The sediment is dominated by very fine, fine, and medium silt (4- 31 µm). The grain size appears to remain relatively constant throughout the core, except for coarsening upwards from 20 cm to the top of the core, coincident with an increase in shell fragments (Fig. 12). This pattern of limited temporal variability of the dominant grain sizes (i.e., range of 4- 31 µm) suggests consistent levels of depositional energy over time at this core location.

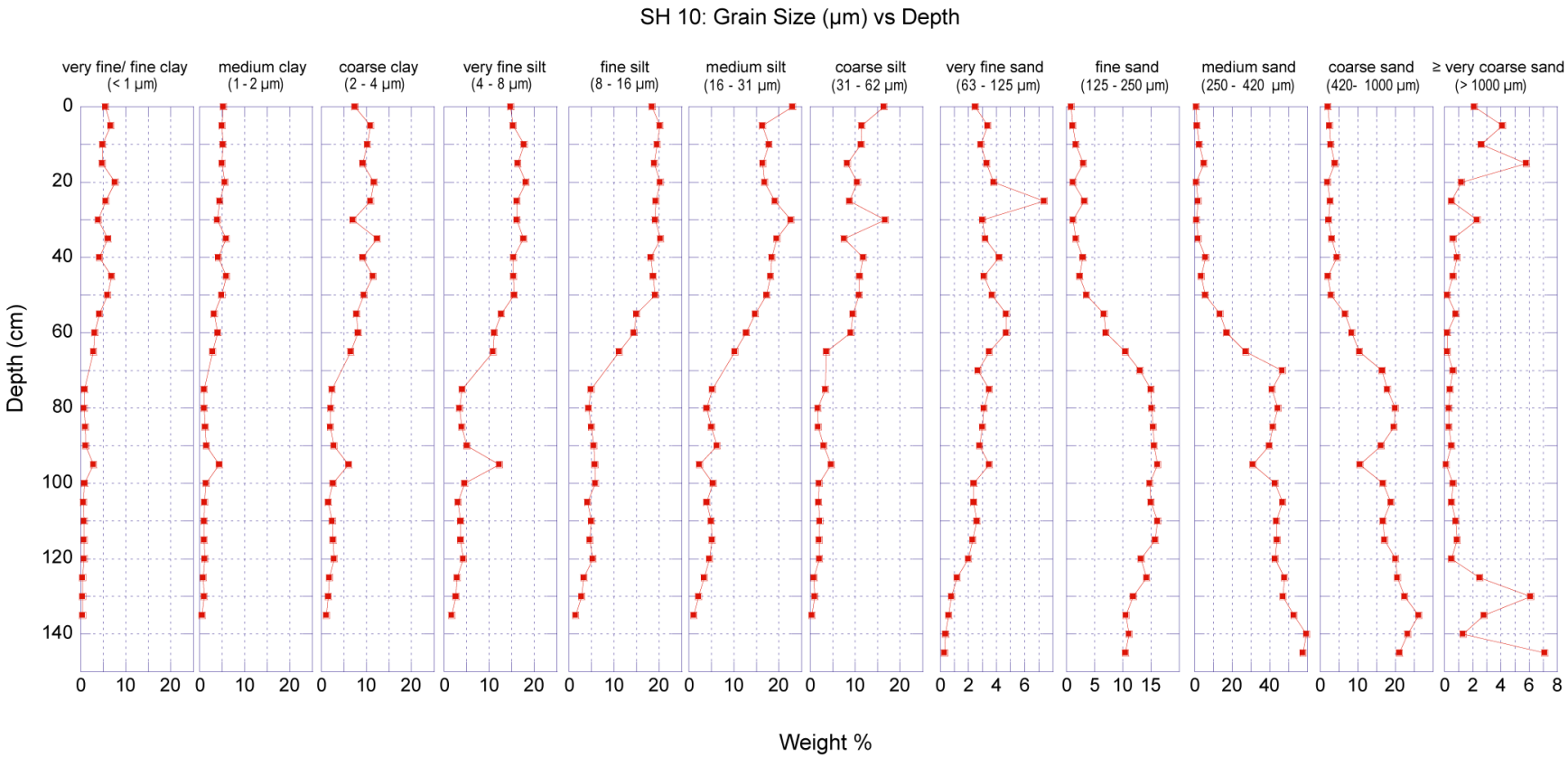

Figure 20: Grain size (weight %) versus depth (cm) results for core SH 10. The deepest sediments are predominantly composed of fine to coarse sand (125- 1000 µm). The sediments fine upwards from 75 cm to the top of the core to a grain-size range of coarse clay (2-4 µm) to coarse silt (31- 62 µm).The fining upwards trend correlates with a lithology shift from muddy sand to mud upwards (Fig. 12) and suggests a decrease in depositional energy over time.

55

Minerals, Shell Fragments, Microfossils, and Accessories (> 63 µm)

Percentages of quartz, pyrite, and iron oxide in the coarse-grained fraction of the sediment were determined by visual observation. The sediments are dominated by quartz, up to 90% (Figure 21). Quartz grains in the bay vary in size, roundness, surface texture, and color. Grains are: 1) clear and angular, with fresh conchoidal fractures; 2) cloudy in appearance and subangular to subrounded; 3) lesser amounts of pitted and/ or frosted and rounded; and 4) rarely, quartz grains (orange and pink) are stained with iron oxide (< 1%). Other mineral components include grains of black- dark gray pyrite (< 5%), and iron oxide (up to 20%; upper 35 cm of sediments near the beaches) (Fig. 22).

Predominantly angular, sharply broken (and lesser amounts of rounded) shell fragments (0.5 – 2 cm diameter), and well- preserved shells (1-7 cm diameter) are present in the sediments. The shell layers (shallow marine mollusks; e.g. *Anomia simplex*, *Crepidula fornicata;* see Methods for reference) are mainly found with the mass-wasting deposit near the tip of the spit (SH 6; Fig. 14), in the upper sediments in the backbarrier, and in layers of sediment ~20-30 cm thick offshore from the beaches and proximal to the Shrewsbury River (SH 10). Well-preserved, whole Mussel shells (*Mytilus edulis;* see Methods for reference) were buried in-situ near the tip of the spit (i.e., SH 6; ~6 cm diameter shells, 42- 90 cm depth; ~1.5 cm diameter 0-7 cm depth). Benthic foraminiferal assemblages are present (5-15%) in the upper sediments in the backbarrier section, and rarely (< 1 %) in sediments near the tip of the spit (Fig. 14).

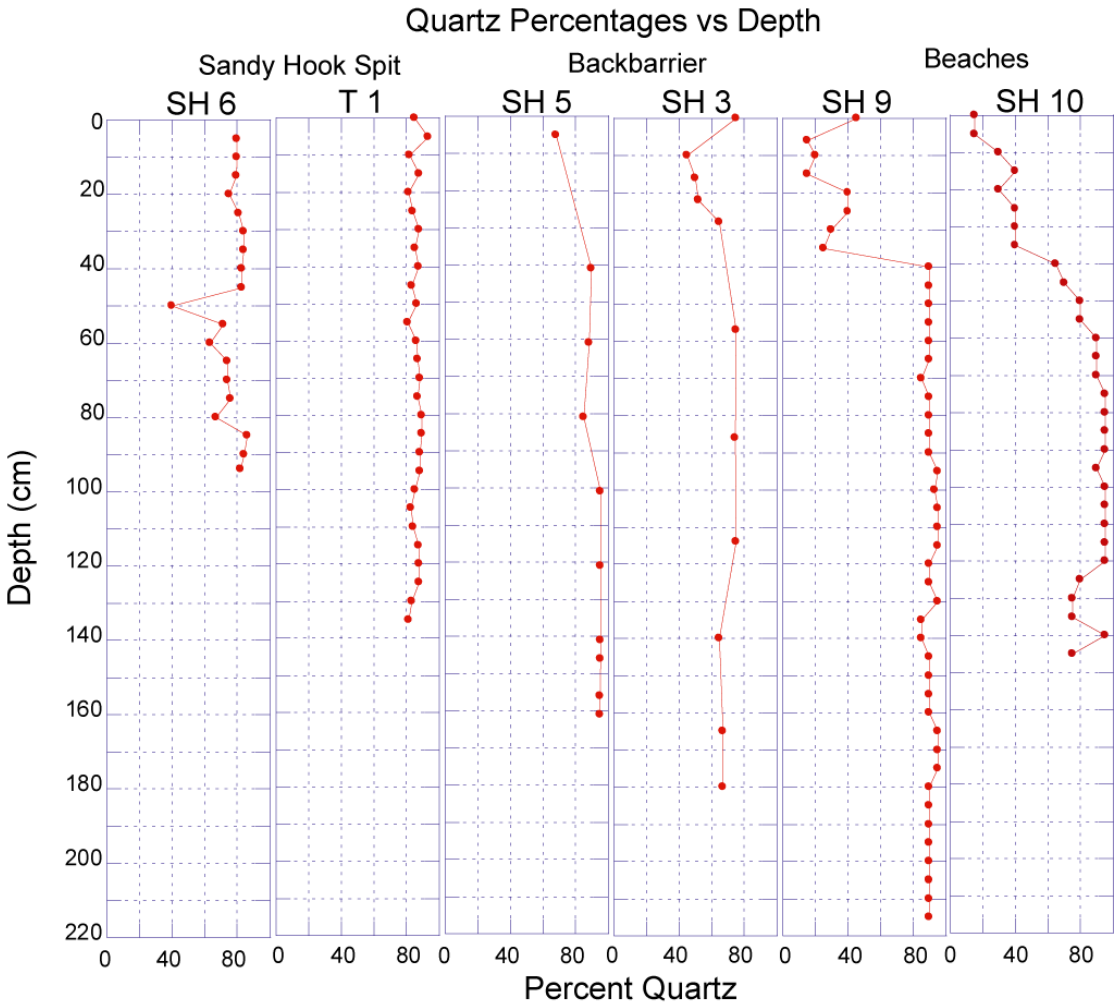

Figure 21: Quartz percentages (>63 µm) are relatively constant across the bay, at approximately 80%. Decreases in quartz percentages are coincident with increases in shell fragments, and therefore decreases in quartz are related to dilution by other components.

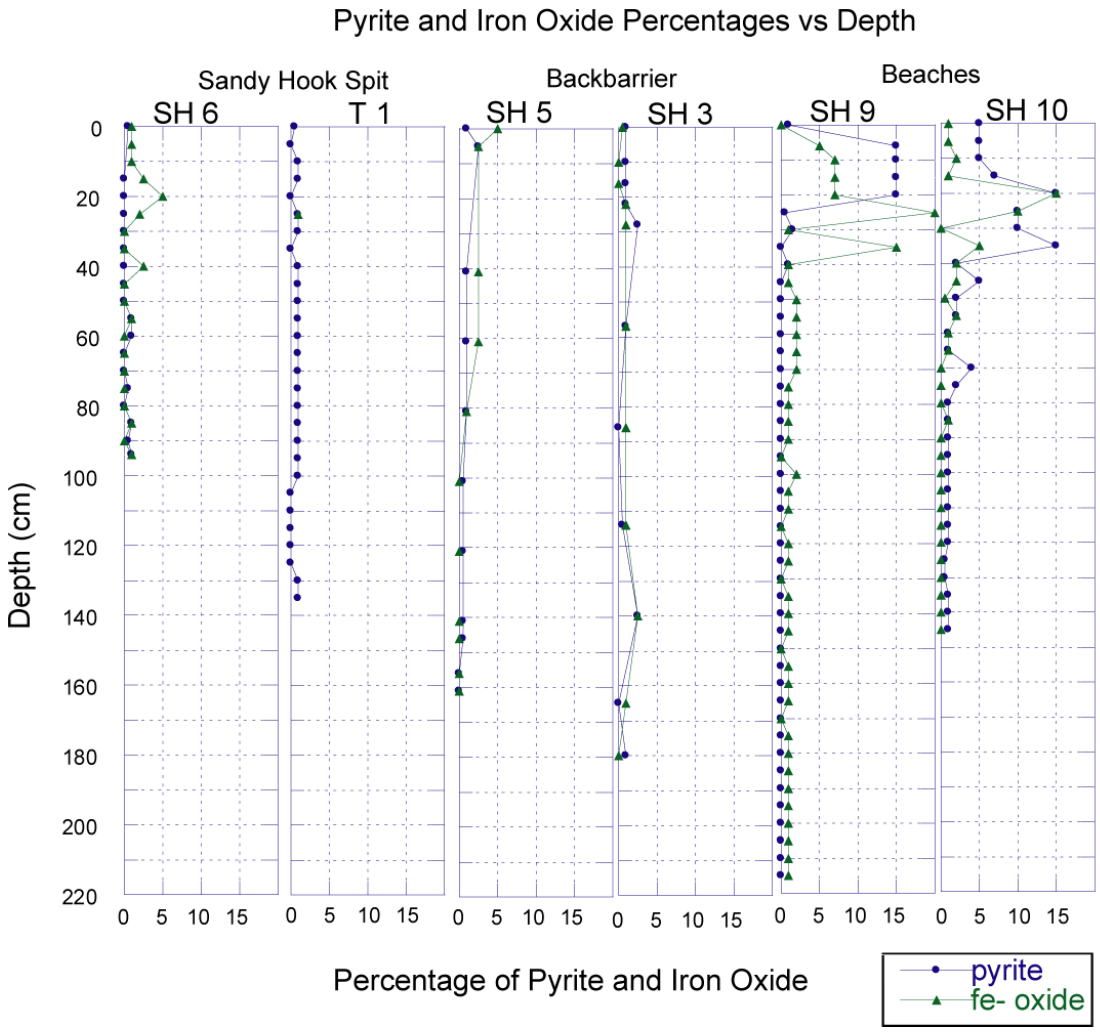

Figure 22: Percentages of pyrite and iron oxide vs. depth. Near the beaches, pyrite and iron oxide exhibit great variability in the upper 40 cm possibly related to increased organic carbon.

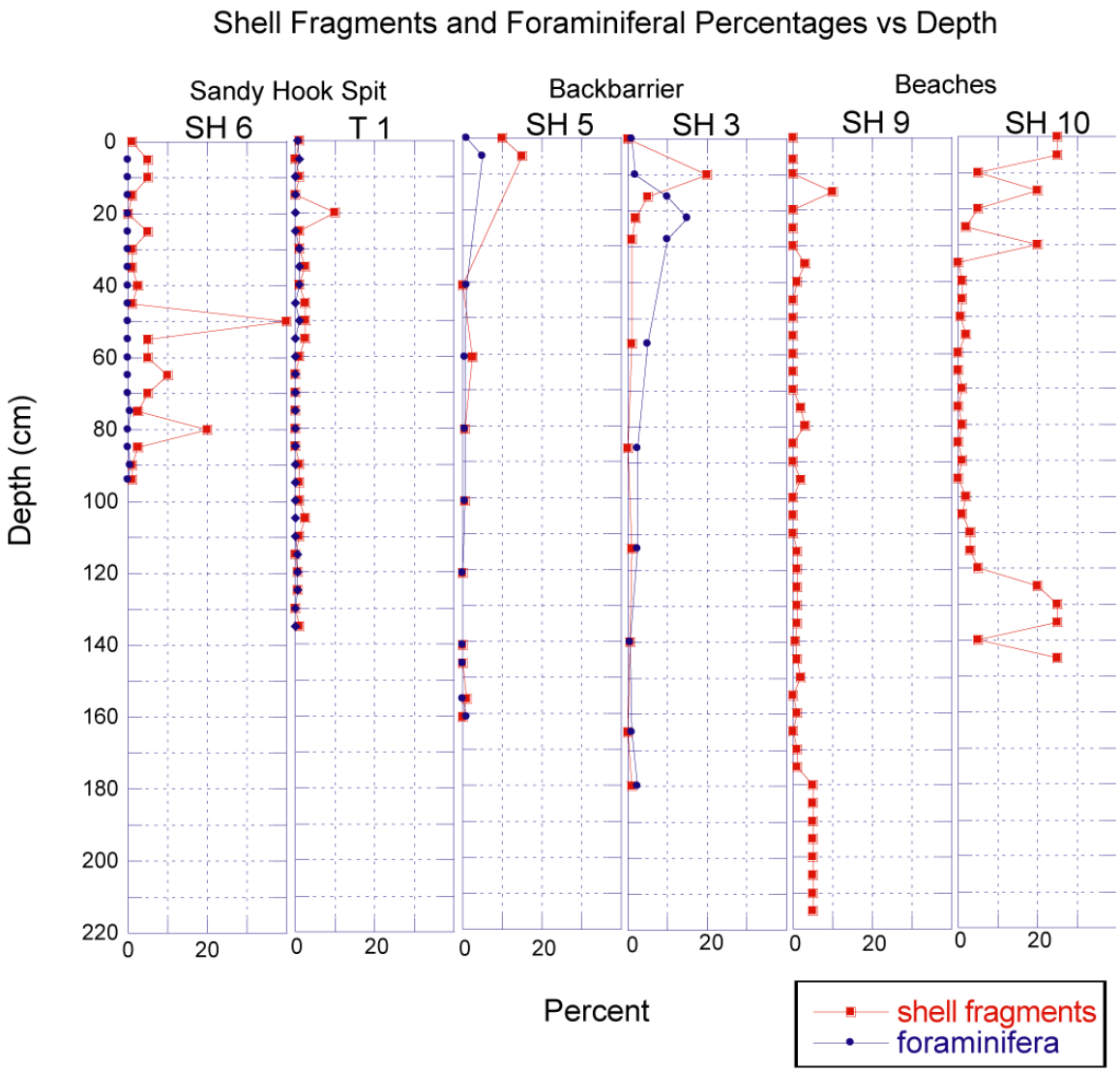

Figure 23: Percentages of shell fragments and foraminifera vs. depth. Shell fragments are present in all the sections of the bay, in varying amounts. The sporadic layers of shell fragments coincide with mass-wasting deposits (Figure 14). The foraminifera are benthic, and are mainly present in the lower energy environment of the backbarrier.

Total Organic Carbon

Results show that the organic carbon content varies depending on depositional environment (Table 5; Fig. 24). Previous studies conducted in and near the Sandy Hook Bay discuss that the elevated values of organic matter (which includes TOC) might be due to

anthropogenic activities and this is considered as a cause for the elevated organic carbon found in the Sandy Hook Bay sediments as well (Coch, 1986; Cohen et al., 2000).

Results show that TOC fluctuates from 1 to 8 % close to the tip of the spit (Core SH 6), remains relatively constant over time (2 to 5%) in the backbarrier sediments (Cores SH 3, SH 5), and shows an increasing trend upwards from 1 to 6% in sediments near the Shrewsbury River and the Atlantic Highlands beaches (Cores SH 9, SH 10). TOC concentrations also increase at the tip of the spit and the backbarrier region (Core T 1). TOC have also been used to track two different sediment sources. The floating mud clasts in Core SH 10 have TOC values of 2% at 122 cm. In contrast, the matrix has TOC values of 4.8%. This suggests a different origin for the mud clasts than the mud in the surrounding matrix.

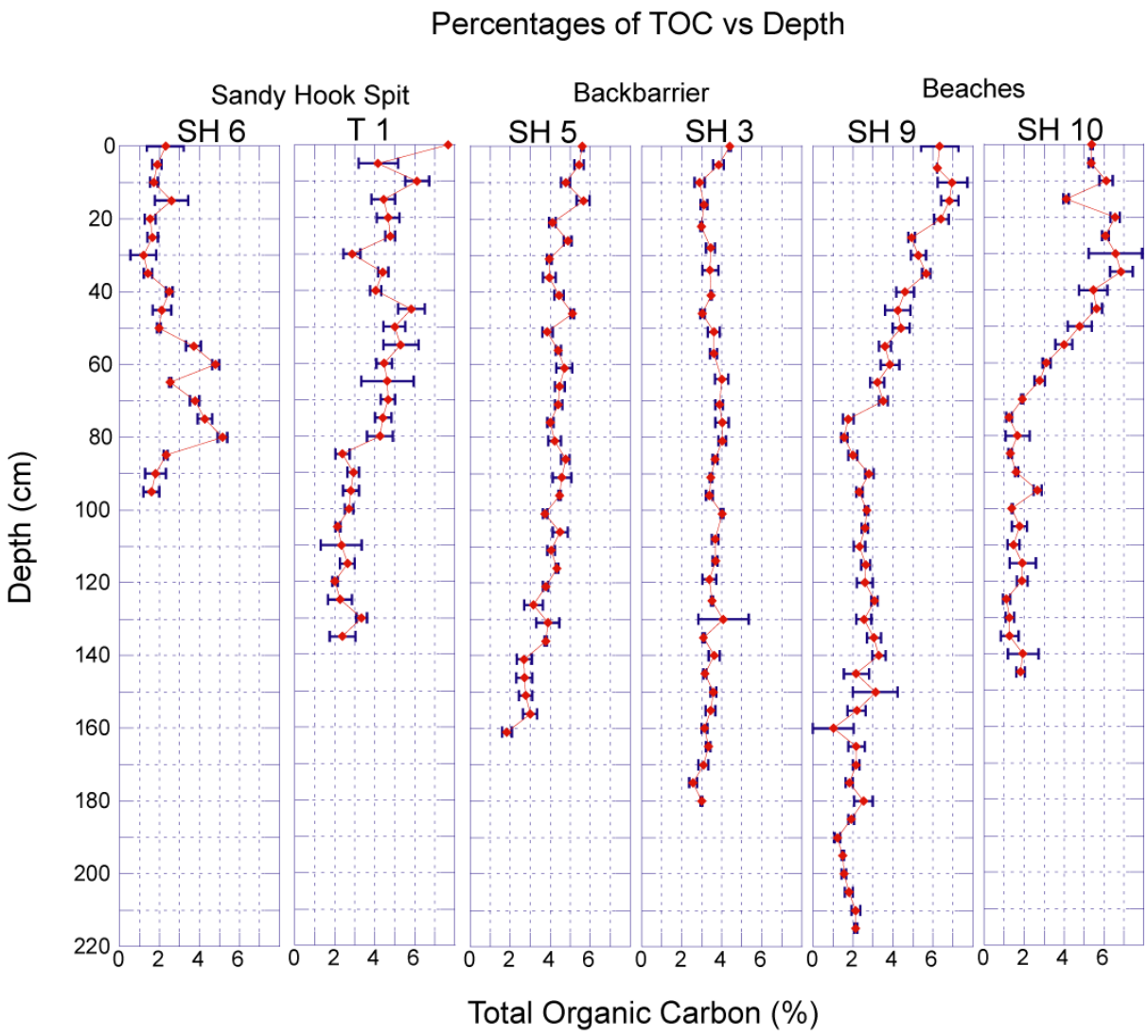

Figure 24: Percent total organic carbon (TOC). Blue lines represent the standard deviation derived from the three trials used in the analysis of each sediment sample. Cores T 1, SH 9 and SH 10 show an increasing trend in TOC. The TOC in the backbarrier sediments remain unchanged. Core SH 6 shows great variability, ranging from 1-8%.

Physical Properties

Physical properties including bulk density and magnetic susceptibility were measured.

Bulk Density

Bulk density is related to the total amount of pore space in the sediments, which is related to grain size and sediment consolidation (Gaugush, 1998; Westrich and Jancke, 2007). Overall results show that bulk density of the sediments varies by depositional environment, evident by increases in Core SH 6, and decreases in Cores SH 9, and SH 10 (Fig. 25).

Sandy Hook Spit: Near the spit, bulk density ranges from 1.4 to 2.2 g/cc, with greater bulk density (≥ 2 g/cc in the upper 40 cm). This increase in bulk density is correlated with coarser grain size (medium sand and pebbles).

Backbarrier: Here, the bulk density is lower than in other sections (1.4- 1.6 g/cc) with the least variation over time. The low bulk density values correspond with clay and silt, as this section of the bay contains sediments mainly composed of relatively homogeneous muds (Core SH 3; Fig. 25).

Beaches: Bulk density decreases towards the top of the core, which corresponds with silt and clay- sized sediments (~1.5 g/cc; Cores SH 9, SH 10). In contrast, the deeper, coarser sediments (fine- medium sand) are characterized by greater bulk density (~2 g/cc; Fig. 25).

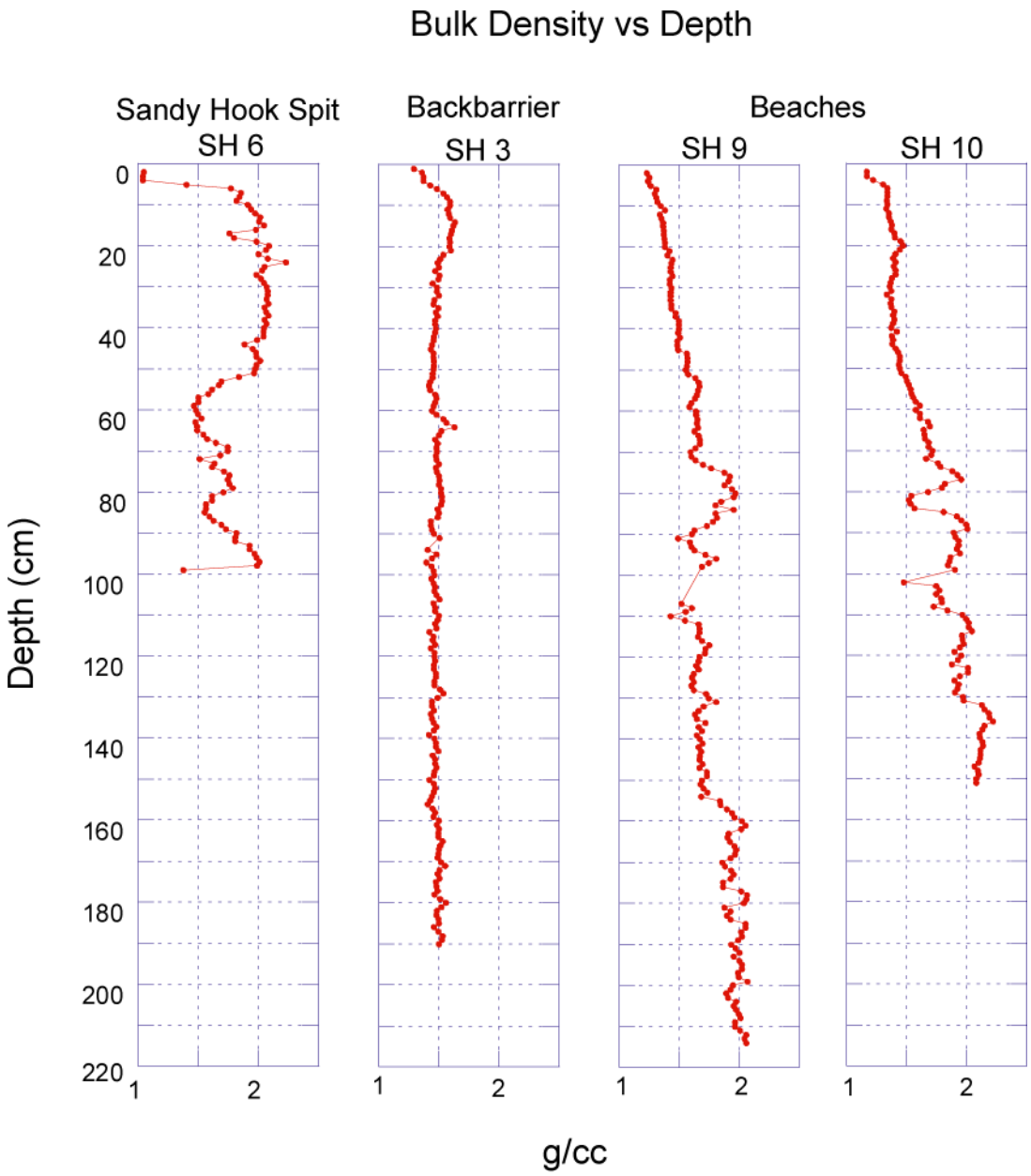

Figure 25: Bulk density values (in g/cc) for Cores SH 6, SH 3, SH 9, and SH 10 analyzed at a resolution of 1 cm. Near the spit, the bulk density is variable, ranging from 1.4- 2.2 g/cc increasing to ≥ 2 g/cc towards the top of the core. Behind the spit, bulk density is more constant, and lower (1.5 g/cc). Near the beaches, the deepest sediments are characterized by greater bulk density, with fluctuations in the mid section, and a decrease in the upper part of the core similar to grain size.

Magnetic Susceptibility

The magnetic susceptibility signal can be indicative of the presence of ferrimagnetic iron-oxides (i.e., magnetite) formed as byproducts of coal combustion, including combustion-related oxidation of materials rich in Fe, Pb, Cu, or Zn, such as oxidation of pyrite to magnetite (Martins et al., 2007 and references therein). Previous studies have also shown that increased magnetic susceptibility signal in sediments could be an indication that the source of the fly ash and other byproducts of burning of fossil fuels are proximal to the depositional environment from which the sediments were recovered (Kapička et al., 1999). In addition to the combustion of fossil fuels, magnetic susceptibility has also been linked to smelting of iron ore to make steel, and cement manufacturing, in recent studies (Plater et al., 1998; Hoffman et al., 1999; Kapička et al., 1999; Petrovsky et al., 2000; Chan et al., 2001; Schmidt et al., 2005; Martins et al., 2007).

In the study area, magnetic susceptibility ranges from 2×10^{-5} SI to 48×10^{-5} SI units in the bay in all three depositional environments, with distinct increases upwards (Figure 26).

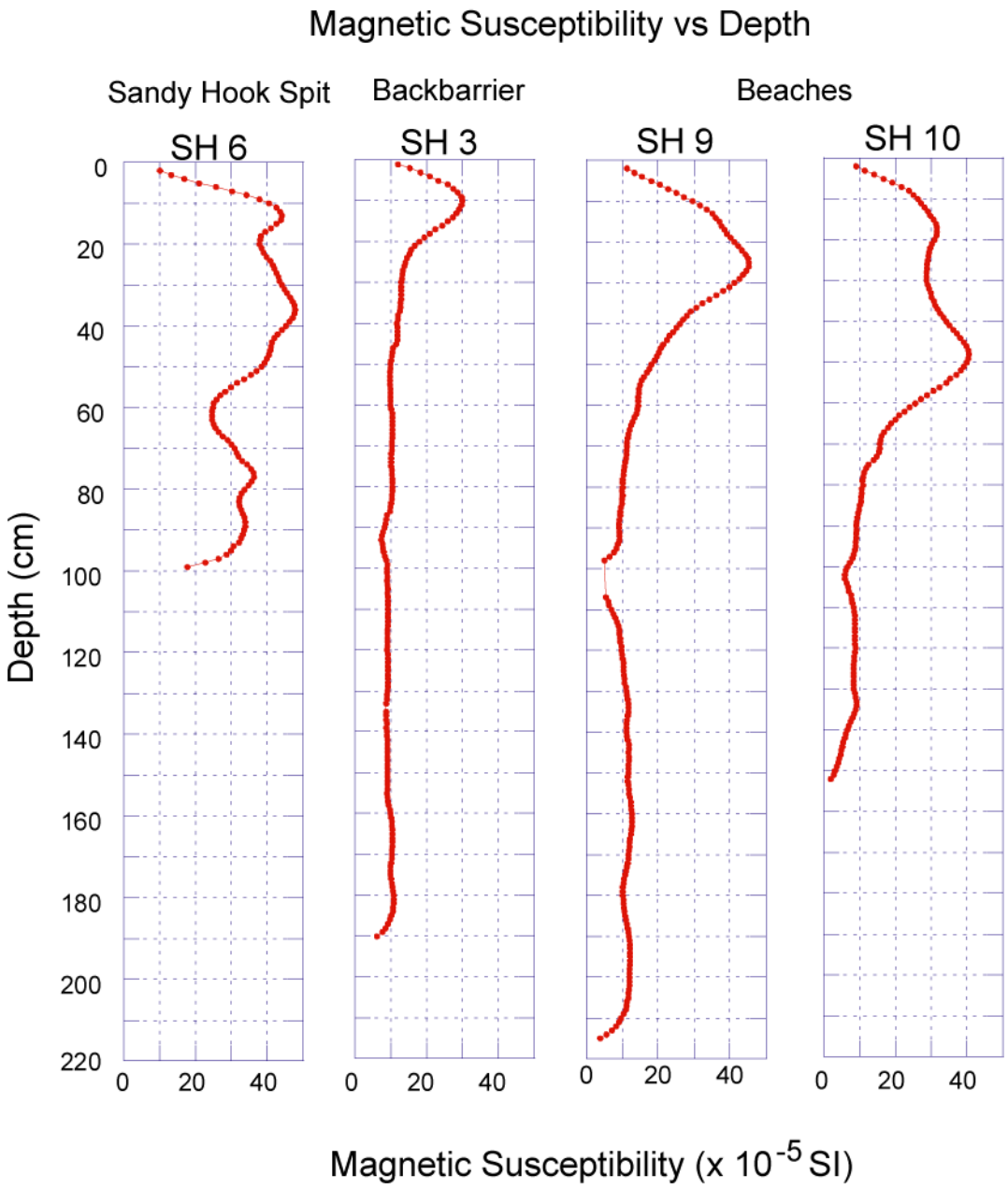

Figure 26: Magnetic susceptibility values for Cores SH 3, SH 9, SH 10, and SH 6 analyzed at a resolution of every 1 cm. Values are given in 10^{-5} SI units. Overall trends reveal an increase in magnetic susceptibility towards the top of the cores.

Age model for Sandy Hook and Raritan Bays

A chronology derived from radiocarbon dates and short-lived radioisotopes was developed for the Sandy Hook Bay cores (1-2 m long), and for the cores from Raritan Bay (4- 5 m long). The Raritan Bay cores were previously studied and described by Gaswirth, (1999) and Gaswirth et al. (2002). The chronology based on the shorter Sandy Hook Bay cores was used as a framework for dating storm deposits and contaminant accumulations. Results from radiocarbon dating of the longer Raritan Bay sediment cores were interpreted within the context of seismic and stratigraphic descriptions of Raritan Bay previously discussed in Gaswirth (1999) in order to date the sea level changes from the LGM through the Holocene.

Radiocarbon Dating

Shells and woody material were used for radiocarbon dating. Mollusk species used for dating, include *Mercenaria mercenaria*, *Crepidula fornicata, Mulinia lateralis, Anomia simplex*, *Anadara transversa* , and *Ensis directus*. Knowledge of the habitats in which these mollusks live was used to date paleoenvironmental changes. The ages of mollusks and woody material recovered from both the Sandy Hook, and Raritan Bay Cores, are late Holocene in age (6520 ^{14}C yr BP - 270 ^{14}C yr BP; Tables 2, 3; Figs. 27, 28).

Gaswirth (1999) determined an older radiocarbon age (31.7 ka ^{14}C yr BP) from one of the Raritan Bay cores (Core RB S08, 350-370 cm). Gaswirth (1999) identified an unconformity separating Late Cretaceous sediments from late Pleistocene strata. Results from this study further show this by dating a wood fragment and obtaining an age of >48,000 years (Core RB 5; 488 cm) representing dead carbon. These sediments could be much older (Table 6; Fig. 28).

Core I.D.	Sample Depth (cm)	Core Water Depth (m)	Type/ Species	^{14}C age	Age Error (+/-)	Age Range (cal. yrs BP)	Medial Age (cal. yrs BP)	Age Range (yrs AD, BC)	Medial Age (yrs AD, BC)
			Mollusk/						
SH5	104	6	*Mercenaria mercanaria (clam)*	550	35	539-625	582*	1325-1411 AD	1368*
SH6	42	9	*Crepidula fornicata (slipper)*	270	40	297-420	356*	1530-1652 AD	1591*
SH6	74	9	*Crepidula fornicata (slipper)*	660	35	81-252	157	1698-1869 AD	1793
SH9	84	6	*Mulinia lateralis (Dwarf surf clam)*	530	40	529-619	574*	1331-1421 AD	1376*
SH9	167	6	*Ensis directus (razor clam)*	1070	40	496-607	546	1343-1454 AD	1404
SH9	209	6	*Anomia simplex (jingle shell)*	1590	35	925-1078	1012	872-1025 AD	938
SH9	213	6	*Anomia simplex (jingle shell)*	1590	40	923-1083	1013	867-1027 AD	937
SH9	215	6	*Anomia simplex (jingle shell)*	1560	40	903-1057	982	893-1047 AD	968
SH10	59	7	*Mercenaria mercanaria (clam)*	605	40	0-145	112	1772-1784 AD	1838
SH10	109	7	*Ensis directus (razor clam)*	920	40	338-341	419	1458-1592 AD	1531
SH10	142	7	*Anomia simplex (jingle shell)*	2210	30	1559-1733	1656	217-391 AD	294
T1	100	7	*Mercenaria mercanaria (clam)*	485	35	514-539	527*	1411-1435 AD	1423*
RB04	362	14	*Anomia simplex (jingle shell)*	5820	40	5999-6179	6095	4230 -4050 BC	-4146
RB04	362	14	*Anadara transversa (ark shell)*	5850	40	6027-6213	6127	4264-4078 BC	-4178
RB05	159	6.1	*Shell Fragment*	6520	45	6766-6961	6867	5012-4817 BC	-4918
RB05	475	6.1	*Woody Material*	3770	35	4087-4159	4138	2278-2251 BC	-2189
RB05	488	6.1	*Woody Material*	>48000		-	Dead carbon	-	-
RBS08	170	4.6	*Ensis directus (razor clam)*	1250	30	621-739	679	1211-1329 AD	1271
RBS08	178	4.6	*Ensis directus(razor clam)*	1250	40	618-748	679	1202-1332 AD	1271
RBS08	178	4.6	*Ensis directus(razor clam)*	1260	30	629-746	688	1204-1321 AD	1262
RBS08	207	4.6	*Mulinia lateralis (Dwarf surf clam)*	805	30	266-405	328	1545-1684 AD	1622

*Table 6: Radiocarbon ages of mollusk shells and wood retrieved from Sandy Hook Bay and Raritan Bay (See Table 1 for Core details). Ages were analyzed by National Ocean Sciences Accelerator Mass Spectrometry Facility (NOSAMS), Woods Hole and calibrated (1 sigma) using Calib 6.0, with the Marine09.14c and Intcal09.14c calibration datasets (Stuiver et al., 2005; Hughen et al. 2009, Reimer et al. 2009). *Ages ≤ 550 ^{14}C yr BP were calibrated using CalPal-2007 online (Danzeglocke et al., accessed 2010) and CALIBomb (Stuiver et al., 2005); Mean age is listed for these samples instead of medial age.*

Mollusk Species	Mollusk Habitat
Mercenaria mercanaria (clam)	In sand or mud in bays or inlets; intertidal flats to water 15 m deep
Crepidula fornicata (slipper)	Found on rocks and other shells; intertidally to water 15 m deep
Mulinia lateralis (Dwarf surf clam)	In sand & mud, water 0.6- 55 m deep
Ensis directus (razor clam)	In sand in bays and inlets; intertidal
Anomia simplex (jingle shell)	Found on rocks, shells, logs, boats & piers, from near low- tide line to 9 m deep
Anadara transversa (ark shell)	Shallow water, sandy bottoms

Table 7: Mollusk species and their corresponding habitat (Rehder,1992; Abbott and Morris, 1995). Mollusks for which habitat conditions are known (i.e., water depths) were used to track relative sea level rise in the region, with the appearance of estuarine mollusk species.

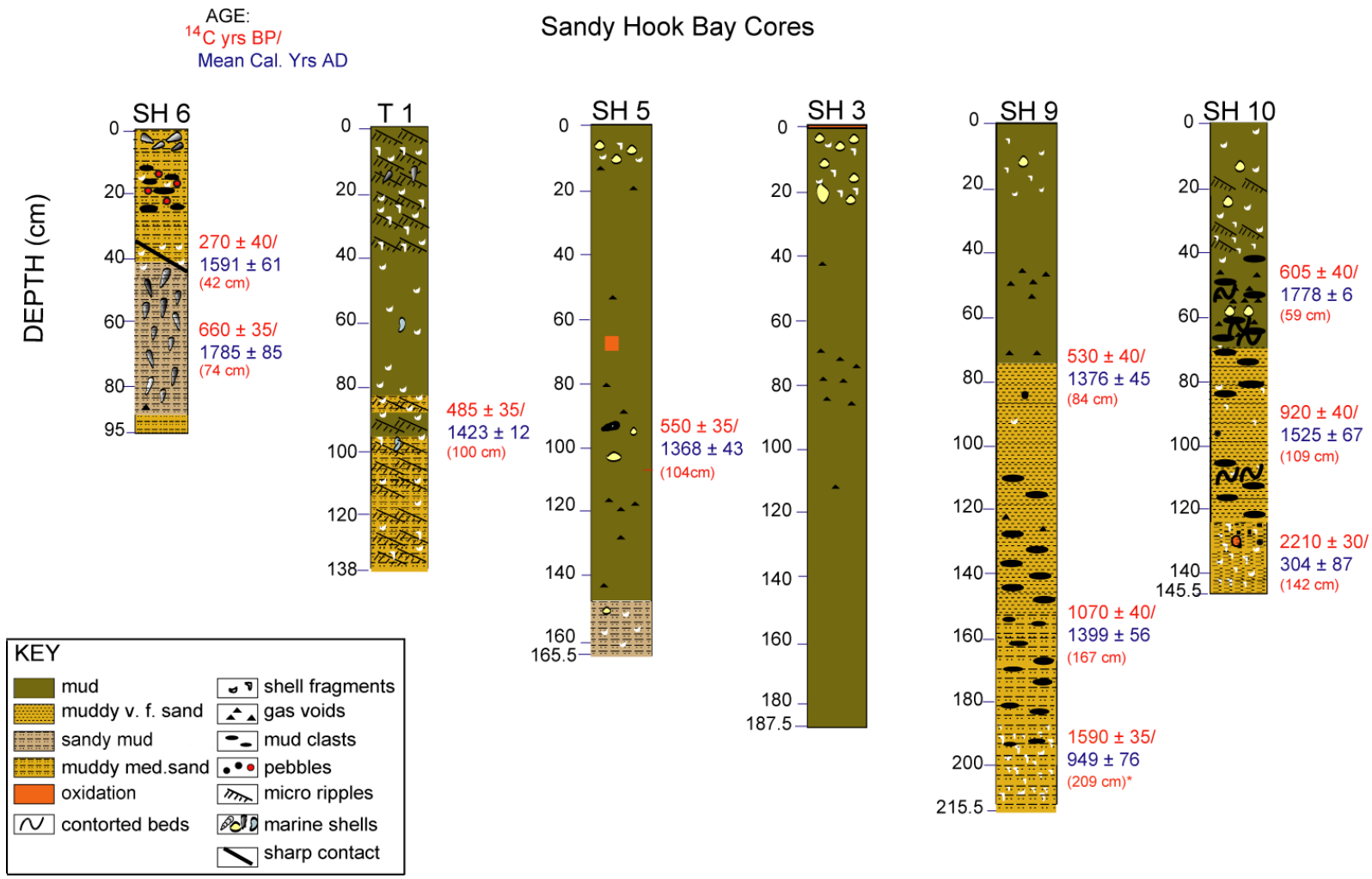

*Figure 27: Lithology of sediment cores with ages as radiocarbon (noted in red) and mean calibrated years AD (noted in blue). *Indicates multiple mollusk samples were analyzed for radiocarbon dates at that depth and resulted in similar dates. For these samples, only one age is listed on the figure; see Table 6 for further details.*

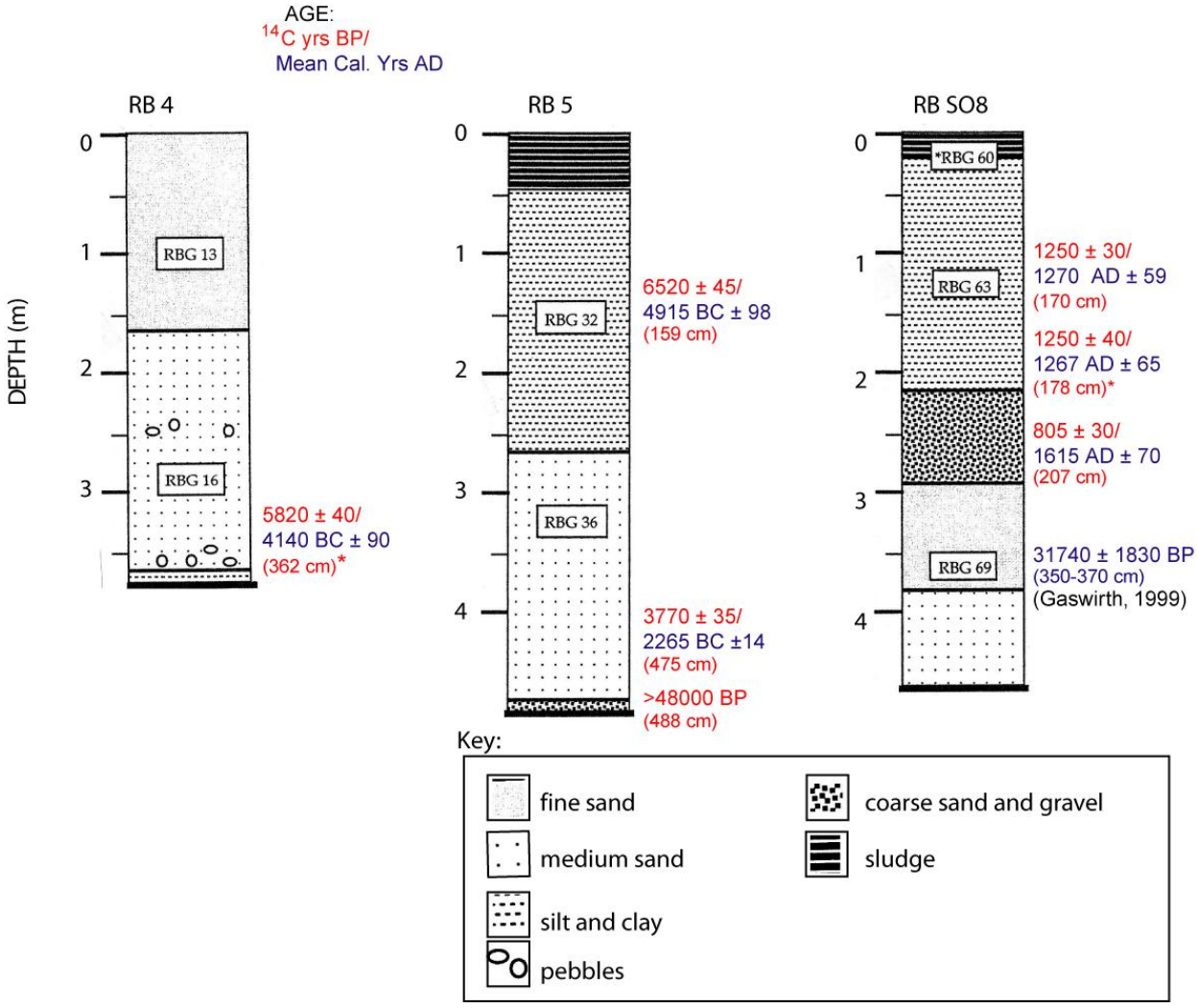

*Figure 28: Lithology modified after Gaswirth (1999) and Sheridan (unpublished) with permission. Ages are shown in radiocarbon (red) and mean calibrated years AD (blue). Cretaceous sands are overlain unconformably by Pleistocene sand and Holocene mud. *Indicates multiple mollusk samples were analyzed for radiocarbon dates at that depth and resulted in similar dates. For these samples, only one age is listed in the figure; see Table 6 for further details.*

Short- lived Radioisotopes

Sediments from Cores SH 9, SH 10, and T1 were analyzed for short-lived radioisotopes, including ^{137}Cs. Results indicate the upper 50 cm sediments in the bay contain short- lived radionuclides. Age estimations (calendar dates) are based on previous studies that interpret the

first appearance of ^{137}Cs in sediment cores (from global fallout) to be from the initiation of nuclear weapons testing (1954), a peak in ^{137}Cs concentration to be from a maximum of nuclear weapon testing (1963), and a second peak of ^{137}Cs associated with a peak in ^{60}Co (1971) to be related to a release of nuclear material from the nuclear reactor at Indian Point (Olsen et al., 1978; Williams et al., 1978; Olsen et al., 1981; Olsen et al., 1984- 1985; Bopp and Simpson, 1989; Figure 29). Micro-ripples and shell fragments in the cores indicate sediment reworking, and this is consistent with the peaks seen in the ^{137}Cs measurements (Figs. 27; 29).

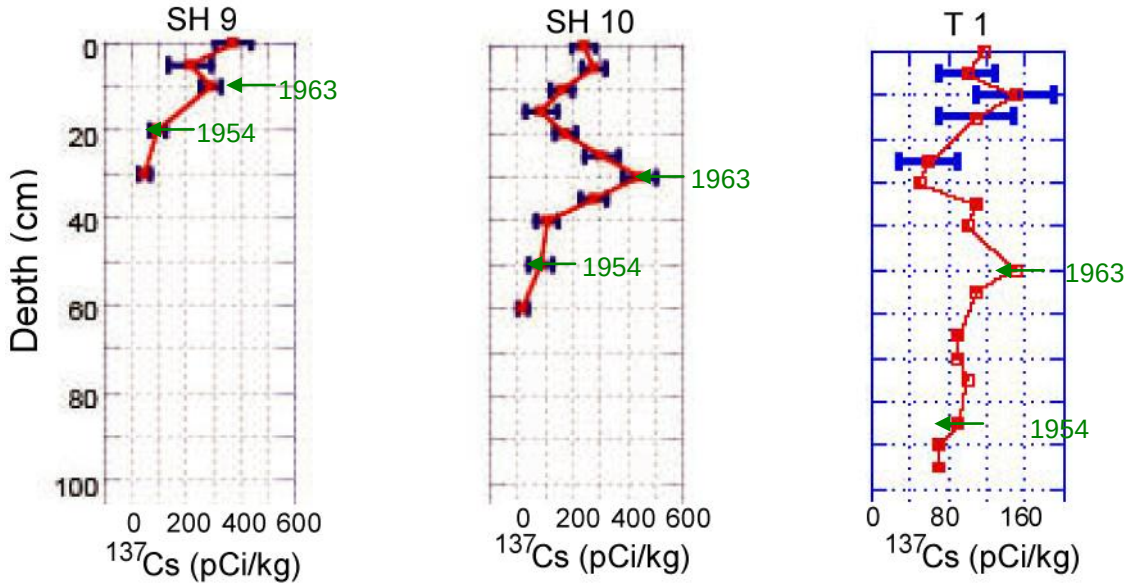

Figure 29: Short-lived radioisotope ^{137}Cs (pCi/kg) detected in sediments from Cores SH 9, SH 10, and T 1. Results indicate the upper 50 cm contain short- lived radionuclides and were deposited post 1950's. The first appearance of ^{137}Cs, as well as subsequent peaks in concentration, mark the 1950's initiation of nuclear testing, the 1960's peak in global fall out (Olsen et al., 1978; Williams et al., 1978; Olsen et al., 1981; Olsen et al., 1984- 1985; Bopp and Simpson, 1989).

Sedimentation Rates

Results show sedimentation rates are highly variable (ranging from 0.03 – 4.0 cm/yr) even in cores recovered from similar depositional environments (e.g., Core SH 10; 2.22 cm/yr vs. Core SH 9; 0.12 cm/yr over past ~200 years; Fig. 30). These trends are consistent with a

shallow water dynamic sedimentary environment. A trend of increased sedimentation rates up-core is noted with greatest in the upper 1 m for all cores (Fig. 30).

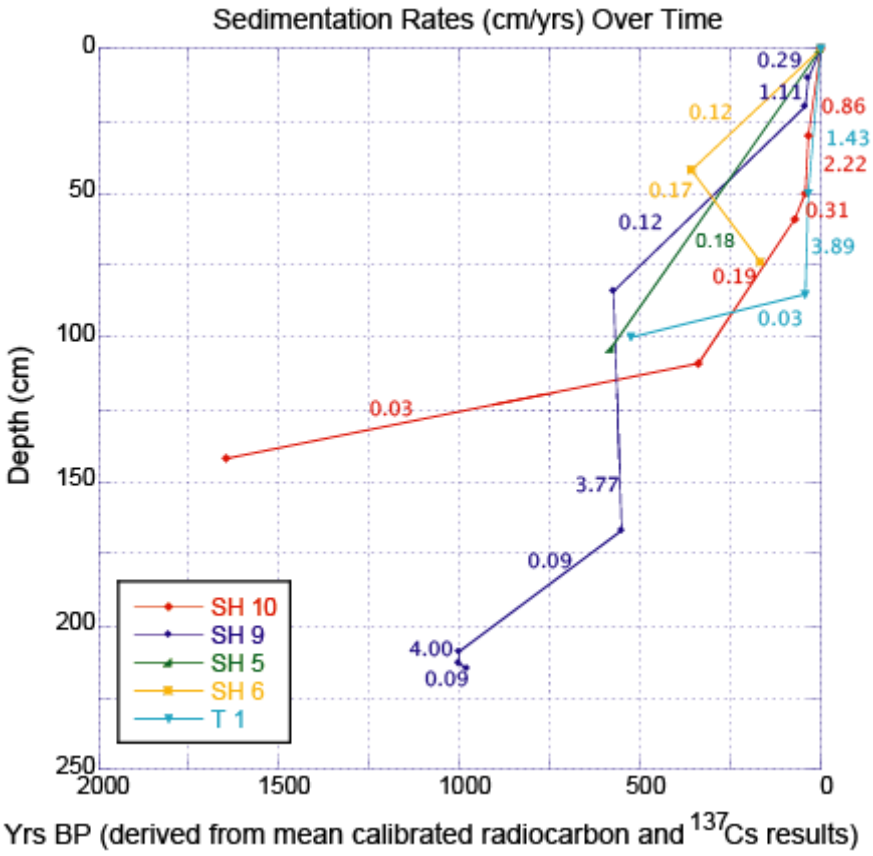

Figure 30: Sedimentation rates calculated from calibrated radiocarbon dates and short- lived radioisotopes (Table 6). Sedimentation rates are highly variable across the bay, ranging from 0.03 – 4.0 cm/yr. Sedimentation rates increase in sediments younger than 500 years.

Chronology for Mass-wasting Deposits

Ages of the events related to six deposits of mass-wasting and sediment reworking in the cores were determined from mollusk shells sampled beneath the deposits. In some cases where dateable material was absent, samples were taken from within the deposit. It is recognized that the samples from the mass-wasting deposits are reworked and could be older but the confidence of the ages of these shells is based on the dates being in appropriate chronological order up-core, despite apparent sediment reworking (i.e., Core SH 10). Where possible, dates were confirmed

by adjacent samples, which yielded similar age results (i.e., Core SH 9; 209 cm, 213 cm, 215 cm; Table 8).

The deposits include (with mean age AD): Deposit SH10-3 (304 AD), Deposit SH9-2 (949 AD), Deposit SH9-1 (1399 AD), Deposit SH10-2 (1525 AD), Deposit SH6-1 (1591 AD), and Deposit SH10-1 (1778 AD) (Figs. 27, 31; Table 8). The ages of the deposits indicate there are erosional unconformities present in the sediments that range from 250- 1220 years.

The upper boundary of Deposit SH10-3 is marked by an abrupt change to muddy very fine sand with mud clasts and represents a 1220 year gap with Deposit SH10-2, while the unconformity between SH10-1 and SH10-2 spans 250 years. The upper boundary of Deposit SH9-2 is marked by a change in lithology from muddy medium sand with abundant shell fragments to sand without shell fragments, and represents an unconformity of 450 yrs with Deposit SH9-1. The sediments above Deposit SH9-1 (i.e., 1376 AD; 84 cm) are close in age to the lower boundary of this thick deposit (~80 cm thick) (Figs. 27, 31; Table 8), indicating a mass- wasting event. Sediment reworking and/or bioturbation are evident where a younger shell was retrieved from a deeper section than an older shell (i.e., Core SH 6, 1785 AD at 74 cm; 1591 AD at 42 cm; Figs. 27, 31; Table 8).

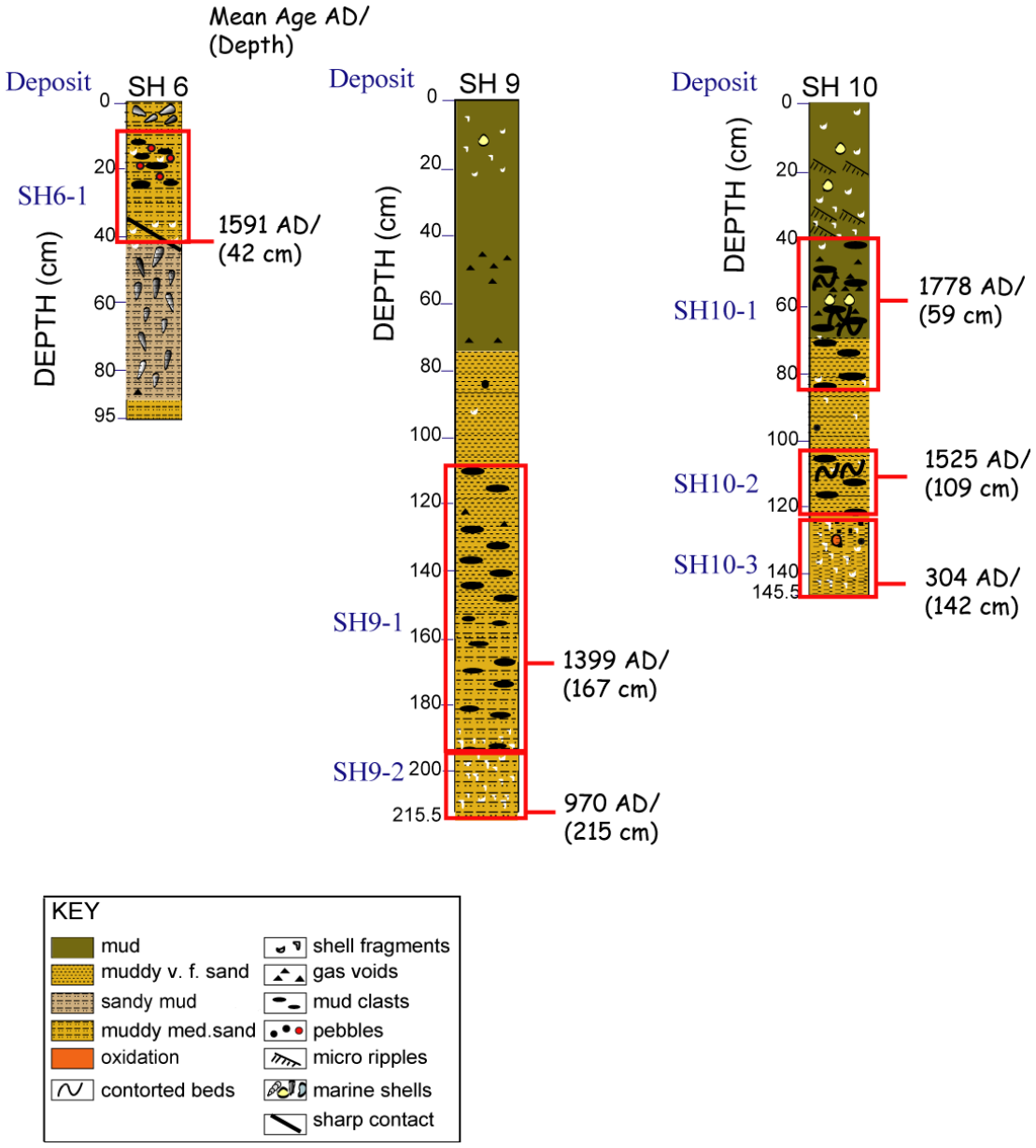

Figure 31: Lithology of sediment cores SH 6, SH 9, SH 10. The chronology based on radiocarbon dates (Table 6) is shown to the right of each lithology column as the mean calibrated age in years (AD). Mass-wasting deposits are bounded by red boxes.

Deposit	Top Depth (cm)	Basal Depth (cm)	Depth From Which Ages Were Obtained (cm)/ Mean Age (AD)
Deposit SH10-3	124	145.5	142-143 cm/ 304 AD
Deposit SH9-2	198	215.5	209 cm/ 949 AD
Deposit SH9-1	118	195	84 cm/ 1376 AD & 167 cm/1399 AD
Deposit SH10-2	124	113	109 cm/ 1525 AD
Deposit SH6-1	13	41	42 cm/ 1591 AD & 74 cm/ 1785 AD
Deposit SH10-1	42	83	59 cm/ 1778 AD

Table 8: Storm deposits labeled in Figure 32, with depths of upper and lower boundaries, and the depth from which ages were obtained. Ages listed are the mean calibrated age in years (AD).

Spatial and Temporal Heavy Metal Distribution

Results for x- ray fluorescence elemental analysis (at 5 cm and 2 cm resolution) indicated that heavy metals are detectable, above background levels, in the upper 100 cm of the sediment cores (Figs. 32- 37). Results reveal the link between increased magnetic susceptibility and metal concentrations above background levels in the upper sediments, denoting an anthropogenic origin of these metals, and are herein described as contaminants (Fig. 26).

Distribution of Metals Relative to Depositional Environment in the Bay

Overall, results from XRF analysis indicate that metal contaminant variability is related to depositional environment in the bay. The following trends were observed:

Tip of the Spit

Results show metal concentrations near the tip of the spit (i.e., Core SH 6) are greater in the muddy sediments from 50 to 80 cm and decrease in the upper 50 cm, coincident with the changes to coarser grain sizes (i.e., sand, pebbles; Core SH 6; Figs. 27, 32).

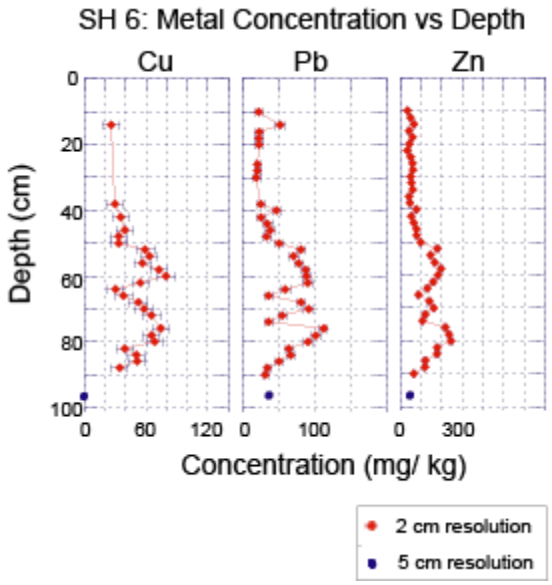

Figure 32: Metal contaminants (Cu, Pb, and Zn) in Core SH 6 are greater in the deeper sediments (i.e., 50- 80 cm depth) and decrease upwards, coincident with the coarser grain size up-core (i.e., pebbles, sand).

Cu and Pb concentrations also increase from 80 to 50 cm in Core T1 (Fig. 33). This interval is composed of sandy mud, with adult, whole, and well- preserved mussel shells, suggesting an undisturbed interval of sediments with mollusks buried in situ (Fig. 27).

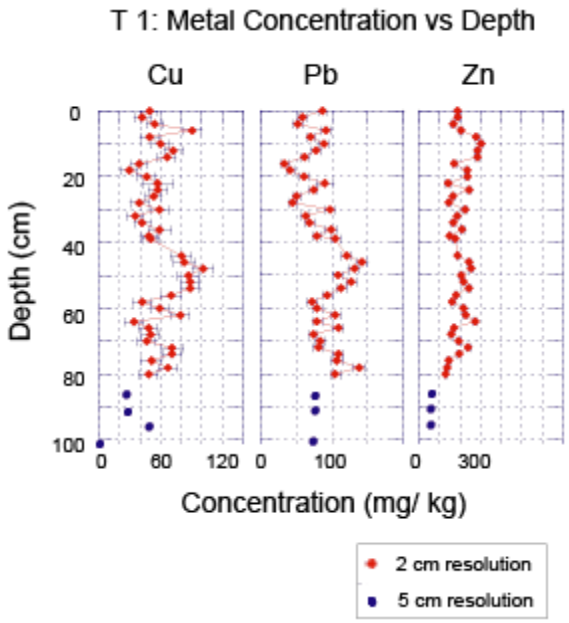

Figure 33: Metal contaminants (Cu and Pb) in Core T 1 are slightly higher between 50 – 80 cm, but generally show variability throughout that is related to sediment reworking as evidenced by microripples present in the core (Fig. 28).

Backbarrier

In contrast with results from near the tip of the spit, metal concentrations detected here (specifically Cu and Zn) increase above background levels in the upper ~25 cm of the sediments (Cores SH 5, SH 3; Figs. 34, 35).

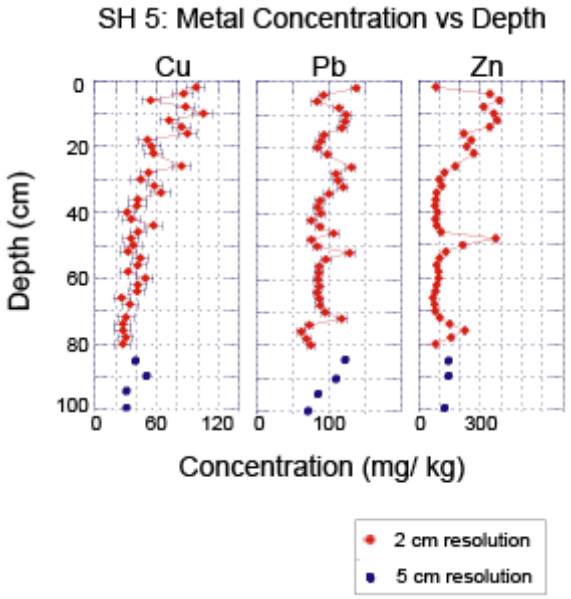

Figure 34: Metal contaminants (Cu, Pb, and Zn) in Core SH 5 are greater in the upper (0- 25 cm depth) sediments. A peak in Zn is also noted at 50 cm.

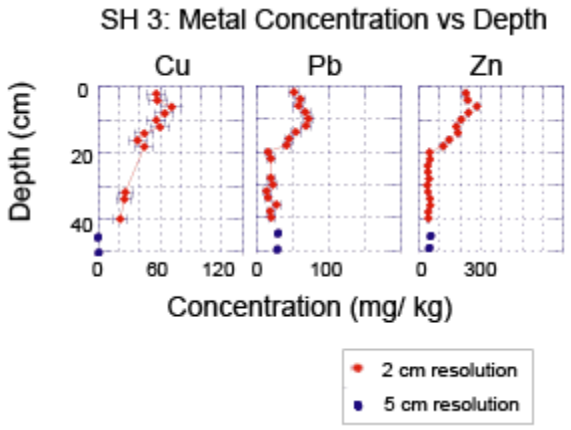

Figure 35: Metal contaminants (Cu, Pb, and Zn) in Core SH 3 are greater in the upper (0- 20 cm depth) sediments. This increase also corresponds with increased magnetic susceptibility for the same depth interval (Fig. 27).

Beaches

The pattern of increasing contaminant concentration up-core of Cu, Pb, and Zn, seen in the backbarrier sediments is also found offshore from the beaches (Cores SH 9, SH 10; upwards from 50 to 60 cm depth to the top of the cores; Figs. 36, 37). Consistent with results from the

backbarrier sediments, the increased concentrations of metal contaminants in the upper sediments also correspond with increased magnetic susceptibility for the same depth interval (Fig. 26).

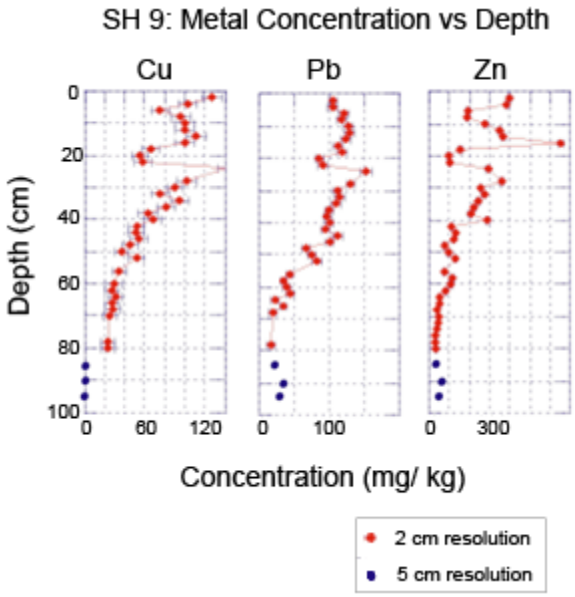

Figure 36: Metal contaminants (Cu, Pb, and Zn) in Core SH 9 increase above background levels in the upper (0- 50 cm depth) sediments.

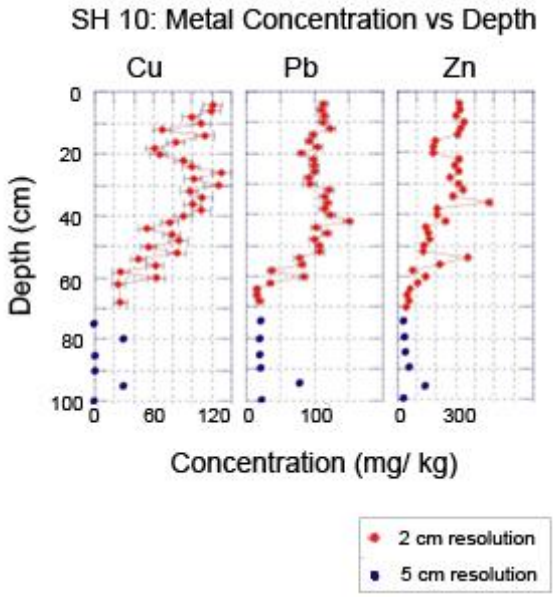

Figure 37: Metal contaminants (Cu, Pb, and Zn) in Core SH 10 increase above background levels in the upper (0- 60 cm depth) sediments.

Multi-proxy Approach for the Interpretation of Sedimentation and Environmental Impact

Results for magnetic susceptibility, grain size variability, total organic carbon, metal concentration, and lithology were correlated and interpreted within the context of an age model. This multi-proxy approach for studying metal concentration in sediment deposits revealed the following trends in each depositional environment.

Near the tip of the spit, metal concentrations are greater in the deeper sediments, coincident with increased silt and clay content (< 1%) and greater TOC, related to lower-energy deposition (marked by well-preserved mussel shells; e.g., SH 6; 40- ~90 cm depth; Fig. 38). TOC and metal concentrations are decreased in the sand-rich sediments at the top (0 - 40 cm) coincident with rapid deposition associated with the mass-wasting deposit. Magnetic susceptibility and coarse-grained composition remain relatively high throughout the core. Results show metal concentrations are related to the TOC content in this section of the bay.

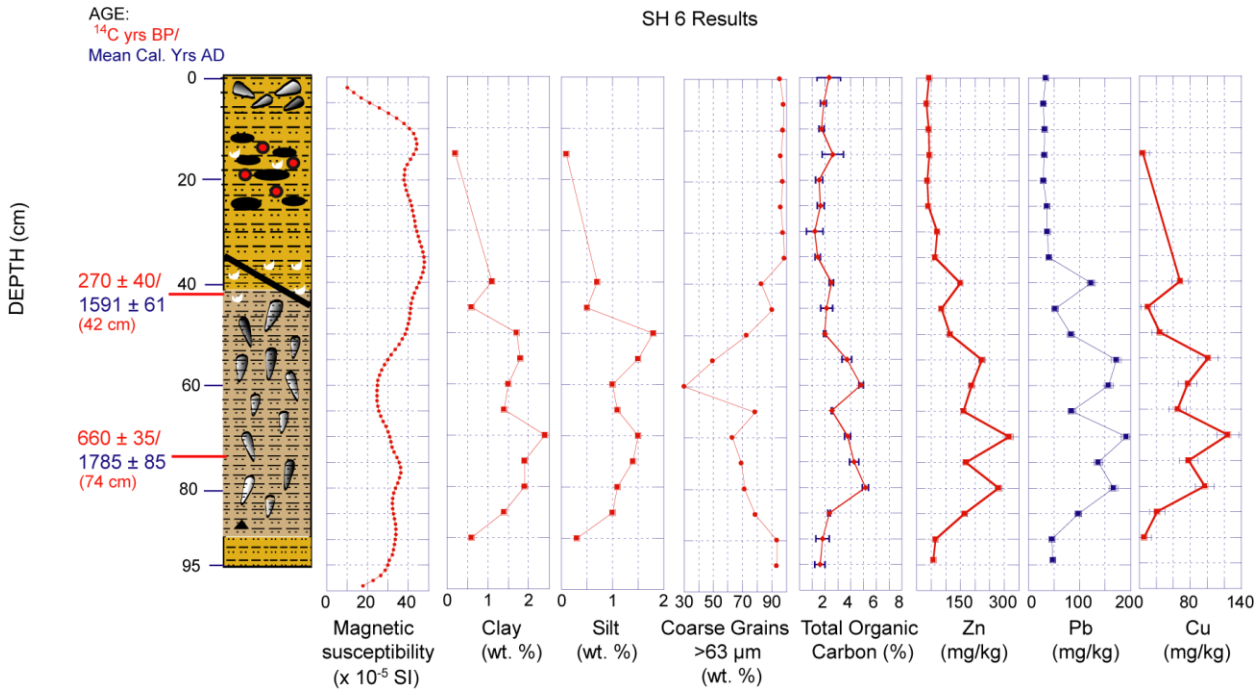

Figure 38: Elements of the study, lithology, magnetic susceptibility, grain size variability, TOC and metals for sediments deposited near the tip of Sandy Hook Spit (Core SH 6). Key for lithology symbols is shown in Figure 27. The metal concentrations are lower in the upper sediments (0 - 40 cm), coincident with low TOC, and a mass-wasting deposit. The deeper sediments exhibit greater metal concentrations coincident with greater TOC, and lower- energy deposition.

Greater metal concentrations in backbarrier sediments (e.g., Core SH 3) are associated with increases in fine grains, and magnetic susceptibility (Fig. 39). The TOC content remains relatively constant throughout the core. This is in contrast to findings near the tip of the spit, where metal concentrations were greater coincident with greater TOC (Fig. 38).

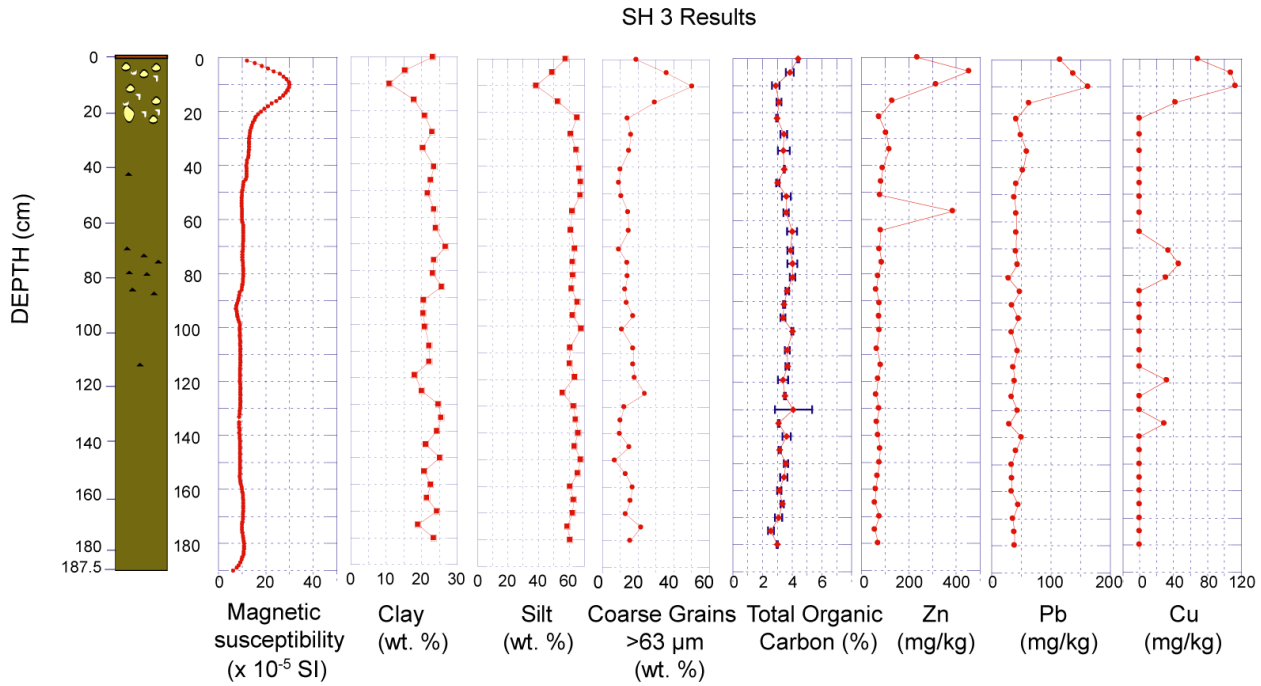

Figure 39: Elements of the study, lithology, grain size variability, magnetic susceptibility, TOC and metals Zn, Pb, and Cu for sediments deposited in the backbarrier setting of Sandy Hook Bay (Core SH 3). Key for lithology symbols is shown in Figure 27.

Furthermore, sediments deposited offshore from the beaches (e.g., Core SH 10; Fig. 40) reveal a pattern of greater metal concentrations that increase with greater magnetic susceptibility, TOC, and clayey silt.

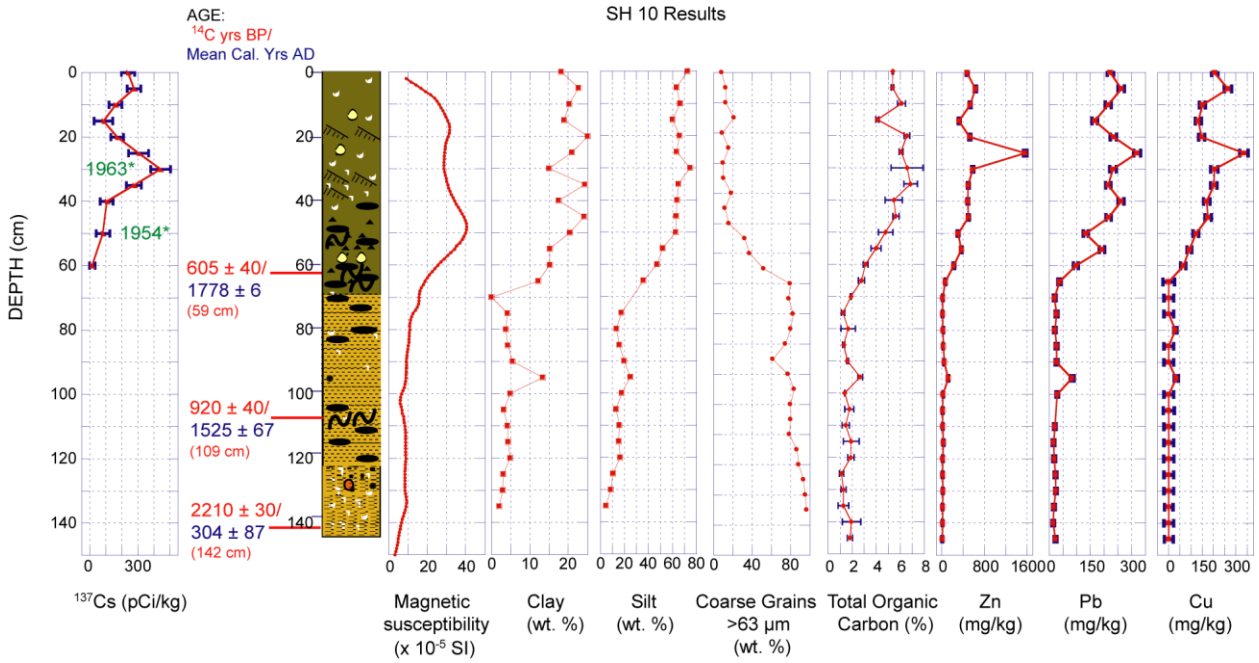

Figure 40: Elements of the study, including lithology, magnetic susceptibility, grain size variability, TOC and metals Zn, Pb, and Cu for sediments deposited offshore from the beaches (Core SH 10). Key for lithology symbols is shown in Figure 27.

DISCUSSION

Sea level Rise in Raritan and Sandy Hook Bays from the Last Glacial Maximum to the Holocene

Sediment facies interpretations, seismic reflection profiles, and a chronology based on radiocarbon dates, were used to decipher the changes that occurred from when the sea was at its lowest level (i.e., during the Last Glacial Maximum), to when it entered the Sandy Hook and Raritan Bays, and as sea level rose to its present-day height.

Late Cretaceous to late Pleistocene Unconformity

In a previous study of the Raritan and Sandy Hook Bays, an unconformity was identified in the sediment cores and interpreted to be a contact between Late Cretaceous and late Pleistocene strata dated as 31.7 ^{14}C ka BP (Vibracore RB S08, 350-370 cm; Gaswirth, 1999). In this study, the unconformity was further confirmed by the radiocarbon dating of mollusk shells and woody material taken from the same Raritan Bay cores. An age of > 48.0 ^{14}C ka BP indicates dead carbon and a late Pleistocene or older age (Vibracore RB 5, 488 cm depth). Results suggest that the unconformable contact between Late Cretaceous and late Pleistocene strata may be evidence of shelf exposure and erosion during lowstands of sea level. This is consistent with Gaswirth (1999) interpretation of a major paleochannel, which remains from fluvial systems that cut into Cretaceous basement sediments during the late Pleistocene.

Late Pleistocene to Holocene Relative Sea Level Rise

Previous studies have shown that the region that is presently the Raritan Bay was located just south of the glacial ice margin, in the proglacial forebulge, and is not influenced by glacial

rebound as much as the Long Island Sound and the Hudson River regions, both depressed under the weight of the glacier (Dillon and Oldale, 1978; Peltier, 1998, Gornitz et al., 2002; Peltier and Fairbanks, 2006; Milne and Mitrovica, 2008; Engelhart et al., 2011a). The up-warped land in the proglacial forebulge is expected to exhibit evidence of subsidence, i.e., more rapid rates of relative sea level rise after deglaciation than areas that were not previously up- warped (e.g., Peltier, 1998; Engelhart et al., 2011a). In contrast, land previously depressed by the glacial ice would present evidence of isostatic rebound (Dillon and Oldale, 1978; Peltier, 1999, Gornitz et al., 2002).

Ages of estuarine bivalves (e.g. *Anomia simplex*) retrieved from sediments which filled a paleochannel (Gaswirth, 1999) suggest sea level first flooded the Raritan Bay region ~6.1 cal. ka BP, consistent with estimates by Fairbanks (1989) and Siddall et al. (2003). This is in contrast to estimates of sea level rise in Long Island Sound (~13.5 to 10.0 cal. ka BP) and the Hudson River (~11.5 cal. ka BP) possibly related to isostatic depression due to glacial ice (Weiss, 1974; Lewis and DiGiacomo- Cohen, 2000; Varekamp, 2005; Peltier and Fairbanks, 2006; Milne and Mitrovica, 2008; Engelhart et al., 2011b). This suggests the study area was not affected greatly by the glacial ice. Furthermore, the mixed ages of shells retrieved from the long Raritan Bay cores (i.e., Core RB 5; 6.9 cal. ka BP at 159 cm depth above 4.1 cal. ka BP at 475 cm depth) indicate abundant reworking of sediments following the initial flooding of sea level into the bay. The reworking is interpreted as being due to shoreline processes.

Studies from other regions have shown that as the sea reached its approximate present-day level, modern coastal sedimentary features (e.g., barriers, spits; infilling of incised valleys) developed and still persist presently around the world (Dabrio et al., 2000; Covelli et al., 2006). For example, the Gulf of Cadiz in Southern Spain has been described by Dabrio et al. (2000) as

an incised valley, which developed during the lowstand of sea level associated with the Last Glacial Maximum. The region was subsequently flooded as sea level rose, creating estuaries (e.g., Odiel-Tinto, Guadalete) that were partially enclosed (similar to the Sandy Hook Bay) by the formation of spits 4,000 to 6,000 years ago due to littoral transport along the Gulf of Cadiz coast (Dabrio et al., 2000). The estuaries have since been infilled with sediments (Dabrio et al., 2000). The Gulf of Trieste, in the Adriatic Sea, has had a similar evolution since the Last Glacial Maximum, with the formation of coastal lagoons due to littoral drift as sea level rose to its present height (Covelli et al., 2006).

Sediment Facies

Facies analysis revealed that the latest Holocene sediment in the bay is dominated by low energy deposition in a back- barrier environment created by the development of the Sandy Hook Spit, interrupted by storm events (e.g., storm surge, fluvial flooding) which have either left unconformities due to erosion, or mass-wasting deposits.

The deposition patterns in the Sandy Hook Bay are comparable to that of the models for partially-closed, bar-built estuaries (typically wave- dominated and microtidal), and bays related to spits (Kumar and Sanders, 1974; Davis, 1983 and references therein; Reinson, 1992; Dalrymple et al., 1992; Dyer, 1994; e.g., Fig. 41). More specifically, bar-built (or bar-mouth) partially-closed estuaries generally exhibit a fining-upwards signature in sections influenced by marine energy as sea level rise continues, filling in the bay with silts and muds (Davis, 1983 and references therein; Reinson, 1992; Dalrymple et al., 1992). Such a fining-upwards trend of grain size is evident in Sandy Hook Bay by thick homogeneous clayey- silt, which is punctuated by

mass wasting deposits (i.e., washover and debris flow deposits) characterized by thinner sections containing concentrations of pebbles, shell fragments, and mud clasts.

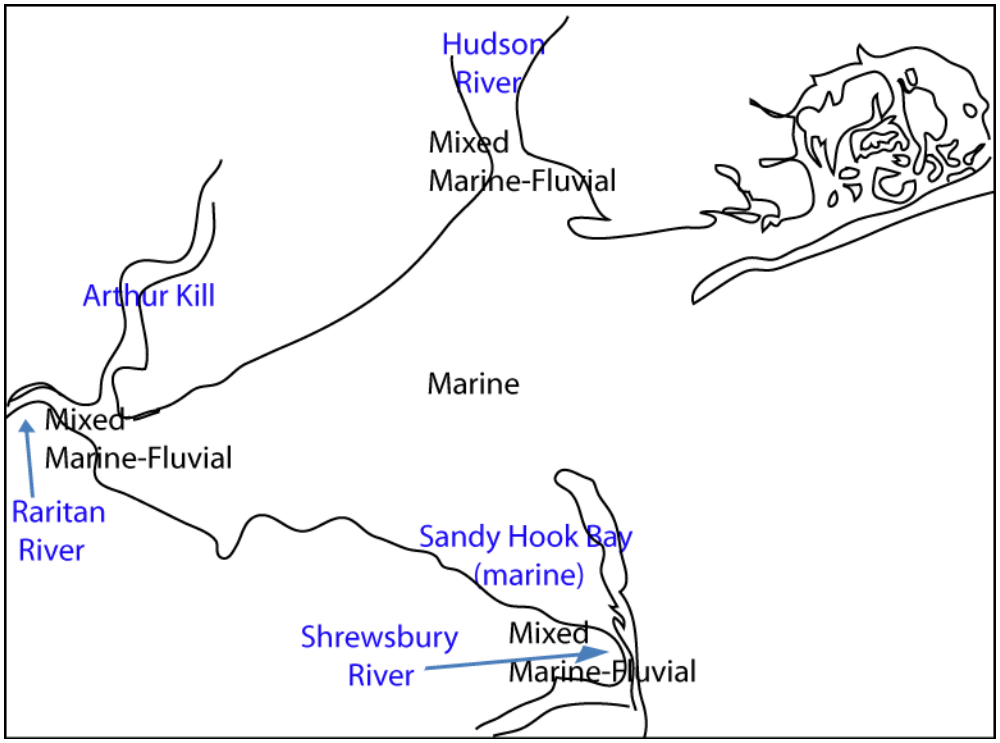

Figure 41: Sandy Hook Bay with depositional environments dominated by mixed marine and fluvial influence labeled according to the model of a typical partially-closed estuary described in Reinson (1992). Map outline modified from GeoMapApp©.

Three sedimentary facies have been characterized based on properties such as grain size variability, components, such as shells, (fragments, and whole), and evidence of soft-sediment deformation (e.g., contorted mud clasts) (Table 9; Figs 42 - 44). The facies include the following:

Facies 1: *fine- grained homogeneous mud to sandy mud with marine shells and gas voids*

Facies 1 is characterized by clayey- silt in the upper sediments of the bay, with contains shell fragments (e.g., thin layers ~10-20 cm thick; single fragments are also found sporadically), whole well- preserved shells include clams, mussels, oysters, rare gastropods, and whole slipper

shells (Fig. 42). In some cases, whole clam shells are ~5 cm diameter, mussels are ~ 6 cm. Rare fish parts (e.g., teeth, piece of vertebrae) are present. Also present are gas voids, sporadic micro-ripples, and areas of oxidized reddish- orange sediment. Rare pyritized woody material and pyritized planktonic foraminifera are present. Aeolian (subrounded, frosted) quartz grains were present in some sections, possibly associated with dunes on the spit.

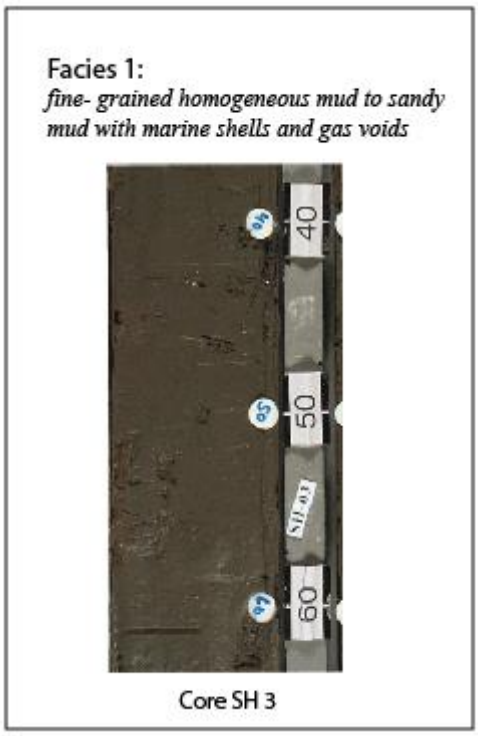

Figure 42: Photograph representing a section of Facies 1, lagoonal deposits; Core SH 3

Interpretation of Facies 1; Lagoonal Backbarrier Deposits

Sediments classified as Facies 1 are interpreted as having been deposited in a relatively low-energy environment setting behind and protected by the Sandy Hook Spit. The sediment originated from mixed sources of suspended marine, fluvial, and in some cases, aolian sediments. These homogeneous fine-grained sediments are comparable to modeled subaqueous backbarrier lagoonal deposits composed of thick sections of mud and silt (Reinson, 1992). The

presence of gas voids indicates the formation of gas bubbles due to the biodegradation of organic matter in the sediments (Schubel, 1974), further suggesting a calm environment, which allows for the build-up of organic-rich sediments.

Foraminifera are present in some sections where low- energy muds are present, suggesting in- situ deposition rather than sediment transport. Rare pyritized planktonic foraminifera are present indicative of reducing conditions in the organic rich mud (Miall, 1984; 1990).

Ripple marks, layers of broken shell fragments, and whole shells indicates occasional occurrences of higher-energy sediment transport. This temporary increase in energy may be due to tidal currents, offshore beach processes, episodes of storm surge, or flooding related to nearby rivers. In some cases thin (~20 cm) deposits at the base of the core (Cores SH 5, SH 9, SH 10) are composed of drier, more indurated sediments, marked by an erosional surface contact with overlying sediments . These sections are interpreted as either related to deposition when the spit was shorter and those locations were less protected from open ocean, or may be indicative of a erosion related to a past storm event (as opposed to a storm event that causes increased deposition to occur).

***Facies 2**: Muddy very fine- to medium sand with contorted mud clasts*

Facies 2 is characterized by muddy very fine- to medium sand with mud clasts (some of which are contorted), and sporadic gas voids (Fig. 43). Also present are rounded pebbles (quartz composition), fish teeth, and a single red bed sandstone fragment ~7 cm in diameter, flat, trapezoidal in shape, with subrounded edges. The muddy clasts are more reddish in color, and

have a slightly greater total organic content than the muddy sediments of Facies 1. Sporadic sandy pockets are present. The absence of shell fragments is noted.

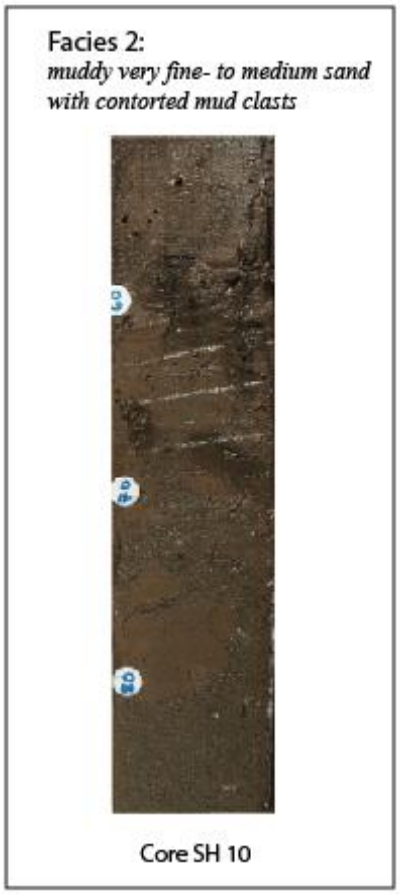

Figure 43: Photograph representing a section of Facies 2, debris flows; Core SH 10

Interpretation of Facies 2; Debris Flow Deposits

Facies 2 is interpreted as debris flow deposits related to storm events, possibly due to flooding from upriver, which affected the distal beach environments. TOC results show that the floating mud clasts (e.g., SH 10, 122 cm depth) have a higher TOC content than the surrounding matrix, suggesting a terrestrial origin for the mud clasts (e.g. transported from a tributary). The absence of shell fragments in the deposits also suggests a non-marine origin.

The single, large sandstone fragment is interpreted as having been eroded from the underlying Englishtown sand (an Upper Cretaceous rock formation containing sand beds cemented by iron oxide), related to a meander in a paleochannel (6-13 m deep) near where Core SH 10 was recovered (Lewis and Kummel, 1940; Minard, 1969; Gaswirth, 1999). An alternative interpretation is that the fragment originated upstream from Cretaceous sandstones exposed along the river-beds of the Navesink and Shrewsbury Rivers, or along the shore of the Atlantic Highlands, NJ (Cook, 1889; Lewis and Kummel, 1940). The large size of this fragment, and the lack of other similar samples in the cores, suggests the mode of transport was a short interval of discharge with high energy (such as due to a flood) from the river. The flat, oval- shape, and sub-rounded edges further suggest fluvial transport (Boggs, 2001).

Facies 3**:** *muddy medium sand with mud clasts, shell fragments, and pebbles*

Facies 3 is a thin deposit (20- 30 cm thick) composed of described as muddy medium sands which contain floating mud clasts, well- rounded pebbles with a surface oxidization residue, and shells fragments (Fig. 44). A sharp angular contact with underlying sediments is noted.

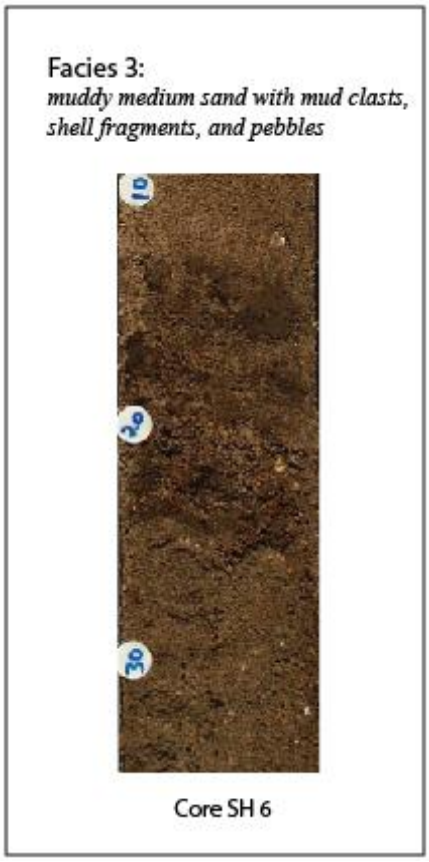

Figure 44: Photograph representing a section of Facies 3, washover deposit; Core SH 6

Interpretation of Facies 3; Washover Deposit

Facies 3 is interpreted as a washover deposit based on the presence of an abrupt, angular dipping contact at the base of the deposit, shells and shell fragments, thin concentrated layer of pebbles, and mud clasts, and is comparable to descriptions of washover deposits in previous studies (Miall, 1984; 1990; Reinson, 1992; Sedgwick et al., 2003 and references therein; Foxgrover, 2009 and references therein). In contrast to Facies 2, interpreted to be related to fluvial flood deposition, Facies 3 contains shells and is therefore interpreted as a washover deposits. Washover deposits generally form when storm surge breaches a barrier or spit, resulting in the transport of barrier (i.e., from erosion of dunes) sediments into the backbarrier facies (Reinson, 1992). There is evidence seen on aerial photographs and maps of historic

shorelines of a prior overwash event related to Sandy Hook Spit that formed the washover fan Plum Island located on the eastern coastline of Sandy Hook Spit (Fig. 45; USGS, 2003).

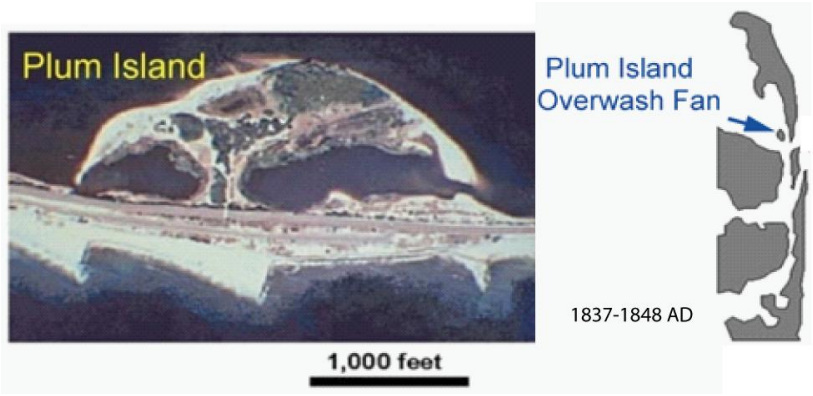

Figure 45: Aerial photograph of Plum Island, and a map showing its location along the Sandy Hook Spit. Plum Island has been identified as a washover deposit. (Modified after USGS, 2003).

The washover deposit both overlies and underlies deposits classified as Facies 1. The older sediment below the washover deposit (upper boundary marked by an abrupt angular dipping contact) is characterized by a thick sandy mud deposit with whole, well-preserved mussel shells (~6 cm diameter; Fig. 46). The sediments overlying the washover deposit (at the top of the core) contain small (1.5 cm diameter; Fig. 46) whole, well-preserved mussels which suggest the recolonization of the previous mussel community. Upon further investigation of the mussel species, it is apparent that the presence of smaller mussel shells (*Mytilus edulis;* blue mussels) is related to a regrowth of the community rather than a shift to a different mussel species, which would have suggested a habitat shift. This process indicates that the washover deposit is related to a short-lived event that buried the mussels in situ, and once deposition associated with non-storm conditions was restored, the mussel community was reestablished.

Mussel shell from the 42-95 cm depth interval Mussel shells from the 0-13 cm depth interval

Figure 46: Photographs of Mytilus edulis (blue mussel) shells found in muddy-sandy beds recovered from near the tip of the spit (Core SH 6, Facies 1). The mussels taken from above the washover deposit are smaller than those found below the washover deposit, indicating a recolonization of the mussel community after a mass-wasting event.

Type of Deposit	Facies	Core	Depth Intervals
muddy- sandy mussel beds	1	SH 6	0-13; 42- 95 cm
mud beds	1	T1	40- 83 cm
mud beds	1	SH 5	0-5; 15-143 cm
mud beds	1	SH 3	0-2; 24–187.5 cm
mud; muddy- sandy beds	1	SH 9	0-5; 22-110 cm
mud; muddy- sandy beds	1	SH 10	0-18; 83- 100 cm
mud; muddy-sandy beds; related to tidal currents near the tip of the spit	1	T1	0- 40; 83- 138 cm
possible storm deposit; past deposits related to less-protected area	1	SH 5	5-15; 143- 165.5 cm
possible storm deposit	1	SH 3	2- 24 cm
possible storm deposit; deposition related to beach processes	1	SH 9	5-20; 195- 215.5 cm
deposition related to beach processes; mouth of Shrewsbury River	1	SH 10	18-40; 125-145.5 cm
debris flow deposit	2	SH 9	110- 195 cm
debris flow deposit	2	SH 10	40- 83; 100-123 cm
washover deposit	3	SH 6	13-42 cm

Table 9: Sedimentary deposits and facies classification in the Sandy Hook Bay.

Growth of the Sandy Hook Spit

The Sandy Hook Spit was formed during the Holocene by northward movement of sediment along the New Jersey coast due to longshore currents (Ashley et al., 1986 and references therein; van Gaalen, 2004 and references therein; Hoffman, 2004; Rosati, 2005 and references therein; Pendleton et al, 2005; Psuty and Pace, 2008 and references therein).

Widening of the spit is related to overwash events, which formed washover fan deposits (Davis, 1983).

The characterization of the growth of the spit over time has previously been documented using aerial photography, including the direction of growth of the tip as well as widening and/or narrowing of the spit (Minard, 1969; Pendleton et al., 2005). As discussed in detail in the Background chapter, the rate of growth of the spit has been estimated to be ~9.4 m/yr (~31 ft/yr) using aerial photography and location of the lighthouse on the Sandy Hook Spit (Hoffman, 2004).

The data collected and analyzed documents changes over time and in depositional energy at each core site in the bay. From north to south along the spit, the core presently located by the tip of the spit is composed of coarser sediments, as it is exposed to wave activity, and tidal currents. It is also located near a channel in the bay (Core SH 6). This suggests that when the Sandy Hook Spit was younger and shorter, core sites to the south would have at one time been near the tip of the spit. This is illustrated by Core T1 and SH 5, which have coarser sediments at the base with fine sediment above.

Using Cores T 1 and SH 5 as references for the time it took for the spit to grow, the fining upwards shift occurs at an approximate depth of 100 cm and was dated as 514- 539 cal. yrs BP (1423 mean age AD). This date is interpreted as the approximate timing of when the tip of the spit grew past the location of Core T 1, resulting in its fining-upward trend more closely associated with backbarrier deposition. The spit grew approximately ~1875 m (derived from Fig. 7; Background chapter; (Fig. 47)) from 1423 AD to 1997 (the year of core recovery). The calculated growth therefore occurred at an approximate rate of ~3.3 m/yr. Based on Core SH 5, dated as 539- 625 cal. yrs BP (1368 mean age AD) at a depth of 104 cm, the tip of the spit grew

~2300 m at a rate of 3.7 m/yr (Fig. 47). Dates derived from two different cores indicate a rate of growth of the spit that is a far slower rate than estimated using the Sandy Hook Lighthouse as a marker for growth, as well as estimates made using the change in the shoreline of the spit (6.8-9.4 m/yr; Fig. 7, Background Chapter; Hoffman, 2004; Pendleton et al., 2005). The discrepancy in growth rate may be due to changes that occur over short time periods to a coastline, including accretion and erosion, which may result in less accurate growth estimates derived from aerial photos.

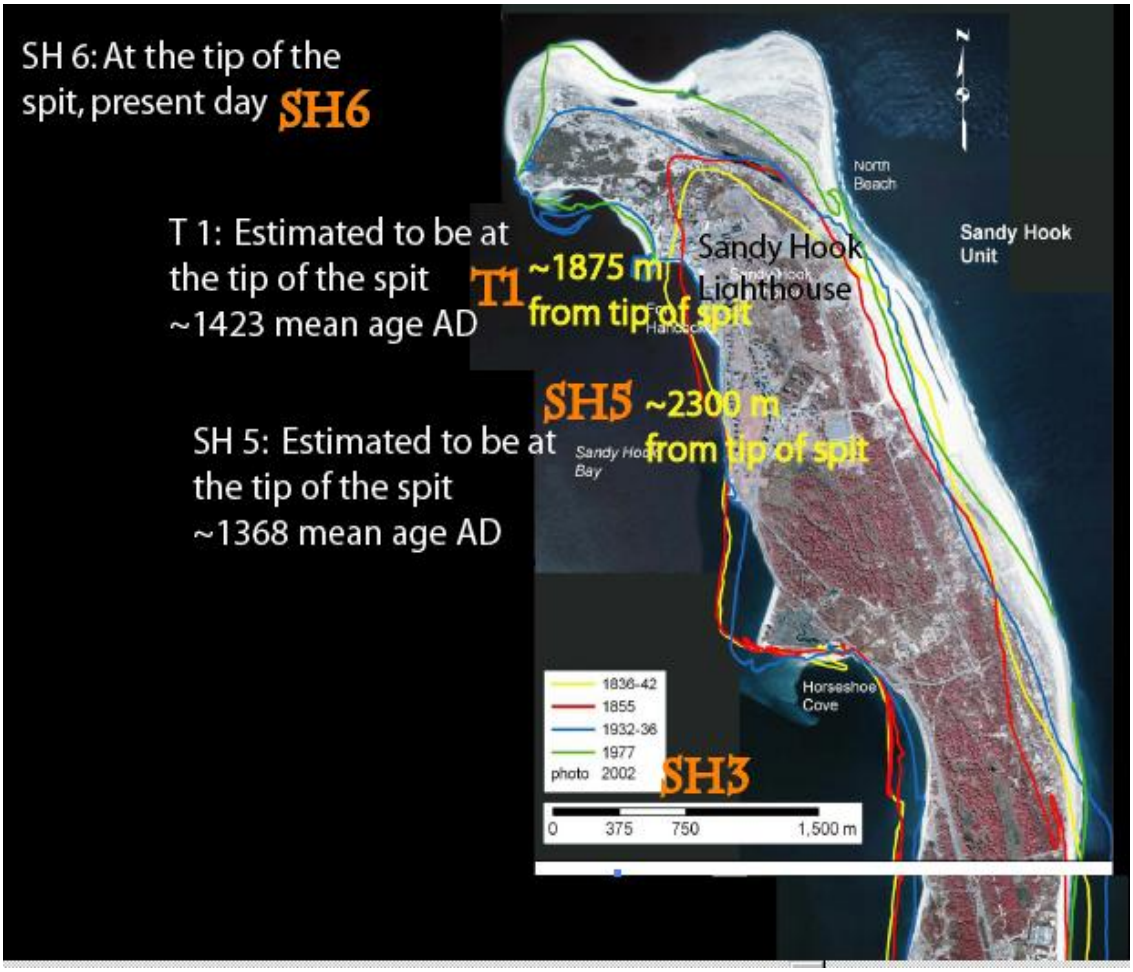

Figure 47: A compilation of aerial photos and historical data of Sandy Hook, New Jersey, modified from Pendleton et al. (2005, with permission). See Figure 7 for details. Estimated dates (mean age AD) are shown of when Cores SH 5, and T 1 were at the tip of the spit before it grew to its present-day position. Distance from the present-day tip of the spit to Cores SH 5, and T 1 are shown in meters (derived from the bar scale provided with the aerial photograph).

Sedimentary Record of Storms

The mass wasting deposits (i.e., washover, debris flow deposits) exhibit characteristics typical of intervals of increased energy (e.g., concentrations of pebbles, broken shell fragments, distorted mud clasts) and are unconformable with sediments related to lower-energy transport and deposition (Miall, 1990). These deposits are interpreted as having been deposited during storm events. By identifying and dating the debris flow and washover deposits, the objective was to determine the effects of storms on the area (i.e., deposition, erosion), to link the deposits with previous storm events that have affected the Northeastern coast, and to quantify the frequency of storm occurrence in the study area.

Six deposits of reworked sediments (i.e., washover and debris flow deposits) found in the Sandy Hook Bay cores were identified as evidence of storm occurrences. These deposits include (with mean age AD): Deposit SH10-3 (304 AD), Deposit SH9-2 (970 AD), Deposit SH9-1 (1399 AD), Deposit SH10-2 (1525 AD), Deposit SH6-1 (1591 AD), and Deposit SH10-1 (1778 AD), and are described in detail in the Results Chapter.

Links to Historical and Prehistorical Storms

The storm deposits identified in this study exhibit similar characteristics to those identified in previous studies of the Northeast coastal region described as having distinct sand layers interbedded among fine-grained mud with sharp contacts at the lower boundaries of the deposits(Donnelly et al., 2001a; 2001b; 2004; Dougherty et al., 2004; Buynevich et al., 2004; Scillepi and Donnelly, 2007), as well as "soft sediment deformation in adjacent muds (Donnelly et al., 2004)." Past studies focused on marsh and backbarrier sediments where evidence of storm activity (e.g. washover events related to storm surge) is expected to be found (Donnelly et al.,

2001a; 2001b; 2004; Buynevich et al., 2004; Dougherty et al., 2004; Scillepi and Donnelly, 2007). The Sandy Hook Bay cores were also recovered from a backbarrier environment, along with areas proximal to beaches and the mouth of the Shrewsbury River, which makes it likely that evidence of storm events would be preserved in the sediment record.

More specifically, the deposit related to Facies 3 (washover deposits; Core SH 6) is comparable to washover deposits described in previous studies (Donnelly et al., 2001a; 2001b; 2004; Dougherty et al., 2004; Buynevich et al., 2004; Scillepi and Donnelly, 2007), as it is composed of muddy very fine sand with concentrated pebbles, angular shell fragments, and mud clasts that overlies homogeneous muddy sediments with a well-preserved mussel population buried in- situ. The sharp, angular contact at the base of the washover deposit further suggests a rapid interval of coarser-grained deposition. Soft sediment deformation in the form of contorted mud clasts (with slightly higher TOC than surrounding muddy sediments) identified in sediment cores as debris flow deposits recovered from near the beaches, and near a subaqueous channel (e.g., Core SH 10, Gaswirth, 1999; Sheridan, unpublished data), suggesting a fluvial source related to storm- related river flooding.

The storm deposits dated as 970 AD, 1399 AD, 1525 AD, 1591 AD, and 1778 AD can be linked with prehistoric storms, and recorded hurricanes, that struck parts of New Jersey and Long Island during the periods of 550- 1400 AD, 1034-1190 AD, 1278-1438 AD, 1477-1642 AD (or a 1693 hurricane), and 1788 AD and/or 1821 AD (Donnelly et al., 2001b; 2004; Scillepi and Donnelly, 2007; Table 10). More specifically, the 970 AD event is correlated with deposits found at Brigantine Beach, NJ (550- 1400 AD), and Hicks Beach, Long Island, NY (1034-1190 AD) (Donnelly et al., 2004; Scillepi and Donnelly, 2007; Table 10). The 1399 event can be correlated with hurricane deposits discovered at Whale Beach, NJ (1278-1438 AD) suggesting

that the hurricane impacted ~150 km of coastline (Donnelly et al., 2001b; Table 10). The deposits dated as 1525 AD and 1591 AD, from two separate cores (SH 6, SH 10) indicates there was a storm event that occurred in the study area (Table 10). This storm is possibly related to an event found in Hicks Beach, NY (1477-1642 AD) which the authors interpreted to be related to either a prehistoric 16th century storm, or a 1693 hurricane (Scillepi and Donnelly, 2007; Table 10). The 1778 AD storm deposit is correlated to deposits found in both Whale Beach, and Brigantine Beach, NJ, and western Long Island, NY, which were attributed to either a 1788, or 1821 hurricane (Donnelly et al., 2001b; 2004; Scillepi and Donnelly, 2007; Table 10).The span of the deposits related to this storm (whether it was the 1788, or 1821 AD hurricane) indicates its large impact of at least ~250 km of coastline.

Storm Deposit/ Type (this study)	**Mean Age (AD)**	**Correlated with Previously Identified Storm Deposits; Location and Ages (AD)**	**Correlated with Documented Historic Storms**	**Reference**
SH9-2/shell fragment layer (possible storm lag deposit)	970 AD	Brigantine Beach, NJ (550-1400 AD); Hicks Beach, Long Island, NY (1034-1190 AD)	prehistoric storm	Donnelly et al., 2004; Scillepi and Donnelly, 2007
SH9-1/ debris flow from river flood	1399 AD	Whale Beach, NJ (1278-1438 AD)	prehistoric hurricane	Donnelly et al., 2001b
SH10-2/debris flow from river flood	1525 AD	Hicks Beach, NY (1477-1642 AD)	prehistoric 16th century storm, or a 1693 hurricane	Scillepi and Donnelly, 2007
SH6-1/ washover deposit	1591 AD			
SH10-1/ debris flow from river flood	1778 AD	Whale Beach, and Brigantine Beach, NJ, Western Long Island, NY	1788, or 1821 hurricane	Donnelly et al., 2001b; 2004; Scillepi and Donnelly, 2007

Table 10: Compilation of storm deposits identified and dated in Sandy Hook Bay as compared to storms documented in previous studies as well as historic storms.

Storms that are more recent were dated using methods involving short-lived radioisotopes, (i.e., ^{137}Cs) discussed in previous studies (Olsen et al., 1978; Williams et al., 1978; Olsen et al., 1981; Olsen et al., 1984- 1985; Bopp and Simpson, 1989). An age of 1963 AD was assigned for the upper 10 - 30 cm of cores recovered from near the beaches (i.e., Cores SH 9, SH

10), and the age of 1954 AD was assigned to the upper 20- 50 cm, indicating vastly different rates of sedimentation for the time interval of 1954- 1963. Based on this chronology, the broken shell layers identified in the upper sediments (e.g., Cores SH 3, SH 5, SH 9; upper 20 cm) may have been deposited during the "Ash Wednesday Nor'easter" of 1962 which has been documented as having a large impact on the local study area (Dolan et al., 1988; Zhang et al., 2002). The hiatuses that separate the storm deposits within the cores are interpreted to be related to the time it took for the shoreline to equilibrate after large-scale erosional events so that sediments could be preserved, rather than a measure of how many storms have hit the region over time. These hiatuses include large unconformities found in the sediment which range in age from 250 to 1220 yrs. Previous studies discuss similar results of a recovery period of the beach profile after an erosional event (Donnelly et al., 2001a; Zhang et al., 2002; Hill et al., 2004). There is great variability in proximal depositional environments through time. Cores recovered within close proximity to each other do not show evidence of preservation of the same storms, which is also an observation made in studies of other regions (Donnelly et al., 2004). This is consistent with the conclusion determined by Donnelly et al. (2004) that large sections of a coast need to be examined and high density coring needs to be conducted in order to document all the storms that have struck a coastal region.

It is noted that recent studies have examined the possibility that a prehistoric tsunami event might have impacted the area encompassing the New York- New Jersey coasts estimated to have occurred ~ 2300 years BP (Goodbred et al., 2006; Krentz et al., 2008; Cagen and Abbott, 2009). In this study, a potential alternative hypothesis (other than being a storm deposit) is that the unconformity associated with Deposit SH10-3 (304 AD) could be related to this type of event.

Temporal and Spatial Variability of Contaminants Related to Sedimentary Processes

Urban estuaries can be greatly impacted by contamination from anthropogenic activities such as commercialization and industrialization (e.g., Bothner et al., 1998; Seger & Davis; 1984; Kennish, 1997; Buchholtz ten Brinket al., 1997; Plater et al., 1998; Rosales- Hoz et al., 2003; Tovar- Sánchezet al., 2004; Prudêncio et al., 2007). More specifically, the Hudson-Raritan Estuary including the NY/NJ Harbor, has been affected by the surrounding urbanized metropolitan region and its sources of pollution (e.g., heavy metals including lead, zinc, and copper) (Breteler, 1984; Mueller and Werme, 1984; Breteler et al., 1984; Connor et al., 1984; Long et al., 1995; Crawford et al., 1995; Wolfe et al., 1996 and references therein; Sanudo-Wilhelmy and Gill, 1999; Mecray et al., 1999; Feng et al., 1998; 2002; and references therein; Adams and Benyi, 2003; Tovar- Sánchez et al., 2004; Kenna et al., 2006; Nitsche et al., 2010).

Prior to 2004, research conducted in the Raritan Estuary has been focused primarily on the water quality (e.g., Greig and McGrath, 1977; NJDEP, 1998; Sañudo- Wilhelmy and Gill, 1999; Zimmer, 2004), and contamination of the surface sediments in the estuary (e.g., Long et al., 1995; Wolfe et al., 1996; Cohen et al., 2000; Adams and Benyi, 2003). A main objective of this study was to determine how metals have accumulated over time in a shallow urban bay that is vulnerable to natural processes (e.g., storms, tidal circulation, growth of a sand spit, fluvial input). Interpretations can be made based on the compiled results as to why metals are being concentrated in some locations but not in others.

It is important to note that elemental analyses for this study were conducted using a hand-held XRF and a wet-chemistry total digestion analysis was not conducted. As a result, it is noted that concentrations of the metals in the sediments discussed here may be greater than the results from the XRF may show.

Temporal and Spatial Patterns of Heavy Metal Contamination in Sandy Hook Bay

Results show great variability in the burial of contaminants even among sites that are within close proximity to each other, indicating that the processes that occur in the bay (i.e., frequent reworking of sediments due to mixed influences such as tides, storm energy, and river input) play a major role in contaminant accumulation, perhaps having a greater impact than proximity to sources of pollution. As described in the Results chapter, metals are present in low, constant concentrations in the older sediments, and increase in the younger sediments (i.e., 0-~80 cm) of the bay. The minimum values are interpreted to be background concentrations related to natural sources, such as weathering of continental rocks (Windom et al., 1989; Kennish; 1997; Eby, 2004; Bianchi, 2007 and references therein).

The following is an interpretation of how metal concentrations (e.g., Pb, Cu, Zn) vary by depositional environment (Figs. 48 - 50):

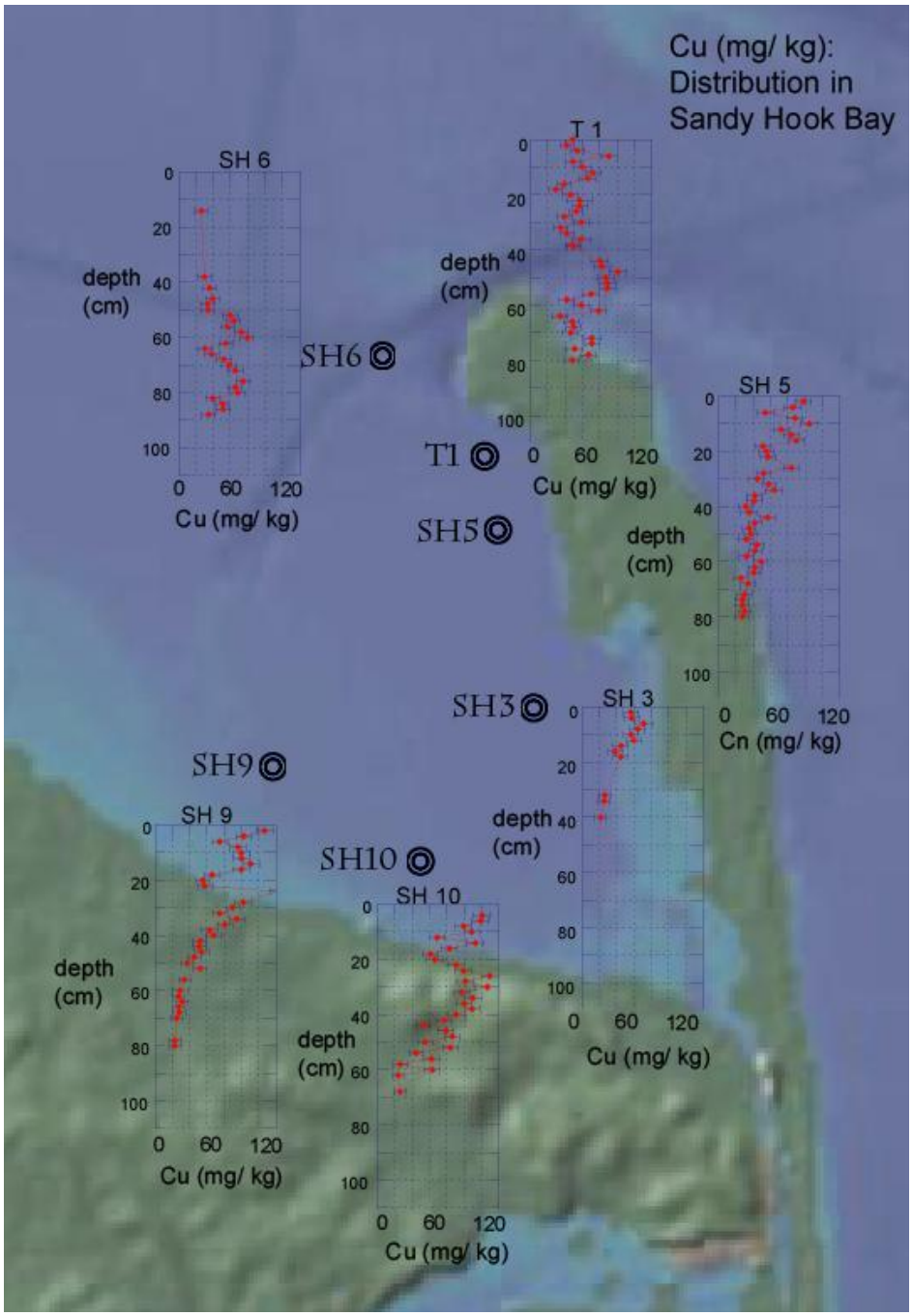

Figure 48: Spatial and temporal variability of copper concentrations in Sandy Hook Bay sediments; at resolution of 2 cm.

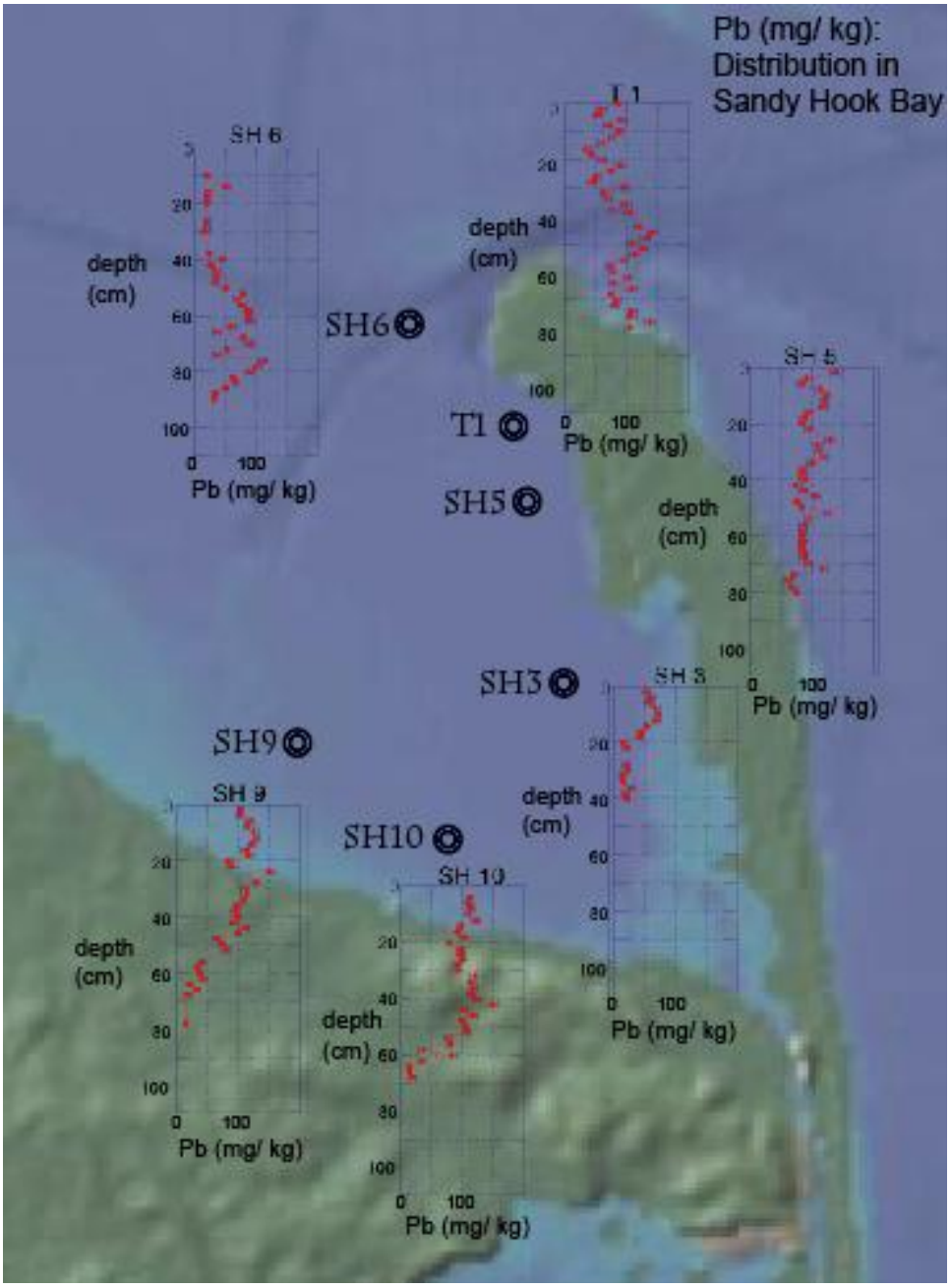

Figure 49: Spatial and temporal variability of lead concentrations in Sandy Hook Bay sediments; at resolution of 2 cm.

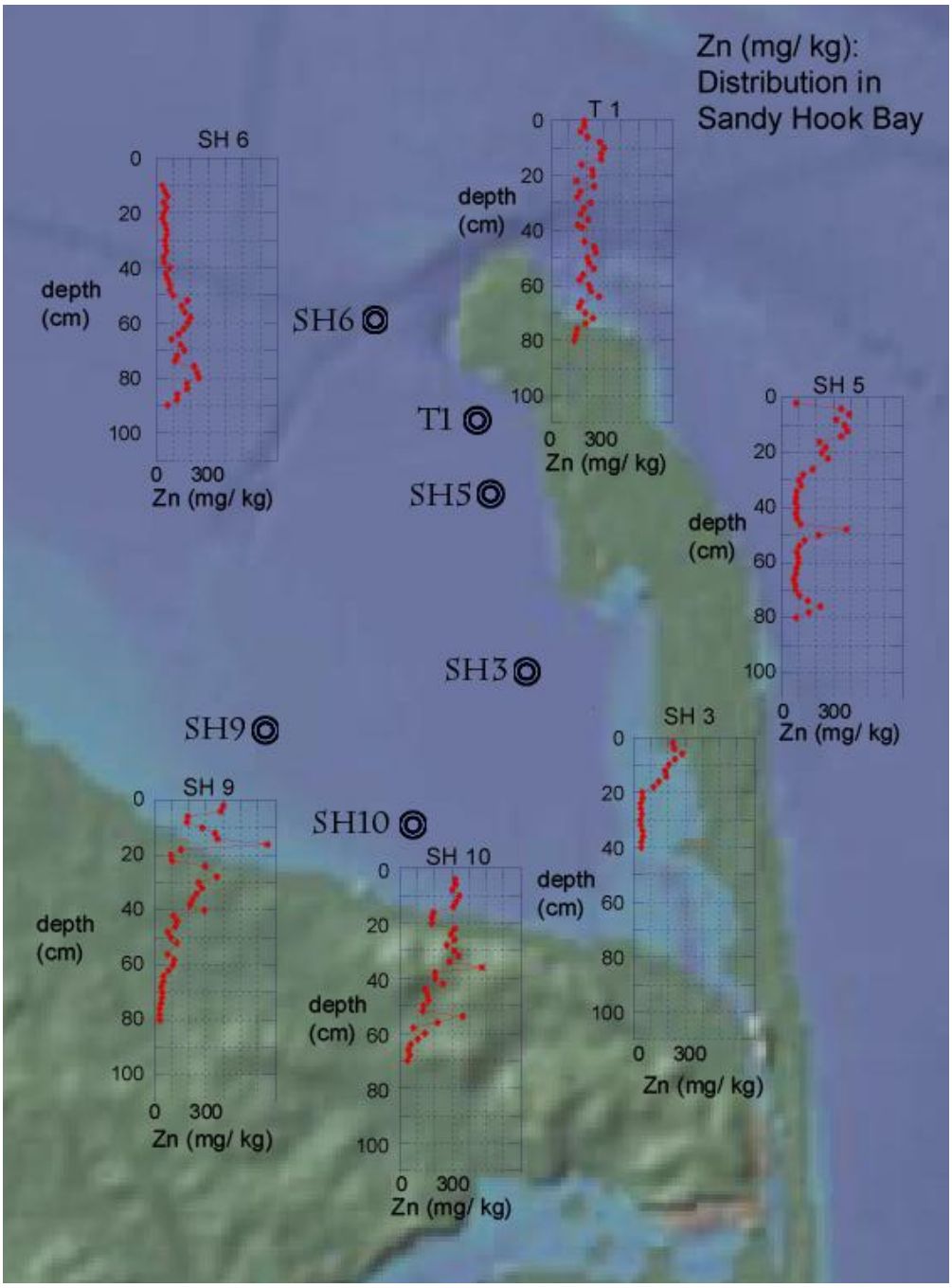

Figure 50: Spatial and temporal variability of zinc concentrations in Sandy Hook Bay sediments; at resolution of 2 cm.

Sandy Hook Spit

Proximal to the tip of the spit metals were detected at greater concentrations in the deeper sediments (Figs. 48 - 50) where the sediments are less disturbed.

Backbarrier

In contrast to the tip of the spit, the sediments recovered from the backbarrier and proximal to the mouth of the Shrewsbury River are characterized by greater metal concentrations in younger (upper) sediments (Figs. 48 - 50), with lower concentrations in the deeper sediments. The long-term deposition of fine-grained backbarrier sediments reveals the impact of anthropogenic activities more concisely than sections of the bay where low-energy deposition has been interrupted by mass-wasting events.

Beaches

Metal concentrations in sediments recovered from offshore from the New Jersey beaches, and proximal to the mouth of the Shrewsbury River are greater in the upper sediments (Figs. 48 - 50), with lower concentrations (similar background levels as seen in the backbarrier) in the deeper sediments. The metal concentrations here are greater than those detected elsewhere in the bay, which is interpreted to be a record of urban runoff from the shore, and/or discharge from the Shrewsbury River.

Background vs Anthropogenic Levels of Metal Concentrations

Background concentrations for Pb, Cu, and Zn derived from Sandy Hook Bay sediments are comparable to values determined in previous studies of nearby waterways. This includes background values from the Hudson Estuary that range from 15.4 (+/- 2.5) to 25 ppm Pb, 14.4 to 25 ppm Cu, and ~80 ppm Zn (William et al., 1978; Bopp and Simpson, 1989; Hirschberg et al., 1996; Kenna et al., 2006). Background levels of Pb in Long Island Sound were found to be 20 ppm (McHugh et al., 2007).

Concentrations of Pb, Zn, and Cu greater than background levels in Sandy Hook Bay sediments are based on correlations with other proxies of anthropogenic sources (e.g., magnetic susceptibility, Cs^{137}) and as compared to results from previous studies (e.g., Bopp and Simpson, 1989; Bopp et al. 1993; Hirschberg et al., 1996; Plater et al., 1998; Benoit et al., 1999; Hoffman et al., 1999; Kapička et al., 1999; Chan et al., 2001; Martins et al., 2007, Nitsche et al., 2010).

Radionuclides as a Proxy for Anthropogenic Activities

The greater concentrations of metals in the upper sediments recovered offshore from the beaches correspond with an age of 1950's (and younger) based on radionuclide chronology, documenting an anthropogenic source of the metals in the upper sediments of Sandy Hook Bay. Results show the pattern of variability to be the most similar between copper and ^{137}Cs which may be related to bioturbation or reworking of the sediment at ~20 cm depth (Fig. 51).

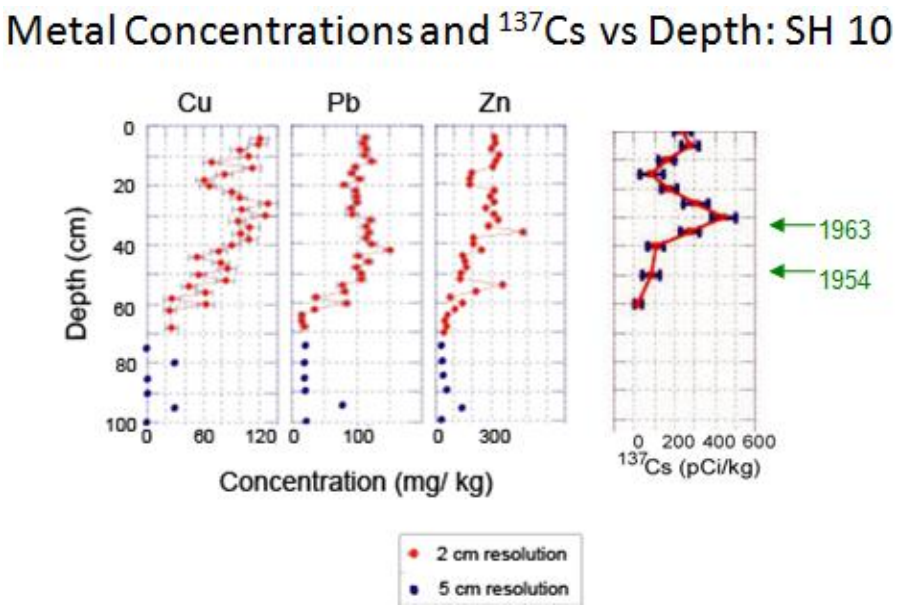

Figure 51: The chronology based on the radionuclide ^{137}Cs varies similarly to metals, specifically copper. The greater values of metals coincident with ^{137}Cs suggests anthropogenic sources of the metals in sediments estimated to be from the 1950's and younger.

Magnetic Susceptibility as a Proxy for Anthropogenic Activities

The correlation between increased magnetic susceptibility and greater concentrations of metal contaminants, as well as lower magnetic susceptibility with uncontaminated sediments, has led to magnetic susceptibility being used as a proxy for anthropogenic activities (e.g., Kapička et al., 1999; Chan et al., 2001; Martins et al., 2007 and references therein).

Results from this study and previous studies conducted in similar environments elsewhere (e.g., Santos Estuary, Brazil; Penny's Bay, Hong Kong) support the use of magnetic susceptibility as an indication of anthropogenic activity and that it further correlates with an increase in metal concentrations (Fig. 52; e.g., Chan et al., 1998; 2001; Martins et al., 2007).

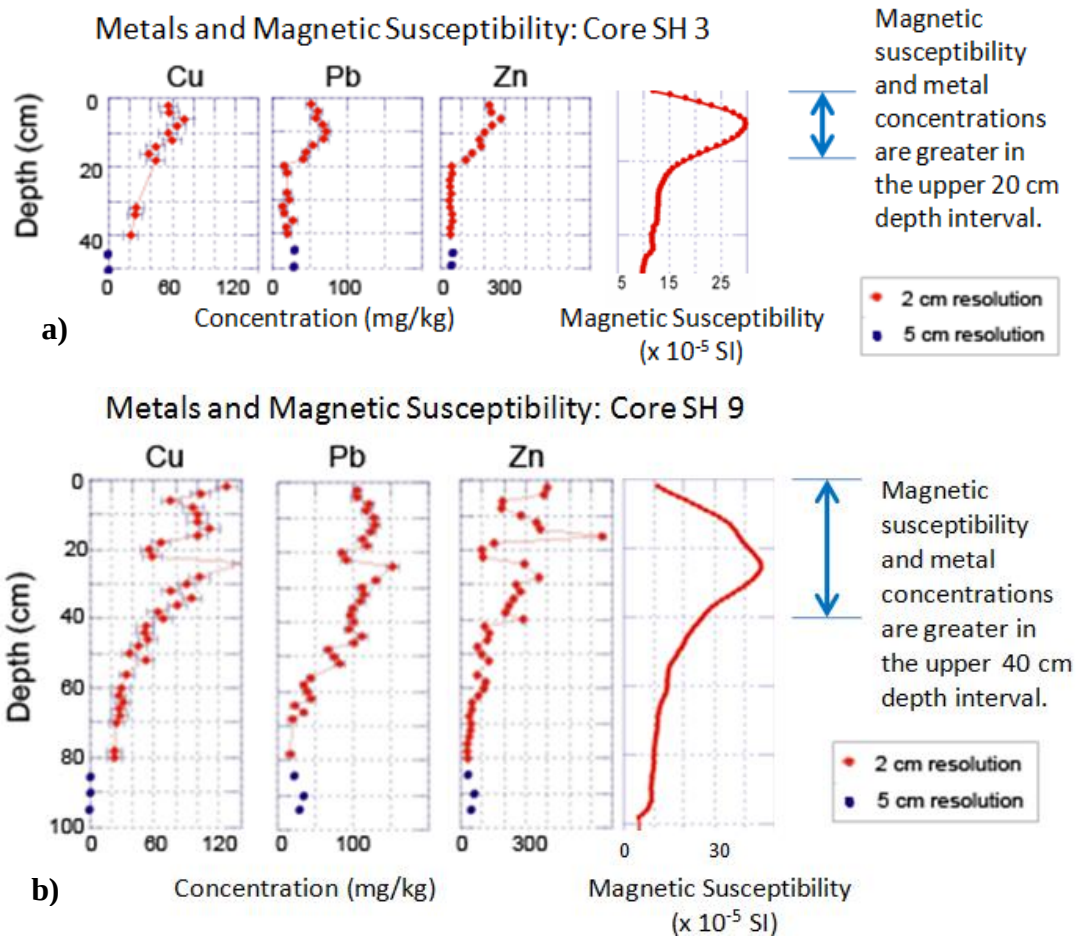

Figure 52: a) The depth interval (0-20 cm) at which metal concentrations (i.e., Cu, Pb, Zn) are greatest coincides with the depth interval of the greatest magnetic susceptibility in sediments recovered from the backbarrier region of the Sandy Hook Bay (Core SH 3) b) The depth interval (0-40 cm) at which metal concentrations (i.e., Cu, Pb, Zn) are greatest coincides with the depth interval of the greatest magnetic susceptibility in sediments recovered from near the beaches (Core SH 3).

Contaminant Transport and Deposition

Sediment properties can play a significant role in how certain contaminants are transported and buried (Kennish, 1997; Mecray et al., 1999; Paulson, 2005). The metal contaminants are coincident with increased TOC and increases in fine-grained sediments, due to the tendency of metals to adhere to organic matter and clays (Olsen et al., 1984; Lick and Huang, 1993; Santschi et al., 1997; Hedges and Keil, 1999; Sañudo-Wilhelmy and Gill, 1999; Cohen et al., 2000; Brady and Weil, 2002; Cantwell et al., 2002; Kersten and Smedes, 2002; Eby, 2004;

Bianchi, 2007). Previous studies conducted worldwide (e.g., Guanabara Bay, Brazil; Victoria Harbour, Hong Kong; Berre Lagoon, France) also found a strong correlation of TOC with metal concentrations (Neto et al., 2006; Accornero et al., 2008; Tang et al., 2008).

The distribution of TOC varies by depositional environment, indicating a strong influence from depositional and erosional processes. The overall trends of TOC (average value for each core) show TOC is greatest in the backbarrier environment and lowest in areas with higher energy processes including, near the tip of the spit, offshore from the beaches, and near the Shrewsbury River (Fig. 53).

Results show the overall average TOC in the Sandy Hook Bay to be 3.39% (ranges from 1 – 8 %), which is comparable to previous studies of the Sandy Hook Bay which found TOC to be 2-3% (NOAA, 1995) and an average of 3.53% in the Lower Bay surface sediments (calculated from organic matter result of 6.09%; Coch, 1986). TOC content was found to be similar, but slightly higher, in sediments from neighboring waterways including Western Long Island Sound (≥ 3%; Poppe et al., 2000; 3.8- >10 %; McHugh et al., 2007) and the Lower East River (3.6- 4.8%; NOAA, 1995). The increased values of TOC in the upper sediments are interpreted to be from anthropogenic inputs to the waterways similar to those obtained for western Long Island Sound (Poppe et al., 2000; McHugh et al., 2007).

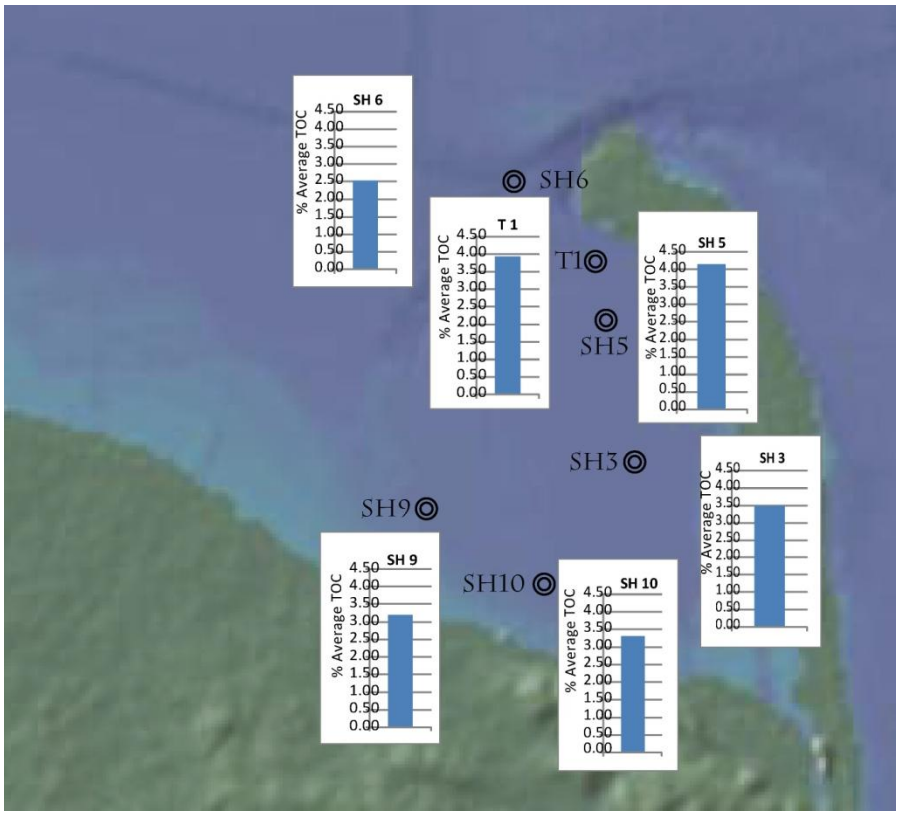

Figure 53: Bar graphs represent the average value of TOC for all sediment samples recovered from each core. Average TOC is greatest in the northern section of the backbarrier where depositional energy is relatively low. Average TOC is lower at the tip of the spit and offshore from the beaches, where energy is greater.

Multiproxy Approach to Approach to Interpretations of Metal Distribution

Compilations of metal concentrations, magnetic susceptibility, grain size variability, total organic carbon, lithology, and age data revealed that sections interpreted as higher energy deposits tend to be related to lower levels of metal contaminants (Figs. 38- 40). This is apparent in sediments near the tip of the spit (SH 6) where the sediment above the sharp angular contact, described as a mass-wasting deposit and coarser grain size (Figs. 14, 38), coincides with minimal concentrations of metals and TOC (SH 6; 0 - 40 cm depth). Lower-energy deposition and finer grain sizes coincide with increased metal concentrations and greater TOC (Fig. 38). These findings may be result of coarse grains associated with higher energy deposition, greater erosion

of contaminated metals during such events, or indicate that slow deposition of finer-grained sediment accumulates the greatest concentrations of metals adsorbed to sediments. In such undisturbed sediments, the metal contaminants are more likely to show the accumulation patterns of metal contaminants over time. This is seen in the backbarrier section (SH 3; Fig. 39) where only the upper sediments (upper ~ 20 cm) are contaminated above background levels, which corresponds primarily with increases in silt. Despite the dominance of clay and silt in the backbarrier, metals are detected above background levels solely in the upper sediments.

Finally, metal concentrations detected in sediments deposited offshore from the beaches (e.g., Core SH 10) appear to vary with changes in grain size including the shift from muddy very fine sand to mud (~ 65 cm depth), and increases in TOC, and magnetic susceptibility upwards (Fig. 40). This suggests the metal concentrations are due to a combined influence by sediment properties (i.e., grain size variability and TOC which is also correlated to fine grained sediments) as well as increased anthropogenic effects on the area associated with modern times.

Results of this study show that the correlation between sediment properties and metal concentrations varies by location in the bay. If only the backbarrier sediments had been studied, the results would show the primary factor in contaminant burial to be anthropogenic input and this would be the location where future contaminant analyses would be focused. However, to characterize all the depositional environments, all the regions of the bay should be studied.

Possible Sources of Contaminants

The sources of pollution to the Sandy Hook Bay are vast, including discharge from the Hudson River, Raritan River, off-shore dumping sites of sewage sludge and contaminated dredge spoils (in the New York Bight), the Newark Bay, Passaic River, Arthur Kill landfill, sewage treatment discharge, storm sewer overflows, atmospheric sources of particulates, oil spills, and

runoff from the entire watershed (Mecray et al., 1999; Tovar-Sánchez et al., 2004 and references therein; Steinberg et al., 2004; Gao et al. 2002; Mueller and Werme, 1984). Prior studies of contaminants in sediments have inferred possible sources by correlating variability of metals with that of other metals, as two metals with coincident variability may have the same source, or same mode of transport (Hirschberg et al., 1996; Feng et al., 1998; Mecray et al., 1999; Benoit et al., 1999; Chillrud et al., 2003). Strong relationships between metals determined in this study, including Cu and Pb, (r^2= 0.778 derived from scatter plot; Pearson Correlation =0.837, SPSS 16.0, Microsoft, 2007) suggest the metals may have been transported from the same source, and/or by the same mode of transport (i.e., dissolved vs. solid phase).

Implications for the Health of Ecosystems

Human consumption of contaminated shellfish is a major mode of ingestion of contaminants from the Hudson-Raritan Estuary (Connor et al., 1984 *in* Breteler, 1984). Therefore, the health of the Hudson- Raritan Estuary is crucial to the shellfish industry. Results from this study suggest that remediation of the contamination of bottom sediments in a shallow marine coastal environment requires thorough investigation to determine where the contaminant accumulation would be expected, and where it would not be. The time spent investigating where contaminants are accumulating, and where they are not, may save monetary resources and time that would otherwise be used to clean sections that are flushed out naturally.

FUTURE STUDIES

Further research of other Mid-Atlantic coastal areas may identify additional storm deposits in that may correlate with the Sandy Hook Bay deposits. This would confirm the extent

of the impact of the historical and prehistorical storms and the ages assigned to those storms in this study.

The correlation of TOC in sediments with metal concentrations indicates a need for controlling the sources of TOC along with controlling metal input to the waterways. This includes mitigation of contaminants associated with combined sewer outflow from locations throughout the watershed.

Results from this study can be improved upon by obtaining new and well-positioned sediment cores that will provide an improved chronology from short-lived radioisotope and radiocarbon results, as well as obtaining results for contaminants using wet chemistry. Preliminary analyses for lead were performed by an independent laboratory on a small selection of samples using an ICP Spectrometer (Analytical Chemists, Farmingdale, NY). The samples were chosen based on peaks in lead previously detected with the XRF. Results indicate further testing should be conducted with wet chemistry methods in order to confirm the metal concentrations derived during XRF analyses, which do not correlate well with the ICP results (Figure 54). Furthermore, XRF is useful primarily as a rapid, non-destructive method to determine trends in metal variability in sediments. The wet chemistry procedure associated with use of the ICP Spectrometer can subsequently be used to determine accurate concentrations, which would have environmental applications, including assessment and predictions of the health of an ecosystem.

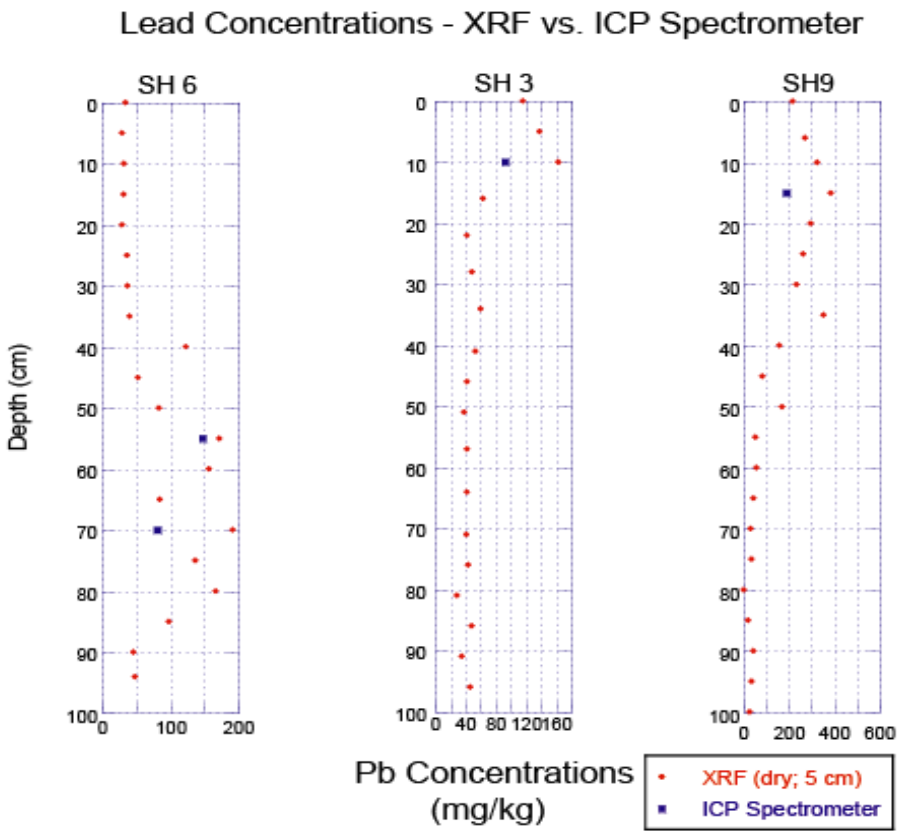

Figure 54: Lead concentrations derived using wet chemistry (ICP Spectrometer; Analytical Chemists, Farmingdale, NY) as compared to XRF results (dry sediment, 5 cm resolution) for three sediment cores representative of each depositional environment (Core SH 6; tip of Sandy Hook Spit, Core SH 3; backbarrier section, and Core SH 9; proximal to the beaches). Concentrations derived from XRF methods do not correlate well with the ICP results, indicating a need for further analysis in order to attain better accuracy.

With regard to environmental applications, lead in sediments has previously been determined to be toxic at a level of 10% of occurrences at 47 ppm, and a level of 220 ppm associated with toxicity at a level of 50% of occurrences (Long et al., 1995; Paul and O'Connor, 2004). Results here show that the concentrations of lead in Sandy Hook Bay sediments range from 81- 190 ppm (Figure 54), indicating the sediments of Sandy Hook Bay are potentially toxic to organisms that inhabit the substrate.

Furthermore, fishing restrictions should be maintained in areas where contaminants are accumulating in fine-grained upper sediments (i.e., backbarrier, offshore from the beaches). From the cores studied, shellfish taken from the area by the tip of the spit (Core SH 6) may pose the least health hazard because the contaminants are buried deeper in the core, and the upper sections show little sign of being contaminated.

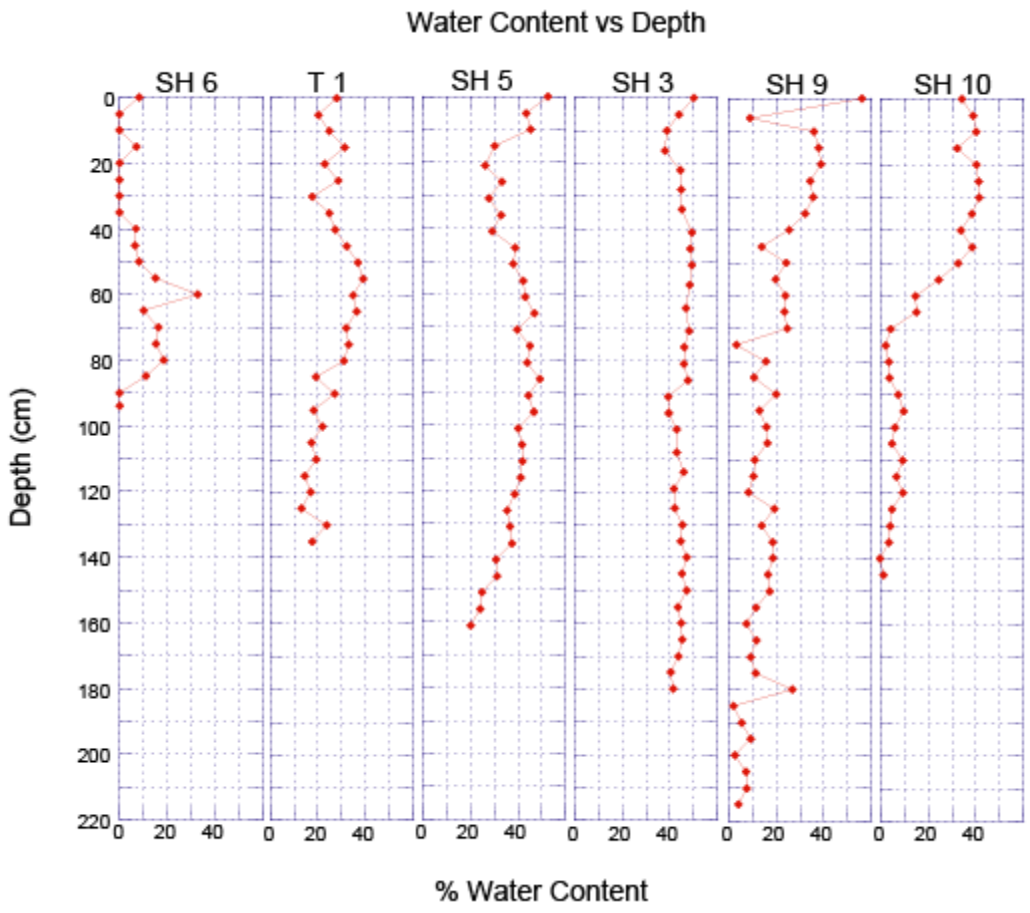

Appendix A: Water Content vs. Depth for all Cores

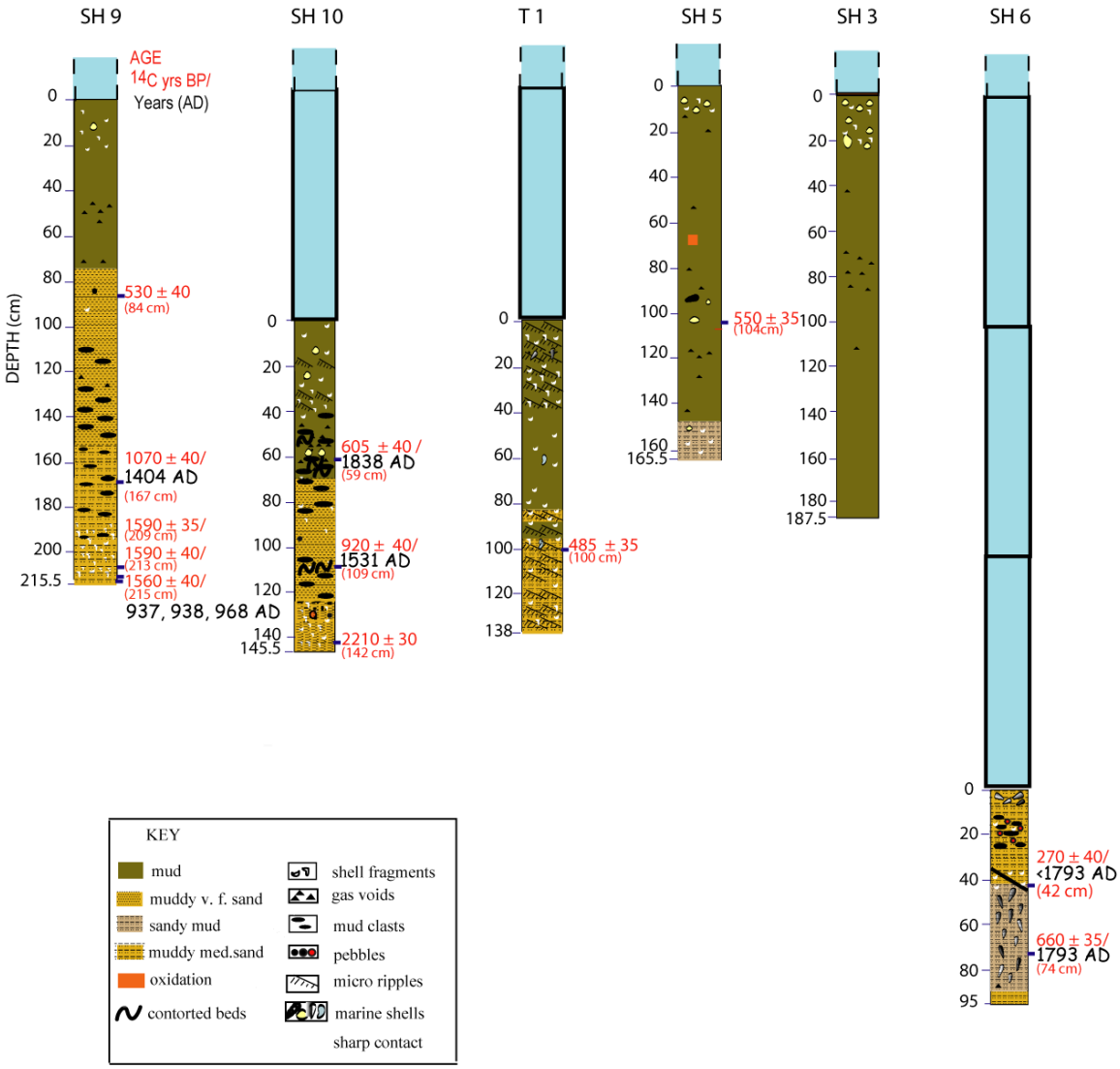

Appendix B: Representation of sediment cores SH 9, SH 10, T1, SH 5, SH 3, and SH 6 positioned with the water surface at the same level. Blue rectangles represent water. All cores were aligned with the top of the water surface positioned at the same level and truncated to fit on the page. Results from cores matched by water depth suggest a correlation between the ripple mark deposits associated with abundant shells and shell fragments in SH 10 (20- 40 cm) and T1 (0- 40 cm). Mud clast deposits in SH 9 and SH 10 appear coincident as well. The muddy sediments in the top of SH 3, SH 5, and SH 9 with abundant shells and shell fragments appear to coincide as well as the depths at which gas voids are evident. SH 6 is located in much deeper water because it is located the closest to the end of the Sandy Hook Spit, where it is closest to the open ocean.

Appendix C: Visual Descriptions of Sediment Composition (5 cm Resolution)

CORE SH 3 visual descriptions:

SH 3: 0 – 187.5 cm

- Oxidation is present at the top of the core evident as a reddish- orange color sediment.
- 4 - 24 cm there are abundant shells- whole clam shells (~1.5 cm diameter), with both valves well- preserved, as well as shell fragments
- 17 - 24 cm there is a well preserved bivalve, with both valves present (~9 cm diameter)
- 70 - 86 cm there are abundant gas voids, and rare gas voids at 43 and 112 cm

CORE SH 5 visual descriptions:

SH 5: 0- 165.5 cm

- The sediment color is anomalously red in color and oxidized at 65- 70 cm
- At 5- 11 cm, there are scattered, well- preserved single valve clam shells (1 cm in diameter). At 94 cm there is a gastropod, and a whole bivalve that extends to 109 cm. At 104 to 105 cm, there is a well- preserved clam shell 4 cm in diameter. There are scattered shells at 95 and 108 cm. Scattered shells at 150 cm.
- There are gas voids from 14- 20 cm, at 55 cm, 80- 95 cm, 117 - 120 cm, 129 - 146 cm

CORE SH 6 visual descriptions:

SH 6 : 0-13 cm, 42- 95 cm

- 0 to 7 cm is composed of crumbly and dry sediment
- 42 to 90 cm contains many well- preserved mussel shells, including both valves, at approximately 6 cm diameter.
- 0 to 7 cm contains smaller, well- preserved mussel shells, (~1.5 cm diameter), there are also well- preserved shells.
- Shells fragments present at 15 cm.
- There is a gas void at 85 cm

SH 6 : 13- 41 cm

- 13- 25 cm contains muddy coarse to medium sand with floating mud clasts (~ 2 to 4 cm diameter) and well- rounded reddish pebbles (~ .5 cm diameter).
- Shells fragments are present at 36 to 43 cm.
- At 41 cm, there is an angular dipping contact with the sediments above.

CORE SH 9 visual descriptions:

SH 9: 0- 75 cm

- There are rare shell fragments from 5 to 22 cm.
- Whole clam shell (5 cm long) with both valves, at 10 to 15 cm.
- Sporadic gas voids at 72 cm, and abundant at 45 to 56 cm.
- Woody and organic material increases from 40 to 0 cm relative to the rest of the core.

SH 9: 76- 215.5 cm

- At 92 cm, there is one rare shell fragment
- At 84- 86 cm, there is a rounded quartz pebble present.
- There are rare gas voids present at 122- 125 cm.
- There are layers of mud clasts from approximately 110 to 195 cm.

- Scattered shell fragments are found 185 to 189 cm, becoming shell fragment layers from 198 to 215.5 cm.

CORE SH 10 visual descriptions:

SH 10: 0- 40 cm

- Well- preserved clam shells at 13 cm (2 cm diameter), and at 24 cm
- Shell fragments from 30 to 40 cm, and between 5 and 38 cm.
- Micro-ripples present 18- 20 cm and 30- 40 cm.

SH 10: 40- 145.5 cm

- From 40 cm- 85 cm and 100- 124 cm there are mud clasts, some of which are contorted
- Single, well- preserved clam shells at (2 cm diameter) 59 to 60 cm.
- Rare shell fragments at 70 - 72 cm, 82 cm, 91 - 95 cm, and 106 - 111 cm.
- There are abundant shell fragments 124 to 145.5 cm
- At 125- 130 cm there is a rock that is 7 cm in diameter, and appears to be a flat, rounded, red bed sandstone fragment
- Rounded pebbles at 98 cm and at130 cm
- Gas voids present from 45 to 66 cm. These can be described as rare from 57 to 66 cm and abundant from 48 to 57 cm.

CORE T 1 visual descriptions:

T 1: 0- 83 cm

- 0 – 40 cm contain micro-ripples
- At 15 to 16 cm there are scattered whole, well- preserved mussel shells at 3 cm diameter
- There are scattered shell fragments from 7- 8 cm, 20- 29 cm, and 35- 40 cm.
- There are rare shell fragments from 40- 50 cm, 75 cm, 80-90 cm, and well preserved shell at 55- 65 cm (oyster)

T 1: 83 - 138 cm

- There are scattered shell fragments found from 80- 130 cm
- Whole shell at ~ 95 to 100 cm
- There are micro-ripples from 83 to 138 cm
- There are rare shell fragments 80-90 cm, and well preserved shell at 98 cm

Appendix D: Photographs of Shells from Sandy Hook Bay and Raritan Bay Cores



Anomia simplex


Ensis directus



Mercenaria mercenaria


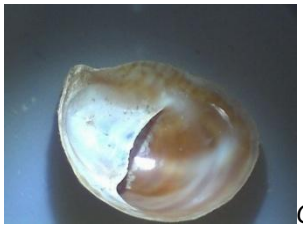
Crepidula fornicata

Works Cited

Abbott, R. T., Morris, P. A. (1995). *Shells of the Atlantic and Gulf Coasts and the West Indies.* New York: Houghton and Mifflin Company, 350 pp.

Accornero, A., Gnerre, R., Manfra, L. (2008). Sediment Concentrations of Trace Metals in the Berre Lagoon (France): An Assessment of Contamination. *Archives of Environmental Contamination and Toxicology, 54 (3),* 372- 385.

Ashley, G.M., Halsey, S.D., Buteux, C.B. (1986). New Jersey's Longshore Current Pattern. *Journal of Coastal Research*, 2 (4), 453-463.
Stable URL: http://www.jstor.org/stable/4297224

Bard, E., Arnold, M., Maurice, P., Duprat, J., Moyes, J., Duplessy, J.-C. (1987).Retreat velocity of the North-Atlantic polar front during the last deglaciation determined by ^{14}C accelerator mass spectrometry. *Nature,* 328, 791-794.

Benoit, G., Wang, E.X., Nieder, W.C., Levandowsky, M., Breslin, V.T. (1999). Sources and History of Heavy Metal Contamination and Sediment Deposition in Tivoli South Bay, Hudson River, New York. *Estuaries,* 22 (2), Part A, 167-178.
Stable URL: http://www.jstor.org/stable/1352974

Bianchi, T. S. (2007). *Biogeochemistry of Estuaries*. New York: Oxford University Press, 706 pp.

Blake, E.S., Rappaport, E. N, Landsea, C.W. (2007). The deadliest, costliest, and most intense United States tropical cyclones from 1851 to 2006 (and other frequently requested hurricane facts). *NOAA Technical Memorandum NWS TPC-5*, 43 pp.

Boggs, S. Jr. (2001). *Principles of Sedimentology and Stratigraphy, Third Edition*. New Jersey: Prentice Hall, 726 pp.

Bopp, R. F., Simpson, H. J., Olsen, C.R., Trier, R. M., Kostyk, N. (1982). Chlorinated hydrocarbons and radionuclide chronologies in sediments of the Hudson River and Estuary, New York. *Environ. Sci. Technol.*, 16(10), 666–676.

Bopp, R. F., Simpson., H. J. (1989). Contamination of the Hudson River: the sediment record, *in* Corell, A. (Ed.), *Contaminated Marine Sediments Assessment and Remediation*. Washington D.C.: National Academy Press, 401- 416.

Bopp, R.F., Simpson, H.J., Robinson, D. W., Chillrud, S. N., Virgilio. A. (1991). Chronologies of persistent contaminants in New York Harbor, Raritan Bay and Jamaica Bay, Abstract, Estuarine Research Federation Conference, San Francisco, CA, Nov. 10-14, 1991.

Bopp, R.F., Simpson, H.J., Chillrud, S. N., Robinson, D.W. (1993). Sediment-Derived

Chronologies of Persistent Contaminants in Jamaica Bay, New York. *Estuaries,* 16(3B), 608-616.

Bothner, M. H., Buchholtz ten Brink, M., Manheim., F.T.(1998). Metal concentrations in surface sediments of Boston Harbor- changes with time. *Marine Environmental Research*, 45 (2), 127-155.

Botton, M. L., Johnson, K., Helleby, L. (1998). Effects of copper and zinc on embryos and larvae of the horseshoes crab, *Limulus polyphemus*. *Arch. Environ. Contam. Toxicol.*, 35, 25-32.

Brady, N. C, Weil, R.R. (2002). The colloidal fraction: seat of soil chemical and physical activity *in* N.C. Brady and R.R. Weil, *The Nature and Properties of Soils, Thirteenth Edition.* New Jersey: Prentice Hall, 316-362.

Breteler, R. J. (1984). Introduction and summary of findings *in* R. J. Breteler (Ed.), *Chemical Pollution of the Hudson- Raritan Estuary.* NOAA Technical Memorandum, NOS OMA 7. 1-4.

Breteler, R. J., Rachlin, J. W., Engel., D. W. (1984). Metals subpanel report *in* R. J. Breteler (Ed.), *Chemical Pollution of the Hudson- Raritan Estuary.* NOAA Technical Memorandum, NOS OMA 7. 12-35.

Broecker, W.S., Andree, M., Wolfli, W., Oeschger, H., Bonani, G., Kennett, J., Peteet., D. (1988). The chronology of the last deglaciation: Implications to the cause of the Younger Dryas event. *Paleoceanography*, 3, 1-19.

Broecker, W. S., Kennett, J. P., Flower, B. P., Teller, J. T., Trumbore, S., Bonani, G., Wolfli, W. (1989). Routing of meltwater from the Laurentide ice sheet during the Younger Dryas cold episode. *Nature*, 341, 318-321.

Buchholtz ten Brink, M., Bothner, M. H., Manheim, F. T., Butman. B. (1997). Contaminant metals in coastal marine sediments: A legacy for the future and a tracer of modern sediment dynamics. *Proceedings of the U.S. Geological Survey (USGS) Sediment Workshop. URL http://water.usgs.gov/osw/techniques/workshop/index.html.*

Buynevich, I. V., FitzGerald, D. M., van Heteren, S. (2004). Sedimentary records of intense storms in Holocene barrier sequences. *Marine Geology*, 210, 135-148.

Cagen, K., Abbott, D. (2009). Evidence for a tsunami generated by an impact event in the New York metropolitan area approximately 2300 years ago. Section I: *in* S.H. Fernald, D. Yozzo, and H. Andreyko (Eds.), *Final Reports of the Tibor T. Polgar Fellowship Progra*m, 2008. Hudson River Foundation. 23 pp.

Camerlenghi, A., Lucchi, R. G., Rothwell, R. G. (1995). Grain-size analysis and distribution in

Cascadia margin sediments, Northeastern Pacific, *in* Carson, B., Westbrook, G.K., Musgrave, R.J., Suess, E (Eds.), *Proceedings of the Ocean Drilling Program, Scientific Results,* 146 (Part 1), 3-31.

Cantwell, M. G., Burgess, R. M., Kester, D. R. (2002). Release and phase partitioning of metals from anoxic estuarine sediments during periods of resuspension. *Environ. Sci. Technol.*, 36 (24), 5328-5334.

Carey, J. S., Sheridan, R. E., Ashley, G.M., Uptegrove, J. (2005). Glacially- influenced late Pleistocene stratigraphy of a passive margin: New Jersey's Record of the North American ice sheet. *Marine Geology,* 218, 155- 173.

Cavin, A., Underwood, M., Fisher, A., Johnston- Karas., A. (2000). Relations between textural characteristics and physical properties of sediments in northwestern Cascadia Basin *in* A. Fisher, E. E. Davis, & C. Escutia, (Eds.). *Proceedings of the Ocean Drilling Program, Scientific Results, 1*68, 67- 84. doi:10.2973/odp.proc.sr.168.013.2000

Cerrato, R. M. (2006). Long-Term and Large-Scale Patterns in the Benthic Communities of New York Harbor *in* J.S. Levinton, & J.R. Waldman, (Eds.). *The Hudson River Estuary*. New York: Cambridge University Press, 242-265.

Chan, L. S., Yeung, C. H., Yim, W. W. S., Or, O. L. (1998). Correlation between magnetic susceptibility and distribution of heavy metals in contaminated sea-floor sediments of Hong Kong Harbour. *Environmental Geology, 36*(1), 77-86.

Chan, L. S., Ng, S. L., Davis, A. M., Yim, W. W. S., Yeung, C.H. (2001). Magnetic properties and heavy- metal contents of contaminated seabed sediments of Penny's Bay, Hong Kong. *Marine Pollution Bulletin*, 42 (7), 596-583.

Chang, S., Zdanowicz, V. S., Murchelano, R. A. (1998). Associations between liver lesions in winter flounder (*Pleuronectes americanus*) and sediment chemical contaminants from north-east United States estuaries. *ICES Journal of Marine Science.* 55, 954-969.

Chillrud, S.N., Hemming, S., Shuster, E.L., Simpson, H.J., Bopp, R.F., Ross, J.M., Pederson, D.C., Chaky, D., Tolley, L-R., Estabrooks, F. (2003) Stable lead isotopes, contaminant metals and radionuclides in upper Hudson River sediment cores: implications for improved stratigraphy and transport processes. *Chemical Geology*, 199, 53-70.

Clark, P. U., Mix, A.C. (2002). Ice Sheet and sea level of the Last Glacial Maximum. *Quaternary Science Reviews*, 21, 1-7.

Coch, N. K. (1986). Sediment Characteristics and Facies Distributions in the Hudson System. *Northeastern Geology*, 8 (3), 109- 129

Coch, N. K., (1994). Geologic effects of hurricanes. *Geomorphology*, 10, 37- 63.

Cohen, J. B., Barclay, J. S., Major, A. R., Fisher, J. P. (2000). Wintering Greater Scaup as Biomonitors of Metal Contamination in Federal Wildlife Refuges in the Long Island Region. *Arch. Environ. Contam. Toxicol.,* 38, 83- 92.

Connor, M. S., Werme, C. E., Rosenmann, K. D. (1984). Public health consequences of chemical contaminants in the Hudson-Raritan Estuary *in* R. J. Breteler (Ed.). *Chemical Pollution of the Hudson- Raritan Estuary.* NOAA Technical Memorandum, NOS OMA 7, 54-60.

Cook, G. H. (1889). Geological map of NJ from original surveys, *NJ State Atlas*, sheet 20, scale 1:316,800, 2 cross sections, shows Terminal Moraine.

Covelli, S., Fontolan, G., Faganeli, J., Ogrinc, N. (2006). Anthropogenic markers in the Holocene stratigraphic sequence of the Gulf of Trieste (Northern Adriatic Sea). *Marine Geology*, 230, 29-51.

Crawford, D. W., Bonnevie, N. L., Wenning, R. J. (1995). Sources of pollution and sediment contamination in Newark Bay, New Jersey. *Ecotoxicology and Environmental Safety*, 30, 85-100.

Dabrio, C. J., Zazo, C., Goy, J. L., Sierro, F. J., Borja, F., Lario, J., Gonzalez, J. A., Flores, J. A. (2000). Depositional history of estuarine infill during the last postglacial transgression (Gulf of Cadiz, Southern Spain). *Marine Geology*, 162, 381- 404.

Dalrymple, R. W., Zaitlin, B. A., Boyd, R. (1992). Estuarine facies models: conceptual basis and stratigraphic implications. *Journal of Sedimentary Petrology*, 62 (6), 1130- 1146.

Danzeglocke, U., Jöris, O., Weninger, B. CalPal-2007online. http://www.calpal-online.de/, accessed 2010.

Davis, R. A. Jr. (1983). *Depositional Systems*. New Jersey: Prentice Hall. 669 pp.

Dillon, W. P., Oldale, R. N. (1978). Late Quaternary sea-level curve: Reinterpretation based on glaciotectonic influence. *Geology*, 6, 56- 60.

Dolan, R., Lins, H., Hayden, B. (1988). Mid-Atlantic coastal storms. *Journal of Coastal Research*, 4 (3), 417- 433.

Donnelly, J.P., Bryant, S.S., Butler, J., Dowling, J., Fan, L., Hausmann, N., Newby, P., Shuman, B., Stern, J., Westover, K., Webb III, T. W. (2001a). 700 yr sedimentary record of intense hurricane landfalls in southern New England. *GSA Bulletin*, 113 (6), 714-727.

Donnelly, J. P., Roll, S., Wengren, M., Butler, J., Lederer, R., Webb III, T. (2001b). Sedimentary evidence of intense hurricane strikes from New Jersey. *Geology*, 29 (7), 615- 618.

Donnelly, J. P., Butler, J., Roll, S., Wengren, M., Webb III, T. (2004). A Backbarrier Overwash Record of Intense Storms from Brigantine, New Jersey. *Marine Geology*, 210, 107- 121.

Donnelly, J. P., Driscoll, N. W., Uchupi, E., Keigwin, L. D., Schwab, W. C., Thieler, E. R., Swift, S. A. (2005). Catastrophic meltwater discharge down the Hudson Valley: A potential trigger for the Intra-Allerod cold period. *Geology*, 33(2), 89-92.

Dougherty, A. J., FitzGerald, D. M., Buynevich, I. V. (2004). Evidence for storm-dominated early progradation of Castle Neck barrier, Massachusetts, USA. *Marine Geology*, 210, 123-134.

Duman, M., Duman, S., Lyons, T. W., Avcı, M., İzdar, E., Demirkurt, E. (2006). Geochemistry and sedimentology of shelf and upper slope sediments of the south-central Black Sea. *Marine Geology*, 227, 51-65.

Duncan, C. S., Goff, J. A., Austin Jr., J. A., Fulthorpe, C. S. (2000). Tracking the last sea- level cycle: seafloor morphology and shallow stratigraphy of the latest Quaternary New Jersey middle continental shelf. *Marine Geology*, 170, 395- 421.

Dyer, K.R. (1994). Estuarine Sediment Transport and Deposition *in* K. Pye (Ed.). *Sediment Transport and Depositional Processes.* Boston, MA.: Blackwell Scientific Publications, 193-218.

Easterbrook, D. J. (1999). *Surface Processes and Landforms, Second Edition*. New Jersey: Prentice Hall, 428- 470.

Eby, G. N. (2004). *Principles of Environmental Geochemistry*. United States: Thomson Brooks/Cole, 514 pp.

Engelhart, S.E., Horton, B.P., Kemp, A.C. (2011a). Holocene sea level changes along the United States' Atlantic Coast. *Oceanography* 24(2),70–79. doi:10.5670/oceanog.2011.28.

Engelhart, S. E., Peltier, W. R., Horton, B. P. (2011b). Holocene relative sea-level changes and glacial isostatic adjustment of the U.S. Atlantic coast. *Geology, 39*(8), 751-754.

Fairbanks, R.G. (1989). A 17,000-year glacio-eustatic sea level record – influence of glacial melting rates on the Younger Dryas event and deep-ocean circulation: *Nature*, 342, 637-642.

Feng, H., Cochran, J. K., Lwiza, H., Brownawell, B. J., Hirschberg, D. J. (1998). Distribution of heavy metal and PCB contaminants in the sediments of an urban estuary: the Hudson River. *Marine Environmental Research*, 45 (1), 69-88.

Feng, H., Cochran, J., Hirschberg, D. J. (2002). Transport and sources of metal contaminants

over the course of tidal cycle in the turbidity maximum zone of the Hudson River Estuary. *Water Research* 36, 733-743.

Foyle, A. M., Oertel, G. F. (1997). Transgressive systems tract development and incised- valley fills within a Quaternary estuary- shelf system: Virginia inner shelf, USA. *Marine Geology*, 137, 227-249.

Foxgrover, A. C. (2009). *Quantifying the Overwash Component of Barrier Island Morphodynamics: Onslow Beach, NC.* Master's Thesis, College of William and Mary, Williamsburg, VA. 163 pp. http://web.vims.edu/library/Theses/Foxgrover09.pdf

Gao, Y., Nelson, E. D., Field, M. P., Ding, Q., Li, H., Sherrell, R. M., Gigliotti, C. L., Van Ry, D. A., Glenn, T. R., Eisenreich, S. J. (2002). Characterization of atmospheric trace elements on $PM_{2.5}$ particulate matter over the New York-New Jersey harbor estuary. *Atmospheric Environment*, 36, 1077-1086.

Gaswirth, S. B. (1999). *The Late Pleistocene to Holocene Glacial History of Raritan Bay, New Jersey*. Master's Thesis, Rutgers University, New Brunswick, New Jersey, 157 pp.

Gaswirth, S., G. M. Ashley, R. E. Sheridan. (2002). Use of seismic stratigraphy to identify conduits for saltwater intrusion in the vicinity of Raritan Bay, New Jersey. *Environmental & Engineering Geoscience*, VIII (3), 209- 218.

Gaugush, R. F. (1998). An in-situ sediment penetrometer for the characterization of sediment type and bottom dynamic conditions. *United States Geological Survey Project Status Report 98-08*, 2 pp.

Gill, R. (Ed.).(1997). *Modern Analytical Geochemistry*. Singapore: Longman Singapore Publishers Ltd., 329 pp.

Gochfeld, M.,Burger, J. (1982). Biological concentration of cadmium in estuarine birds of the New York Bight. *Colonial Waterbirds.* 5, 116-123.

Goodbred, S., Krentz, S., LoCicero, P. (2006). Evidence for a newly discovered 2300- year-old tsunami deposit from Long Island, New York. *Eos Trans. AGU 87*(53), Fall Meet. Suppl., Abstract OS43C-0681.

Gornitz, V., Couch, S., Hartig, E. K. (2002). Impacts of sea level rise in the New York City Metropolitan area. *Global and Planetary Changes*, 32, 61-88.

Goss, M.C., Ashley, G. M., Sheridan, R. E. (1995). Sedimentology and stratigraphy of a first generation estuary at the last glacial limit, Raritan Bay, New Jersey: Annual Meeting, *Northeast Geological Society of America Abstracts,* Cromwell, Connecticut, 49 pp.

Gottholm, B. W., Harmon, M. R., Turgeon, D. D. (1993). Assessment of chemical contaminants

in the Hudson-Raritan Estuary and coastal New Jersey area. *National Oceanic and Atmospheric Administration*, Silver Spring, MD. 19 pp.

Greig, R.A., McGrath, R.A. (1977). Trace metals in sediments of Raritan Bay.*Marine Pollution Bulletin*, 8 (8), 188-192.

Gulick, S. P. S., Goff, J. A., Austin Jr., J. A., Alexander Jr., C. R.,Nordfjord, S.,Fulthorpe,C. S. (2005). Basal inflection- controlled shelf- edge wedges off New Jersey track sea- level fall. *Geology*, 33 (5), 429- 432.

Hedges, J. I., Keil, R. G. (1999). Organic geochemical perspectives on estuarine processes: sorption reactions and consequences. *Marine Chemistry*, 65, 55-65.

Hill, H. W., J. T. Kelley, D. F. Belknap, S. M. Dickson. (2004). The effects of storms and storm-generated currents on sand beaches in southern Maine, USA. *Marine Geology*, 210, 149-168.

Hirschberg, D. J., Chin, P., Feng, H., Cochran, J.K. (1996). Dynamics of Sediment and Contaminant Transport in the Hudson River Estuary: Evidence from Sediment Distributions of Naturally Occurring Radionuclides. *Estuaries, Dedicated Issue: The Hudson River Estuary*, 19 (4) 931-949.

Hoffman, T. (2004). *Shifting Sands of Sandy Hook.* National Park Service. Web: http://www.nps.gov/gate/naturescience/upload/nature_shifting_sands.pdf

Innov-X User Manual Version 2.2, and Soil Appendix (2006)

Itow, T., Loveland, R. E., Botton, M. L. (1998). Developmental abnormalities in horseshoe crab embryos caused by exposure to heavy metals. *Arch. Environ. Contam. Toxicol.*, 35, 33-40.

Jeffries, H. P. (1962). Environmental characteristics of Raritan Bay, a polluted estuary. *Limnology and Oceanography*, 7 (1), 21- 31.

Jones, R. A., Lee, G. F.(1988) Toxicity of U.S. waterway sediments with particular references to the New York Harbor area *in* J.J. Lichtenberg, F. A. Winter, C. I. Weber, L. Fradkin, (Eds.),*Chemical and Biological Characterization of Sludges, Sediments, Dredge Soils, and Drilling Muds, ASTM STP 976*, 403-417.

Kapička, A., Petrovsky´, E., Ustjak, S., Macháčková, K. (1999). Proxy mapping of fly-ash pollution of soils around a coal-burning power plant: a case study in the Czech Republic. *Journal of Geochemical Exploration*, 66, 291–297.

Kemp, R. (1999). *Spss for Psychologists*. Mcmillin Pub Llc**,** 300 pp.

Kenna, T.C., Nitsche, F. O., Sands, E., Bell, R. E., Ryan, W. B., Chillrud, S. N., Ross, J. M.

(2006). Application of field portable X-ray fluorescence spectrometry to rapidly measure metal distributions in sediment cores, *Eos Trans. AGU, 87*(52), Fall Meet. Suppl., Abstract #H33B-1502.

Kenna, T. C., Nitsche, F. O., Herron, M. M., Mailloux, B. J., Peteet, D., Sritrairat, S., Sands, E., Baumgarten, J. (2011). Evaluation and calibration of a field portable x-ray fluorescence spectrometer for quantitative analysis of siliciclastic soils and sediments. *J. Anal. At. Spectrom, 26, 395-405.*

Kennish, M. J. (1997). *Practical Handbook of Estuarine and Marine Pollution*. New York: CRC Press, 524 pp.

Kersten, M., Smedes, F. (2002). Normalization procedures for sediment contaminants in spatial and temporal monitoring. *J. Environ. Monit.*, 4, 109-115.

Kinnear, P.R, Gray., C.D (2004). *SPSS 12 Made Simple, 1st ed.* New York: Psychology Press. 451 pp.

Kovanen, D. J., Easterbrook, D. J. (2002). Paleodeviations of radiocarbon marine reservoir values for the northeast Pacific, *Geology*, 30(3), 243- 246.

Krentz, S., Goodbred, S., Nitsche, F., McHugh, C., Carbotte, S., Slagle, A., Klein, E. (2008). Evidence for a tsunami event and coastal reorganization in the New York Metropolitan region ~2300 yr BP. *EOS Trans. AGU,* 89 (53), Fall Meet. Suppl. Abstract # OS53B-1311.

Kumar, N., Sanders, J. E. (1974). Inlet sequence: a vertical succession of sedimentary structures and textures created by the lateral migration of tidal inlets. *Sedimentology*, *21*(4), 491-532. DOI: 10.1111/j.1365-3091.1974.tb01788.x

Landsea, C. W., C. Anderson, N. Charles, G. Clark, J. Dunion, J. Fernandez-Partagas, P. Hungerford, C. Neumann, M. Zimmer. (2003). The Atlantic hurricane database re-analysis project : Documentation for the 1851-1910 alterations and additions to the HURDAT database. *in*: Murnane, R. J. and K. L. Liu (eds.), *Hurricanes and Typhoons : Past, Present, and Future.* Columbia University Press, 177-221.

Lewis, R.S., DiGiacomo-Cohen, M. (2000). A Review of the Geologic Framework of the Long Island Sound Basin, With Some Observations Relating To Postglacial Sedimentation. *Journal of Coastal Research*, 16 (3), 522–532.

Lewis, R. S., Stone, J. R. (1991). Late Quaternary Stratigraphy and Depositional History of the Long Island Sound Basin. *J. Coastal Res., Spec. Issue*, 11, 1-23.

Lewis, J. V., Kummel, H.B. (revised by Kummel). (1940). *The Geology of New Jersey.* Trenton, NJ: Dept. of Conservation and Development, State of New Jersey, Bulletin 50 Geologic Series. 230 pp.

Lick, W., Huang, H. (1993) *in* Mehta, A. (Ed.). *Coastal and Estuarine Studies: Nearshore and Estuarine Cohesive Sediment Transport*. Washington D.C.: American Geophysical Union, 21- 39.

Long, E. R., Wolfe, D. A., Scott, K. J., Thursby, G. B.,Stern,E. A., Peven, C., Schwartz,T. (1995). Magnitude and Extent of Sediment Toxicity in the Hudson-Raritan Estuary. *NOAA Technical Memorandum NOS ORCA 88,* 242 pp.

Lu, S. G., Bai, S. Q., Xue, Q. F. (2007). Magnetic properties as indicators of heavy metals pollution in urban topsoils: a case study from the city of Luoyang, China. *Geophysical Journal International, 171*(2), 568-580.

Mansfield, E. (1986). *Basic Statistics with Applications.* New York: W. W. Norton. 449- 541.

Martins, C. C., Mahiques, M. M., Bicego, M. C., Fukumoto, M. M., Montone, R. C. (2007). Comparison between anthropogenic hydrocarbons and magnetic susceptibility in sediment cores from the Santos Estuary, Brazil. *Marine Pollution Bulletin,* 54, 226- 246.

Maurer, D., Watling, L., Aprill, G. (1974). The Distribution and Ecology of Common Marine and Estuarine Pelecypods in the Delaware Bay Area. *The Nautilus*, 88 (2), 38- 45.

Mccave, I. N., Hall, I. R.(2006). Size sorting in marine muds: Processes, pitfalls, and prospects for paleoflow-speed proxies. *Geochemistry Geophysics Geosystems,*7(10), 37 pp.

McHugh, C. M.G., Olson, H. C. (2002). Pleistocene chronology of continental margin sedimentation: New insights into traditional models, New Jersey. *Marine Geology*, 186, 389 – 411.

McHugh, C., Pekar, S.F., Christie-Blick, N., Ryan, W.B.F., Carbotte, S., Bell, R. (2004). Spatial variations in a condensed interval between estuarine and open-marine settings: Holocene Hudson River estuary and adjacent continental shelf. *Geology*, 32(2), 169- 172.

McHugh, C. M., Cormier, M., Pant, H., Varekamp, J., Marchese, P., Charles, T., Bowman, A., Vargas, W., Balbas, A., Boteju, J. (2007). History of Contamination and Coastal Hazards in Western Long Island Sound, N.Y.*Eos Transactions AGU*, 88 (52), abstract #OS23B-07.

McHugh, C. M., Hartin, C. A., Mountain, G. S., Gould, H.M. (2010). The role of glacio-eustacy in sequence formation: Mid-Atlantic Continental Margin, USA. *Marine Geology*, 277, 31-47.

McNeely R., Dyke, A. S., Southon, J. R. (2006) Canadian marine reservoir ages, preliminary data assessment, Open File 5049, pp. 3. Geological Survey Canada.

Mecray, E.L., Buchholtz ten Brink, M. R., Butman, B. (1999). Contaminants and marine geology

in the New York Bight: modern sediment dynamics and a legacy for the future: U.S. Geological Survey Fact Sheet FS-114-99.

Menon, M. G., R. J. Gibbs, A. Phillips. (1998). Accumulation of muds and metals in the Hudson River estuary turbidity maximum. *Environmental Geology*, 34 (2/3), 214-222.

Meyer, A., Fisher, A. (1997). Data Report: Grain size analysis of sediments from the northern Barbados accretionary prism, *in* Shipley, T.H, Ogawa, Y., Blum, P., Bahr, J.M. (Eds.), *Proceedings of the Ocean Drilling Program, Scientific Results*, 156, 337-341.

Miall, A. D. (1984). *Principles of Sedimentary Basin Analysis*. NY: Springer- Verlag. 490 pp.

Miall, A. D. (1990). *Principles of Sedimentary Basin Analysis, Second Edition*. NY: Spring-Verlag. 668 pp.

Micromeritics SediGraph 5100 operator's manual. Micromeritics - Inc., Norcross, GA, 2001

Miller, K. G., Sugarman, P. J., Browning, J. V., Horton, B.P., Stanley, A., Kahn, A., Uptegrove, J., Aucott, M. (2009). Sea- level rise in New Jersey over the past 5000 years: Implications to anthropogenic changes, *Glob. Planet. Change*, 66, 10-18. doi:10.1016/j.gloplacha.2008.03.08

Miller, K.G., G.S. Mountain, J.D. Wright, J.V. Browning. (2011). A 180-million-year record of sea level and ice volume variations from continental margin and deep-sea isotopic records. *Oceanography* 24(2), 40–53. doi:10.5670/oceanog.2011.26

Milne, G. A., Mitrovica, J. X. (2008). Searching for eustasy in deglacial sea-level histories. *Quaternary Science Reviews*, *27*(25-26), 2292-2302.

Minard, J.P. (1969). *Geology of the Sandy Hook Quadrangle in Monmouth County, New Jersey: U.S. Geological Survey Bulletin 1276.* 43 pp.

Morgan, G.A., Leech, N.L., Gloeckner, G.W., Barrett, K.C. (2004). *SPSS For Introductory Statistics: Use and Interpretation, Second Edition.* New Jersey: Lawrence Erlbaum Associates, 211 pp.

Mueller, J. A., C. E. Werme. 1984. Contaminant inputs to the Hudson-Raritan Estuary. Pp. 7-11 *in* Breteler, R. J. (ed.) (1984). *Chemical Pollution of the Hudson- Raritan Estuary.* NOAA Technical Memorandum, NOS OMA 7. 72 pp.

Neto, J. A. B., Gingele, F. X., Leipe, T., Brehme, I. (2006). Spatial distribution of heavy metals in surficial sediments from Guanabara Bay: Rio de Janeiro, Brazil. *Environ Geol*, 49, 1051–1063.

Nitsche, F.O., Kenna, T.C., Haberman, M. (2010). Quantifying 20th century deposition in complex estuarine environment: An example from the Hudson River.

Estuarine, Coastal and Shelf Science, 89, 163-174.

NJDEP. (1998). *Raritan and Sandy Hook Bays Sanitary Survey Report 1994- 1997*, Division of Watershed Management, Bureau of Marine Water Monitoring. 48 pp.

Nordfjord, S., Goff,J. A., Austin Jr.,J. A., Sommerfield,C. K.(2005). Seismic geomorphology of buried channels systems on the New Jersey outer shelf: assessing past environmental conditions. *Marine Geology*, 214, 339- 364.

Nordfjord, S., Goff, J. A., Austin, J. A., Gulick, S. P. S. (2006). Seismic facies of incised-valley fills, New Jersey Continental Shelf: Implications for erosion and preservation processes acting during latest Pleistocene- Holocene transgression. *Journal of Sedimentary Research*, 76, 1284- 1303.

Olsen, C.R., H. J. Simpson, R. F. Bopp, S. C. Williams, T. H. Peng, B.L. Deck. (1978). A geochemical analysis of the sediments and sedimentation in the Hudson Estuary. *Journal of Sedimentary Petrology*, 48(2), 401- 418.

Olsen, C. R., H. J. Simpson, T. H. Peng, R. F. Bopp, R. M. Trier. (1981). Sediment Mixing and Accumulation Rate Effects on Radionuclide Depth Profiles in Hudson Estuary Sediments. *Journal of Geophysical Research*, 86 (C11), 11,020- 11,028.

Olsen, C. R., I. L. Larsen, R. H. Brewster, N. H. Cutshall, R. F. Bopp, H. J. Simpson. (1984). A Geochemical Assessment of Sedimentation and Contaminant Distributions in the Hudson- Raritan Estuary. *NOAA Technical Report, NOS OMS 2*. 101 pp.

Olsen, C.R., N. H. Cutshall, I. L. Larsen, H. J. Simpson, R. M. Trier, R. F. Bopp. (1984- 1985). An estuarine fine- particle budget determined from radionuclide tracers. *Geo- Marine Letters*, 4, 157- 160.

Pant, H.K., Reddy, K.R. (2001). Phosphorus sorption characteristics of estuarine sediments under different redox conditions. *J. Environ. Qual.*, 30, 1474-1480.

Paul, J. F., O'Connor, T. P. (2004). Analysis of estuarine sediment contaminant and toxicity data for eliciting responses. *Environmental Monitoring & Assessment Program Symposium Abstracts;* http://www.epa.gov/emap/html/pubs/docs/groupdocs/symposia/symp2004 /Abstracts/paul.html

Paulson, A. J. (2005). Tracing water and suspended matter in Raritan and Lower New York Bays using dissolved and particulate elemental concentrations. *Marine Chemistry*, 97, 60-77.

Peltier, W.R. (1998).Postglacial variations in the level of the sea: Implications for climate dynamics and solid-earth geophysics. *Reviews of Geophysics*, 36 (4), 603-689.

Peltier, W.R. (1999). Global sea level rise and glacial isostatic adjustment. *Global and Planetary Change*, 20, 93-123.

Peltier, W. R., Fairbanks, R. G. (2006). Global glacial ice volume and Last Glacial Maximum duration from and extended Barbados sea level record. *Quaternary Science Reviews*, 25, 3322-3337.

Pendleton, E. A., Thieler, E. R., Williams,S. J. (2005). *Coastal Vulnerability Assessment of Gateway National Recreation Area (GATE) to Sea Level Rise*. 27 pp.

Petrovsky, E., A. Kapička, N. Jordanova, M. Knab, V. Hoffman. (2000). Low-Field Magnetic Susceptibility: a Proxy Method of Estimating Increased Pollution of Different Environmental Systems. *Environmental Geology*, 39 (3-4), 312- 318.

Plater, A. J., J. Ridgway, P. G. Appleby, A. Berry, M. R. Wright. (1998). Historical contaminant fluxes in the Tees Estuary, UK: geochemical, magnetic and radionuclide evidence. *Marine Pollution Bulletin*, 37 (3-7), 343-360.

Posamentier, H. W. (2001). Lowstand alluvial bypass systems: Incised vs. unincised. *AAPG Bulletin*, 85 (10), 1771-1793

Prudêncio, M. I., M. I. Gonzalez, M. I. Dias, E. Galan, F. Ruiz. (2007). Geochemistry of sediments from El Melah lagoon (NE Tunisia): A contribution for the evolution of anthropogenic inputs. *Journal of Arid Environments*, 69, 285- 298.

Psuty, N. P. (1986). Holocene Sea Level in New Jersey. *Physical Geography*, 7 (2), 156- 167.

Psuty, N.P., Pace, J.P. (2008). Sediment management at Sandy Hook, NJ: An interaction of science and public policy. *Geomorphology*, doi:10.1016/j.geomorph.2008.05.036.

Ray, G. L. (2004). *Monitoring of intertidal benthos on the shoreline of Raritan and Sandy Hook Bays, New Jersey: interim report*. A report to the U.S. Army Engineer District, New York, 41 pp.

Rayburn, J. A., Knuepfer, P. L. K., Franzi, D. A. (2005). A series of large, Late Wisconsinan meltwater floods through the Champlain and Hudson Valleys, New York State, USA. *Quaternary Science Reviews*, 24, 2410- 2419.

Rayburn, J. A., Franzi, D. A., Knuepfer, P. L. K. (2007). Evidence from the Lake Champlain Valley for a later onset of the Champlain Sea and implications for late glacial meltwater routing to the North Atlantic. *Palaeogeography, Palaeoclimatology, Palaeoecology*, 246, 62-74.

Rehder, H. A. (1992). *The Audubon Society Field Guide to North American Seashells*. New York: Alfred A. Knopf. 894 pp.

Reid, R. N., Olsen, P. S., Mahoney, J. B.(2002). A Compilation of Reported Fish Kills in the Hudson- Raritan Estuary during 1982 through 2001. *U.S. Dep. Commer., Northeast Fisheries Science Center Reference Document 02-09:*16 pp. Available from: National

Marine Fisheries Service, 166 Water Street, Woods Hole, MA 02543- 1026.

Reinson, G.E. *in* Walker, R.G. and N. P. James (ed.) (1992). *Facies Models, Response to Sea Level Change*. Ontario: Geological association of Canada, Love Printing Service Ltd., 179-194.

Renwick, W. H., Ashley, G. (1984). Sources and Sinks of fine- grained sediments in a fluvial-estuarine system. *Geological Society of America Bulletin*, 95, 1343- 1348.

Rick, T. C., Vellanoweth, R. L., Erlandson, J. M. (2005). Radiocarbon dating and the "old shell" problem: direct dating of artifacts and cultural chronologies in coastal and other aquatic regions, *Journal of Archaeological Science*, 32, 1641- 1648.

Rosales-Hoz, L., Cundy, A.B., Bahena-Manjarrez, J.L.(2003). Heavy metals in sediment cores from a tropical estuary affected by anthropogenic discharges: Coatzacoalcos estuary, Mexico. *Estuarine, Coastal and Shelf Science*, 58, 117- 126.

Rosati, J. D. (2005). Concepts in Sediment Budgets. *Journal of Coastal Research, 21 (2), 307-322.*

Santschi, P. H., Lenhart, J. L.,Honeyman, B. D. (1997). Heterogeneous processes affecting trace contaminant distribution in estuaries: The role of natural organic matter. *Marine Chemistry*, 58, 99-125.

Sañudo- Wilhelmy, S. A., Gill, G. A. (1999). Impact of the Clean Water Act on the levels of toxic metals in urban estuaries: The Hudson River Estuary revisited. *Environmental Science and Technology*, 33 (20), 3477-3481.

Schmidt, A., Yarnold, R., Hill, M., Ashmore, M. (2005). Magnetic susceptibility as proxy for heavy metal pollution: a site study. *Journal of Geochemical Explorations,* 85, 109- 117.

Schubel, J. R. *in* I. R. Kaplan (Ed). (1974). *Natural Gases in Marine Sediments*. New York: Plenum Press. 275- 298.

Scileppi, E., Donnelly, J.P. (2007). Sedimentary evidence of hurricane strikes in western Long Island, New York. *Geochemistry Geophysics Geosystems,* 8 (6), 1-25.

Sedgwick, P.E., Davis, R. A. Jr. (2003) Stratigraphy of washover deposits in Florida: implications for recognition in the stratigraphic record. *Marine Geology,* 200, 31-48.

Shea, D., Lewis, D.A., Buxton, B. E, Rhoads, D. C., Blake, J. A. (1991). *The sedimentary environment of Massachusetts bay: physical, chemical and biological characteristics*. Boston: Massachusetts Water Resources Authority. Report 1991-06, 139 pp.

Siddall, M., Rohling, E. J. Almogi-Labin, A. Hemleben, Ch., Meischner, D.,Schmelzer, I. Smeed, D.A. (2003). Sea-level fluctuations during the last glacial cycle. *Nature,* 423, 853-858.

Smith, E. (1999). Atlantic and east coast hurricanes 1900-98: A frequency and intensity study for the twenty-first century. *Bulletin of the American Meteorological Society*, 80 (12), 2717-2720.

Stallard, M.O., Apitz, S. E., Dooley, C. A.(1995). X-ray fluorescence spectrometry for field analysis of metals in marine sediments. *Marine Pollution Bulletin*, 31 (4-12), 297-305.

Stamoulis, S., Gibbs, R. J., Menon, M. G. (1996). Geochemical phases of metals in Hudson River Estuary sediments. *Environmental International*, 22 (2), 185-194.

Stanley, A., Miller, K. G., Sugarman, P. (2004). *Holocene Sea- level Rise in New Jersey: An Interim Report*. New Jersey Department of Environmental Protection, Division of Science, Research & Technology, 7 pp.

Steinberg, N., Suszkowski, D.J., Clark, L., Way, J. (2004). Health of the Harbor: the First Comprehensive Look at the State of the NY/NJ Harbor Estuary. A report to the NY/NJ Harbor Estuary Program. Hudson River Foundation, New York, NY. 82 pp.

Stone, J. R., Schafer, J. P., London, E. H., DiGiacomo- Cohen, M., Lewis, R. S., Thompson,W. B.(1998). Quaternary geologic map of Connecticut and Long Island Sound Basin. *U. S. Geological Survey Open- File Report 98-371*, 68 pp.

Stuiver, M., Reimer, P. J., Reimer, R. W. (2005). CALIB 5.0; CALIB 6.0.

Swift, D. J. P., Moir, R., Freeland, G. L. (1980). Quaternary rivers on the New Jersey shelf: Relation of seafloor to buried valleys. *Geology*, 8, 276-280.

Szava-Kovats, R. C. (2008). Grain-size normalization as a tool to assess contamination in marine sediments: Is the <63 μm fraction fine enough? *Marine Pollution Bulletin*, 56, 629-632.

Tang, C. W., Ip, C. C., Zhang, G., Shin, P. K. S., Qian, P., Li, X. (2008). The spatial and temporal distribution of heavy metals in sediments of Victoria Harbour, Hong Kong. *Marine Pollution Bulletin,* 57, 816–825.

Teller, J.T. (1987). Proglacial lakes and the southern margin of the Laurentide Ice Sheet. *in*: Ruddiman, W.F., Wright, H.E., Jr. (Eds.), *North America and Adjacent Oceans during the Last Glaciation: The Geology of North America K-3*. Geological Society of America, Boulder, CO, pp. 39-69.

Thieler, E. R., Butman, B., Schwab, W. C., Allison, M. A., Driscoll, N. W., Donnelly, J. P., Uchupi, E. (2007). A catastrophic meltwater flood event and the formation of the Hudson Shelf Valley. *Palaeogeography, Palaeoclimatology, Palaeoecology*, 246, 120- 136.

Thomas, E., Varekamp, J. C., Lewis, R. S (2007).The Flooding of Long Island Sound, *Eos Trans. AGU*, 88 (52), Fall Meet. Suppl., Abstract #PP13B-1277.

Tiedemann, J.A. (1997). Water Quality Issues (Section VI) *in: The biology of the Hudson-*

Raritan Estuary: a teacher's guide. NJSG-97-354, N.J. Sea Grant Program, NJ Marine Sciences Consortium, 18 pp.

Tiedemann, J.A. (1997). Benthic invertebrate species of the Hudson-Raritan estuary (VIII)*in: The biology of the Hudson-Raritan Estuary: a teacher's guide*. NJSG-97-354, N.J. Sea Grant Program, NJ Marine Sciences Consortium, 56 pp.

Tovar- Sánchez, A., Sañudo- Wilhelmy, S. A., Flegal, A. R. (2004). Temporal and spatial variations in the biogeochemical cycling of cobalt in two urban estuaries: Hudson River Estuary and San Francisco Bay. *Estuarine, Coastal and Shelf Science*, 60, 717-728.

Uchupi, E., Driscoll, N., Ballard, R. D., Bolmer, S. T. (2001). Drainage of Late Wisconsin glacial lakes and the morphology and late quaternary stratigraphy of the New Jersey-southern New England continental shelf and slope. *Marine Geology*, 172, 117-145.

US Environmental Protection Agency. (1998). *Sediment Quality of the NY/NJ Harbor System: an Investigation Under the Regional Environmental Monitoring and Assessment Program (R-EMAP). Final Report.* EPA/902-R-98-001, 255 pp.
URL: http://www.epa.gov/emap/remap/html/docs/nynjsed1.pdf

US Environmental Protection Agency. (2003). *Final Report: Sediment quality of the NY/NJ Harbor system: a 5-year revisit 1993/4 – 1998- An Investigation under the Regional Environmental Monitoring and Assessment Program (REMAP*. EPA/902-R-03-002. USEPA- Region 2, Division of Environmental Science and Assessment. Edison, NJ. 51 pp.

US Fish and Wildlife Service. (1997). *Significant habitats and habitat complexes of the New York Bight watershed*. Southern New England - New York Bight coastal ecosystems program, Charlestown, Rhode Island. Http://library.fws.gov/pubs5/web_link/text/toc.htm

United States Geological Survey. (1998). Sandy Hook Quadrangle Topographic Map 7.5 Minute Series.

United States Geological Survey. Stoffer, P., Messina., P. (2003). Geology of New York City Region. *A Preliminary Regional Field-Trip Guidebook.*
URL: http://3dparks.wr.usgs.gov/nyc/common/preface.htm

Vail, P. R. (1987). Part 1 *in*: Bally, A. W. (Ed.). *Atlas of Seismic Stratigraphy, American Association of Petroleum Geologists in Studies in Geology; 1 (27)* Tulsa: American Association of Petroleum Geologists, 1-5.

Vail, P. R., Mitchum,R. M.Jr., Thompson,S.III (1977). Part 3*in* C.E. Payton (Ed.). *Seismic stratigraphy- applications to hydrocarbon exploration*: American Association of Petroleum Geologists Memoir 26, 63- 81.

Valette-Silver, N.J. (1993). The use of sediment cores to reconstruct historical trends in contamination of estuaries and coastal sediments. *Estuaries*, 16, 577-588.

van Gaalen, J. F. (2004). Longshore Sediment Transport From Northern Maine To Tampa Bay, Florida: A Comparison Of Longshore Field Studies To Relative Potential Sediment Transport Rates Derived From Wave Information Study Hindcast Data. M.S. Thesis, College of Marine Science, University of South Florida, 114 pp.

Van Wagoner, J. C., Mitchum, R. M., Posamentier, H. W.,Vail, P. R. (1987). Part 2- Seismic Stratigraphy Interpretation Procedure *in*: Bally, A. W. (Ed.). *Atlas of Seismic Stratigraphy, American Association of Petroleum Geologists in Studies in Geology; No. 27, Vol.1*. Tulsa: American Association of Petroleum Geologists, 11- 12.

Varekamp, J.C., Thomas, E. (2005). The early geological history of Long Island Sound. *EOS Trans.* AGU, 86, (52), Fall Meet. Suppl., Abstract # PP13A-1481.

Varekamp, J. C., Thomas, E., Groner, M. (2005). The late Pleistocene- Holocene History of Long Island Sound, *Seventh Biennial LIS Research Conference Proceedings*, 27- 32.

Veres, D. S. (2002). A Comparative Study Between Loss on Ignition and Total Carbon Analysis on Minerogenic Sediments. *Studia Universitatis Babes- Bolyai, Geologia*, XLVII, 1, 171-182.

Wartel, S. Barusseau, J. P., Cornand, L. (1995). Improvement of grain-size analyses using the automated SEDIGRAPH 5100. KBIN, Brussels, Belgium, 400-426.

Weiss, D. (1974). Late Pleistocene Stratigraphy and Paleoecology of the Lower Hudson River Estuary, *Geological Society of America Bulletin*, 85, 1561- 1570.

Westrich, B., Jancke, T.(2007). *Report on erosion behaviour measurements of undisturbed sediment cores from the Belgian North Sea bed*. University of Stuttgart, Institute of Hydraulic Engineering, 13 pp.

Williams, S. C., Simpson, H. J., Olsen,C. R., Bopp, R. F. (1978). Sources of Heavy Metals in Sediments of the Hudson River Estuary. *Marine Chemistry*, 6, 195-213.

Wilson, T.P., Bonin, J.L. (2007), Concentrations and Loads of Organic Compounds and Trace Elements in Tributaries to Newark and Raritan Bays, New Jersey: *U.S. Geological Survey Scientific Investigations Report 2007-5059*, 176 p.

Windom, H. L., Schropp, S. J., Calder, F. D., Ryan, J. D., Smith Jr., R. G., Burney, L. C., Lewis, F. G., Rawlinson,C. H. (1989). Natural trace metal concentrations in estuarine and coastal marine sediments of the southeastern United States. *Environ. Sci. Technol.* 23 (3), 314- 320.

Wolfe, D.A., Long, E. R., Thursby, G. B. (1996). Sediment Toxicity in the Hudson- Raritan Estuary: Distribution and Correlations with Chemical Contamination. *Estuaries*, 19 (4), 901- 912.

Wright, J D., Sheridan, R. E., Miller, K. G., Uptegrove, J., Cramer, B. S., Browning,J. V. (2009). Late Pleistocene Sea Level on the New Jersey Margin: Implications to Eustasy and Deep-sea Temperature, *Global and Planetary Change*, 66, 93-99.

Yuhas, C. (2002). The Status of Shellfish Beds in the NY-NJ Harbor Estuary. *NJ Sea Grant College Extension Program/NY-NJ Harbor Estuary Program*, 23 pp.

Young, R. A., Hillard, B.F. (1984). Suspended Matter Distribution and Fluxes Related to the Hudson- Raritan Estuarine Plume. *NOAA Technical Memorandum NOS OMA 8,* 32 pp.

Zaitlin, B. A., Dalrymple, R. W., Boyd,R.(1994). The stratigraphic organization of incised-valley systems associated with relative sea- level change. *Incised- Valley Systems: Origin and Sedimentary Sequences, SEPM Special Publication*, 51, 45- 60.

Zhang, K, Douglas, B., Leatherman,S.(2000). Twentieth- century storm activity along the U.S. east coast. *Journal of Climate*, 13, 1748-1761.

Zhang, K, Douglas, B., Leatherman, S. (2002). Do Storms cause long-term beach erosion along the U.S. East barrier coast? *The Journal of Geology*, 110, 493- 502.

Zimmer, B. J. (2004). *Raritan and Sandy Hook Bays Sanitary Survey Report 1997- 2000*, NJDEP, Division of Watershed Management, Water Monitoring Project. 102 pp.

Personal Communication Cited

Coch, N. (2009). person. commun., Queens College, NY

Lotti- Bond, R., Anest, N. (2008). person. commun., Lamont- Doherty Earth Observatory, Palisades, NY

Losefski, G. (2008). person. commun., Lamont- Doherty Earth Observatory, Palisades, NY

Pant, H. (2008). person. commun., Lehman College, Bronx, NY

Sheridan, R. E.(2007; 2008) unpublished data; person. commun., Rutgers University, New Brunswick, N.J.

Wolf, A. (2012), person. commun., Pennsylvania State University, PA